1998

Hydrogen peroxide diel cycling in geothermal waters: Photochemical formation through metal redox cycling

Cindy Wilson
The University of Montana

Recommended Citation

Maureen and Mike
MANSFIELD LIBRARY

The University of **MONTANA**

Permission is granted by the author to reproduce this material in its entirety, provided that this material is used for scholarly purposes and is properly cited in published works and reports.

*** Please check "Yes" or "No" and provide signature ***

Yes, I grant permission _____ ✗ _____

No, I do not grant permission _____

Author's Signature _Cindy Wilson_____

Date _May 22, 1998_____

Any copying for commercial purposes or financial gain may be undertaken only with the author's explicit consent.
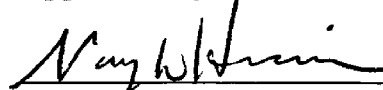
Hydrogen Peroxide Diel Cycling in Geothermal Waters: Photochemical Formation Through Metal Redox Cycling

By

Cindy Wilson

B.S. Montana Tech, 1998

B.S. Montana State University, 1979

Presented in partial fulfillment of the requirements for the degree of

Master of Sciences

The University of Montana, 1998

Approved by:

_____

Chairperson

_____

Dean, Graduate School

5-27-98

Date

UMI Number: EP37388

UMI°

Dissertation Publishing

UMI EP37388

ProQuest°

Hydrogen peroxide diel cycling in surface geothermal waters: Possible formation through metal redox cycling (83 pp.)

Advisor: Nancy W. Hinman

Hydrogen peroxide is widely distributed throughout surface waters where the primary photochemical mechanism of formation involves dissolved organic carbon (DOC). Hydrogen peroxide concentrations in metal-rich surface geothermal waters were determined to examine hydrogen peroxide formation at high temperatures and the possible involvement of metal redox cycling in hydrogen peroxide formation. Hydrogen peroxide was measured every 4 hours over 40 hour periods at four hot springs in Yellowstone National Park. Concentrations were measured in the source pool at all hot springs and in the outflow channel at three hot springs. The hot springs included an alkaline spring (Black Sand Pool), a near-neutral spring (unnamed spring at Nymph Lake), and two acidic springs (Chocolate Pots and an unnamed spring at Nymph Lake).

Diel changes in hydrogen peroxide concentrations suggest that photochemical processes were responsible for its formation. Hydrogen peroxide concentrations reached 200-600nM by late afternoon and decreased to less than 50nM during the night. While the primary hydrogen peroxide formation mechanism involves DOC in other surface waters, DOC concentrations in these geothermal waters varied throughout the sampling periods and did not coincide with hydrogen peroxide concentrations. Instead, iron cycling at three sites coincided with hydrogen peroxide cycling which suggested hydrogen peroxide formation through metal redox cycling. The highest apparent hydrogen peroxide formation with iron redox cycling occurred in lower pH waters (pH ~3.5). This is consistent with hydrogen peroxide formation where the reaction of the hydroperoxyl radical ($HO_2^{\cdot}$) with ferrous iron dominates below pH 4.8.

Laboratory studies using water from Chocolate Pots indicated that hydrogen peroxide formation varied for different regions of the solar spectrum. Hydrogen peroxide formation was greater with UVA radiation (320-400nm) than with UVB radiation (280-320nm). However, UVB radiation formed more hydrogen peroxide per watt of solar radiation than did UVA radiation. Photosynthetically active radiation (PAR, 400-700nm) was responsible to a lesser degree for hydrogen peroxide formation.

Laboratory studies of hydrogen peroxide dark decay indicated that two mechanisms were responsible for hydrogen peroxide decay. The main mechanism for hydrogen peroxide decay involved particulate matter (probably microorganisms) while the secondary mechanism involved soluble matter (i.e. metal ions and chemical reactions such as Fentons type reactions and Haber-Weiss reactions).

Hydrogen peroxide formation and decay through chemical reactions involving metal redox cycling affects the oxidation state and the biovailability of these metals which may affect microbial ecology and evolution. In particular, hydrogen peroxide formation and degradation through metal redox cycling may have been the first steps in the development of superoxide dismutase to control the superoxide radical and the development of catalase-type enzymes to control hydrogen peroxide.

ACKNOWLEDGMENTS

TABLE OF CONTENTS

LIST OF TABLES

LIST OF ILLUSTRATIONS

vi

CHAPTER 1: INTRODUCTION

Hydrogen peroxide (H_2O_2) is widely distributed in the hydrosphere where it has been measured in groundwater (Holm et al., 1987), surface waters (marine, estuarine, and lacustrine ecosystems) (Zika et al., 1985; Cooper and Lean, 1989; Scully et al., 1996) and atmospheric waters (Kok, 1980; Zika et al., 1982; Gunz and Hoffmann, 1990) (Table 1). As the most stable intermediate species in the reduction of oxygen, hydrogen peroxide may shape the biogeochemistry of these aqueous ecosystems by affecting biological processes (Halliwell and Gutteridge, 1984; Imlay and Linn, 1988) and geochemical cycling of metals and non-metals (i.e. Cr, Mn, Cu, Fe, S) (Sunda et al., 1983; Moffett and Zika, 1987; Millero et al., 1989; Pettine and Millero, 1990; Gaede and van Eldik, 1994). The effect of hydrogen peroxide on biological and geochemical processes depends largely on its' concentrations.

Table 1: Typical hydrogen peroxide concentrations in natural waters		
Water source	Range	Reference
rain	<0.1 - 120 µM	Gunz and Hoffmann 1990
snow	<0.6 - 15.6 µM	Gunz and Hoffmann 1990
oceans	10 - 240 nM	Cooper and Lean 1989
lakes	10 - 400 nM	Cooper and Lean 1989
groundwater	<10 - 66 nM	Holm et al., 1987

In surface waters, hydrogen peroxide concentrations are controlled primarily by in-situ formation and decomposition (Cooper et al., 1989) and to a lesser extent by wet and dry deposition of atmospherically formed oxidants (Cooper et al., 1988). Wet deposition, characterized as precipitation of hydrogen peroxide in rain and snow, introduces large hydrogen peroxide concentrations (10^{-6} M) to surface waters over short periods (Zika et al., 1982; Cooper et al., 1987). Dry deposition, characterized as absorption of atmospheric gases ($HO_2^{\cdot}$, H_2O_2, O_2, and O_3) at the air-water interface, continuously introduces small hydrogen peroxide concentrations to surface waters. Dry deposition is believed to contribute less than 2% of the hydrogen peroxide found in most surface waters (Cooper et al., 1988).

In-situ hydrogen peroxide formation and decomposition are continuous processes that occur at various rates resulting in daily (diel) and seasonal variations in hydrogen peroxide concentrations (Cooper et al., 1989). During hydrogen peroxide diel cycling, maximum hydrogen peroxide concentrations are observed mid-afternoon and minimum hydrogen peroxide concentrations are observed pre-dawn (Cooper et al., 1989; Zika et al., 1985). During hydrogen peroxide seasonal cycling, higher hydrogen peroxide concentrations are observed in the summer and lower hydrogen peroxide concentrations are observed in the winter (Cooper et al., 1989). Potential mechanisms for in-situ hydrogen peroxide formation and decomposition in surface waters are photochemical reactions, biological activity, and oxidation-reduction (redox) reactions. Each process forms and degrades hydrogen peroxide at different rates for marine and freshwater environments (Table 2).

Table 2: Hydrogen peroxide formation and decomposition rates in surface waters					
	Formation (nM/hr)			Decomposition	
Mode	Solar radiation	Marine	Lakes	Marine	Lakes
Photochemical	280-400 nm	$5-6^2$	$80-2000^1$	<5 nM^2	
Biological					
Light	400-700 nm	ND	ND		
Dark		[a] $1-2^5$	ND	[b] $5-35$ nM/hr^3	[c] $1-12$ nM/hr^3
Redox reactions	290-600 nm	$<0.2^2$	Negligible[4]		

ND - observed but not determined	[1] Scully et al., 1996
[a] 10^5 cells/liter marine water at a rate of 10^{-14} mole (H_2O_2)/cell·hr	[2] Moffett and Zarifiou, 1990
[b] 3×10^9 cells/liter estuarine water at a rate of 14%/hr	[3] Cooper et al., 1994
[c] 1.3×10^9 cells/liter lake water at a rate of 3%/hr	[4] Moffett and Zika, 1987
nM = 10^{-9} moles/liter	[5] Palenik et al., 1987

Hydrogen peroxide formation in surface waters

Photochemical processes form the majority of hydrogen peroxide found in surface waters (Cooper et al., 1988; Cooper et al, 1994; Scully et al., 1996) with formation rates 5-6 nM/hr in oceans (Moffett and Zarifiou, 1990) and 80-2000 nM/hr in lakes (Scully et al., 1996) (Table 2). The main pathway for photochemical formation of hydrogen peroxide in surface waters is probably the interaction of ultraviolet (UV) radiation (280-

400nm) with dissolved organic carbon (DOC) (Cooper et al, 1994; Scully et al., 1996). The DOC absorbs energy from UV radiation (DOC*) and then reduces oxygen forming the superoxide ion (O_2^{-}) (equations 1 and 2) (Cooper et al, 1994). Disproportionation of the superoxide ion produces hydrogen peroxide and oxygen (equations 3 and 4).

$$DOC \xrightarrow{h\nu} DOC* \tag{1}$$
$$DOC* + O_2 \rightarrow DOC^{\cdot+} + O_2^{-} \tag{2}$$
$$O_2^{-} + H^+ \rightarrow HO_2^{\cdot} \tag{3}$$
$$HO_2^{\cdot} + HO_2^{\cdot} \rightarrow H_2O_2 + O_2 \tag{4}$$

Hydrogen peroxide formation as a by-product of biological activity (i.e. aerobic respiration (equations 5-6), nitrogen acquisition (equation 7), photosynthesis (equations 8 - 9)) has been reported in marine and freshwater environments with formation rates 1-3 nM/hr in marine water (Stevens et al., 1973; Palenik et al., 1987; Palenik and Morel, 1988 and 1990; Moffett and Zarifiou, 1990) (Table 2). While the rates for biological hydrogen peroxide formation are low compared to rates for photochemical hydrogen peroxide formation, biological hydrogen peroxide formation can be significant at night or in waters containing large microbial populations. Additionally, microbes may produce hydrogen peroxide when they are exposed to toxic levels of the superoxide ion or oxygen (equations 10 and 11) (Gottschalk, 1986; Brock et al., 1994).

$$O_2 + e^- \rightarrow O_2^{-} \tag{5}$$
$$O_2^{-} + e^- + 2H^+ \rightarrow H_2O_2 \tag{6}$$
$$L\text{-amino acid} + O_2 \xrightarrow{LAAO} KetoAcid + H_2O_2 + NH_4^+ \tag{7}$$
$$H_2O \rightarrow HO^{\cdot} + e^- + H^+ \tag{8}$$
$$H_2O + HO^{\cdot} \rightarrow H_2O_2 + e^- + H^+ \tag{9}$$
$$O_2^{-} + O_2^{-} + 2H^+ \xrightarrow{SOD} H_2O_2 + O_2 \tag{10}$$
$$O_2 + 2e^- + 2H^+ \xrightarrow{oxidase} H_2O_2 \tag{11}$$
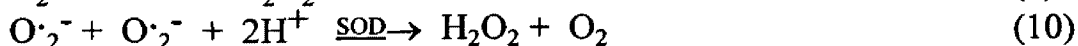
Metal redox reactions (photochemical or chemical) are considered a minor source for hydrogen peroxide formation in surface waters (Table 2) (Cooper et al., 1994). In metal photochemical/chemical redox cycling, reduced metals (Fe, Cu, and Mn) react with the superoxide ion ($O_2^{\cdot-}$) or oxygen forming hydrogen peroxide (Figure 1) (Cooper et al, 1994; Zuo and Hoigne 1992). The oxidized metals absorb sunlight energy and are reduced completing the redox cycle. While formation rates in surface waters have not been determined, formation rates appear to depend on water pH and metal concentrations (Zuo and Hoigne 1992).
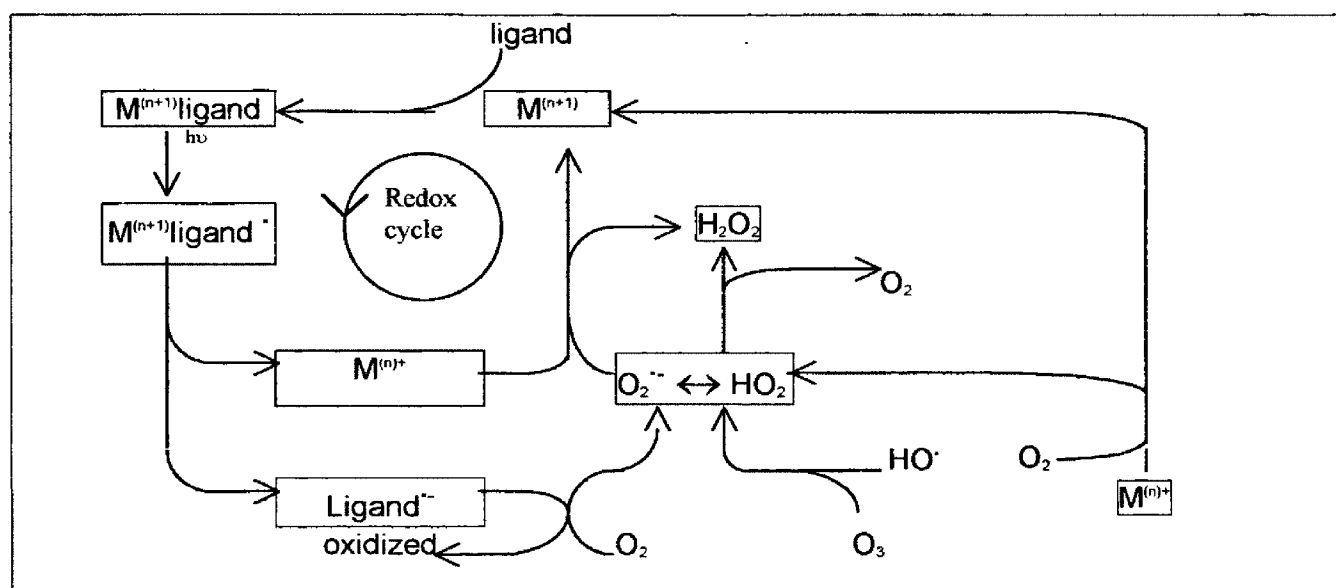
Figure 1: Photochemical/chemical metal redox cycling and hydrogen peroxide formation (ligand: organic, inorganic, none) (after Zuo and Hoigne, 1992).

Hydrogen peroxide removal in surface waters

While photochemical processes form most hydrogen peroxide, photolysis removes insignificant quantities of hydrogen peroxide (Table 2) (Moffett and Zarifiou, 1990). Instead, biological activity is responsible for the majority of hydrogen peroxide removal in surface waters (Moffett and Zarifiou, 1990). Small algae and bacteria (0.2-1.0 μm) produce enzymes, catalase and/or peroxidase, that convert hydrogen peroxide to water (equations 12 and 13) (Moffett and Zarifiou, 1990; Cooper and Lean, 1992). Hydrogen

peroxide removal depends on the kind and number of bacteria present with rates 1-12 nM/hr in lakes and 5-35 nM/hr in estuaries (Cooper and Lean, 1992).

$$H_2O_2 + 2H^+ \xrightarrow{\text{peroxidase}} 2H_2O \qquad (12)$$
$$2H_2O_2 \xrightarrow{\text{catalase}} 2H_2O + O_2 \qquad (13)$$

Hydrogen peroxide-mediated redox cycling of metals and non-metals (Fe, Cu, Mn, Cr, S) is a minor source for hydrogen peroxide removal in most surface waters (Sunda et al., 1983; Moffett and Zika, 1987; Millero et al., 1989; Gaede and van Eldik, 1994). Two possible pathways for hydrogen peroxide oxidation or reduction of metals are Fentons reactions (equations 14 and 15) or Haber-Weiss reactions (equation 16) (Zuo and Hoigne, 1992).

$$M^{(n)+} + H_2O_2 \rightarrow M^{(n+1)+} + HO\cdot + HO^- \qquad (14)$$
$$M^{(n)+} + HO\cdot \rightarrow M^{(n+1)+} + HO^- \qquad (15)$$
$$M^{(n+1)+} + H_2O_2 \rightarrow M^{(n)+} + HO_2\cdot + H^+ \qquad (16)$$
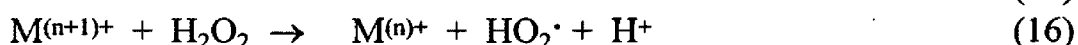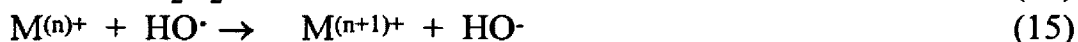
Purpose of the study

Several studies have reported daily variations in metal speciation in freshwaters (McKnight et al., 1988; Collienne,1983; Brick and Moore, 1996). Changes in metal speciation affect the bioavailability of these metals (Moffett and Zika, 1987). It is possible that these changes involve reactions with hydrogen peroxide as observed in marine and atmospheric waters (Moffett and Zika, 1987; Zuo and Hoigne, 1992). Because of the high temperatures in surface geothermal waters and different metal concentrations, it is difficult to extend these studies to surface geothermal waters.

Besides affecting metal bioavailability, hydrogen peroxide at concentrations found in marine and freshwaters may inhibit some microbial processes (Cooper and Lean, 1992). The microbes in geothermal waters are closely related to the earliest organisms and may lack hydrogen peroxide neutralizing enzymes. These primitive microorganisms may use an alternative mechanism, to provide protection from hydrogen peroxide. For these

reasons, a quantitative understanding of hydrogen peroxide formation and decomposition in surface geothermal waters may be important in microbial ecology and evolution.

This prompted a preliminary investigation at two hot springs (Black Sand Pool and Sulphide Spring) in Yellowstone National Park. Results from the preliminary investigation indicated that hydrogen peroxide is present in surface geothermal waters and that concentrations vary with time of day and sunlight exposure (Appendix A).

Based on the results from this preliminary investigation, an extended field study was conducted in surface geothermal waters. The study extended over two 40-hour periods at three locations (Black Sand Pool, Chocolate Pots, and Nymph Lake) and four hot springs in Yellowstone National Park and is the first known report of hydrogen peroxide in surface geothermal waters. The purpose of the extended field study was to 1) determine hydrogen peroxide cycling patterns in surface geothermal waters, 2) examine possible biological formation of hydrogen peroxide, and 3) determine a possible correlation between iron cycling and hydrogen peroxide cycling.

Due to the complexity of hydrogen peroxide formation in surface waters, two laboratory experiments were conducted to examine photochemical hydrogen peroxide formation in water from Chocolate Pots in Yellowstone National Park. In particular, these experiments examined 1) hydrogen peroxide formation by different regions of solar radiation and 2) hydrogen peroxide formation by particulate and non-particulate matter.

This paper presents the results of a multi-phase hydrogen peroxide study in surface geothermal waters in Yellowstone National Park, WY.

Study area

Yellowstone National Park, WY is situated on a volcanic plateau at an elevation over 2200m. Meteoric waters from the mountains north and northwest of the park migrate along faults and fractures to deep beneath the plateau where the waters are heated

(Truesdell et al., 1977; Fournier, 1989). When the heated waters contact rocks, the water leaches dissolved solids (metals and silica) from the rock. These mineralized, heated waters migrate upward along faults and fractures to form surface geothermal springs (Fournier, 1989).

Besides high metal concentrations, hot spring waters contain a diverse microbial population whose distribution is controlled by water temperature and pH (Table 3) (Brock, 1978). The upper temperature limit for non-photosynthetic bacterial growth is greater than 90°C and the upper temperature limit for photosynthetic bacterial growth is 75°C (Brock, 1978). Competition between organisms further reduces the number of species in a system. In the siliceous-alkaline waters of Yellowstone National Park, the predominant photosynthetic organisms are *Synechococcus*, a cyanobacteria, and *Chloroflexus*, a green bacteria (Brock, 1978). These species have several strains with different optimum temperatures for growth and photosynthesis. The upper temperature limit for growth and photosynthesis for these species is 70-75°C. In the very acidic waters (pH less than 4.0) of Yellowstone National Park, the predominant photosynthetic organism is *Cyanidium*, an algae (Brock, 1978). There are several *Cyanidium* strains that grow between 35-57°C, with an optimum temperature for growth and photosynthesis of 48°C (Brock, 1978).

Table 3: Geothermal micobial population growth limits
From Brock, 1978

Organisms		upper temp (°C)	lower pH
Eucaryotes			
	algae	55 - 60	1 - 2
	fungi	60 - 62	1 - 2
Procaryotes			
	cyanobacteria	70 - 75	4
	photosynthetic bacteria	70 - 75	
	chemolithitropic bacteria	> 90	

CHAPTER 2: EXPERIMENTAL DESIGN

Hot spring and site selection

Hot springs were selected according to their accessibility, proximity to electricity, dissolved iron and sulfide concentrations, and pH. Hot springs containing dissolved iron or sulfide were selected to examine metal redox cycling as a mechanism for hydrogen peroxide cycling. Hot springs with different pHs were selected to examine if pH affects hydrogen peroxide concentrations.

Based on these criteria, four hot springs (Black Sand Pool, Chocolate Pots, and two hot springs at Nymph Lake) in Yellowstone National Park (Figure 2) were selected for the hydrogen peroxide field study of surface geothermal waters. These springs contain clear waters with high concentrations of dissolved (<0.45μm) metals and sulfide (Table 4). Of particular interest are iron, manganese, arsenic, and sulfide. Concentrations of these redox-sensitive elements differ between the springs. Iron and manganese concentrations are highest at Chocolate Pots and Nymph Lake-iron spring while arsenic and sulfide concentrations are highest at Black Sand Pool and Nymph Lake-sulfur spring. DOC concentrations also varied between the springs ranging from <0.5mg/l to 8.56mg/l.

Each hot spring consists of a vent, a pool, and a run-off channel. The heated, mineralized waters forming the spring surface at a vent. In the springs studied, the vent was in a depression where water collected forming a pool. Water flowed from the pool in small run-off channels. The water chemistry within a pool-channel system is similar except at Chocolate Pots where the pool is mildly acidic pH with high average iron concentrations and the channel is near neutral pH with lower average iron concentrations (Table 4).

Site selection at a spring was based on microbial types and water temperature. High temperature pools (>75°C) contain non-photosynthetic microbes while cooler temperature pools and channels (<75°C) contain photosynthetic microbes. Photochemical hydrogen peroxide formation probably occurs at all temperatures while biological

photosynthetic hydrogen peroxide formation occurs only at temperatures <75°C. Pools and their chemically similar channels were sampled to examine the relative importance of photochemical processes and photosynthetic processes on hydrogen peroxide formation. Pools were sampled near the outflow channels (Black Sand Pool and Nymph Lake-sulfur spring) or in the center of the pool (Chocolate Pots and Nymph Lake-iron spring). Channels were sampled 5-20 meters downstream from the pool. Channels were sampled in areas with microbial mats and a water temperature ~ 50°C in July. Despite lower temperatures in August, the same sites were sampled in August.

TABLE 4: Hot spring water chemistry							
	Black Sand Pool		Chocolate Pots		Nymph lake		
	pool	channel	pool	channel	sulfur pool	iron pool	iron channel
temp (C)							
July	88.8 +/- 2.2	48.6 +/- 2.1	48.6 +/- 3.1	42.8 +/- 2.1	68.1 +/- 1.5	78.3 +/- 0.8	52.8 +/- 1.1
August	81.4 +/- 2.6	38.2 +/- 4.1	43.9+/- 1.6	39.3 +/- 1.7	63.2 +/- 3.5	67.3 +/- 8.1	45.1 +/- 3.8
pH							
July	8.39 +/- 0.11	8.73 +/- 0.13	5.78 +/- 0.15	7.26 +/- 0.12	6.57 +/- 0.17	3.37 +/- 0.06	3.24 +/- 0.08
August	8.45 +/- 0.15	9.33 +/- 0.18	5.75 +/- 0.11	7.32 +/- 0.10	6.48 +/- 0.17	3.47 +/- 0.29	3.40 +/- 0.25
alkalinity (HCO_3) (mg/l)							
July	289 +/- 21	306 +/- 26	144 +/- 5	148 +/- 5	100 +/- 6	ND	ND
August	313 +/- 5	325 +/- 12	167 +/- 6	168 +/- 8	106 +/- 3	ND	ND
metals (mg/l)							
Fe*	0.163	0.171	5.68	1.69	0.139	2.63	2.17
Mn*	< 0.001	< 0.001	1.445	1.340	0.007	0.188	0.195
As*	1.680	1.778	0.049	0.031	3.98	0.344	0.297
Cr*	0.010	0.011	< 0.004	< 0.004	0.008	0.012	0.008
Cu*	< 0.002	< 0.002	< 0.002	< 0.002	< 0.002	< 0.002	< 0.002
S(-2)(ave)	0.09	<0.01	0.02	0.02	0.13	0.06	0.02
Anions and cations (mg/l)							
Al*	0.454	0.441	0.139	0.074	0.187	1.23	1.29
B*	3.309	3.512	0.461	0.461	7.42	1.79	1.86
Ca*	0.412	0.416	23.64	23.88	1.69	6.78	7.05
Cl#	306	332	25	25	427	99	105
F#	28.2	29.7	4.3	4.1	19.2	2.5	2.6
K*	20.6	21.7	23.5	23.8	7.3	63.6	67.5
Li*	4.15	4.33	0.801	0.827	1.58	0.752	0.792
Mo*	0.048	0.052	0.009	< 0.005	0.128	< 0.005	< 0.005
Na*	493	532	114	115	442	126	142
Si*	173	183	56	57	138	131	137
SO4#	16	18	29	30	51	254	274
ND - none detected			#Analytical error for IC analyses is +/-10%				
			*Analytical error for ICP analyses is +/-15%				
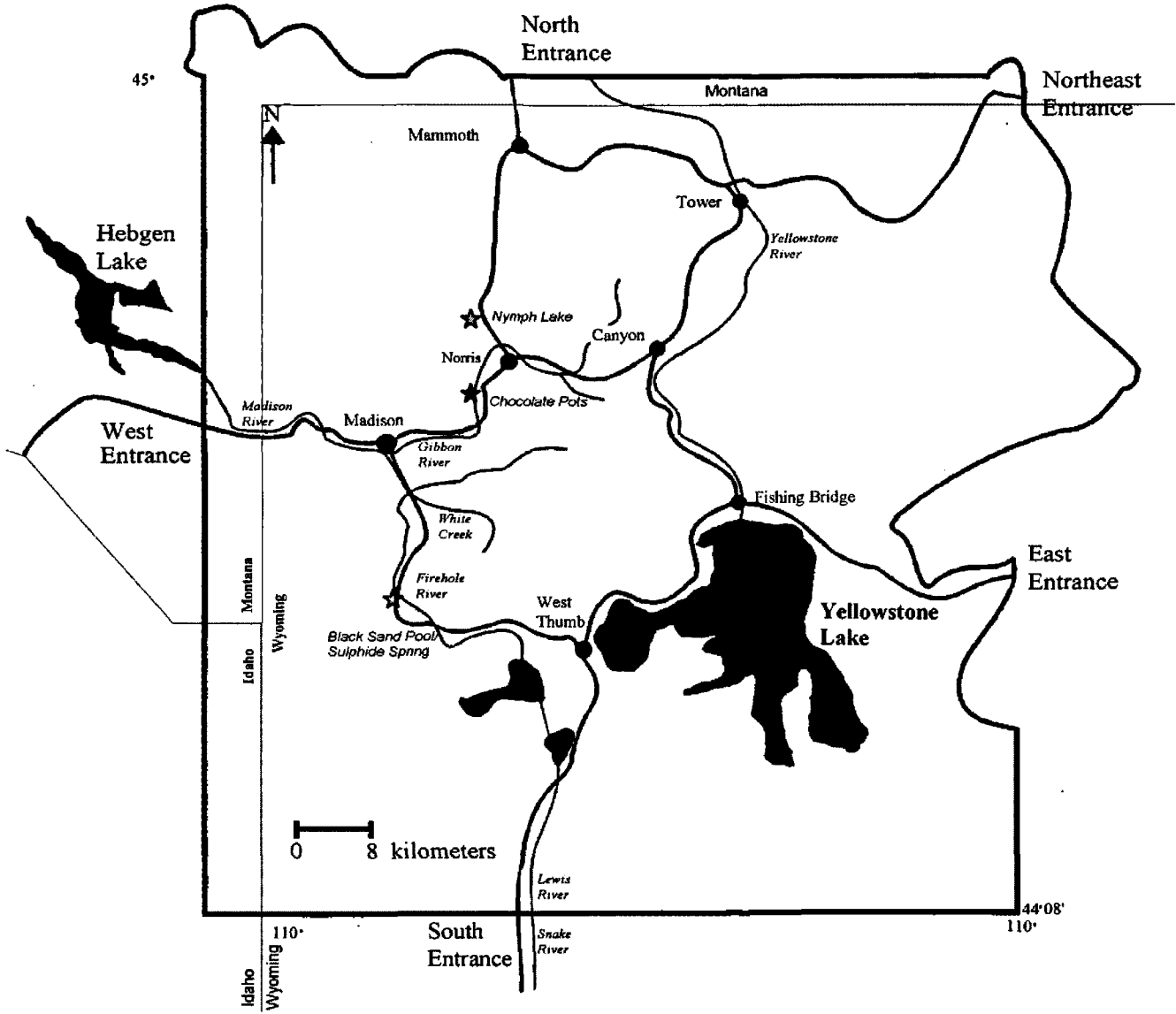
Figure 2: Sampling location in Yellowstone National Park, WY.

Sampling schedule

Each location was sampled over two 40-hour periods during the summer of 1996 (Table 5). A 4-hour sampling interval was established with 4PM as the probable time for maximum hydrogen peroxide concentrations (Scully et al., 1996). Sampling began at 8AM on the first day and ended at midnight on the second day. Samples were collected and analyzed for hydrogen peroxide, dissolved iron (total and ferrous iron) ($<0.45\mu m$), dissolved sulfide, alkalinity, dissolved organic carbon (DOC), dissolved metals/cations (Fe, Mn, Cu, Al, Mo, As, Cr, Li, Ca, Na, K, B, S, Si), and anions (SO_4, Cl, F). Dissolved oxygen (DO), pH, and temperature were monitored every 4 hours. Sunlight intensity measured as photosynthetically active radiation (PAR) was monitored every 30 minutes and weather conditions were monitored continuously.

Table 5: Sampling periods	
Black Sand Pool	July 13-14 and August 20-21, 1996
Chocolate Pots	July 10-11 and August 17-18, 1996
Nymph Lake	June 30- July 1 and August 6-7, 1996

Sample collection and preservation

Water samples were collected and preserved according to the procedures outlined in Table 6. Unfiltered samples for hydrogen peroxide and sulfide analysis were collected by dipping an HDPE sample bottle into the water and allowing the bottle to fill. These samples did not require addition of a preservative. All other water samples were collected with acid-washed plastic syringes (PP/PE Aldrich Z11, 840-0) that were rinsed with spring water prior to sampling. Samples were collected by placing the syringe tip 1-2 inches below the water surface and filling the syringe with spring water. For alkalinity analysis, twenty milliliters of unfiltered water was collected with a syringe. The samples were placed in bottles that were not rinsed. These samples did not require the addition of a preservative. Samples for anions, ferrous iron, dissolved metals/cations, and DOC analyses were filtered in the field with $0.45\mu m$ filters (Gelman nylon acrodisc). Prior to

sample collection, filters and HDPE sample bottles were rinsed with small amounts of spring water. Samples for anions and ferrous iron analyses were filtered but not preserved. Samples for dissolved metals/cations analyses were filtered and acidified to pH 2 with trace metal-grade concentrated nitric acid. Borosilicate glass bottles for DOC samples were acid-washed, rinsed with de-ionized water, and baked at 400°C for one hour in the lab (Standard Methods, 1985). Samples for DOC analysis were filtered and acidified to pH 2 with concentrated hydrochloric acid (Standard Methods, 1985). Samples for dissolved metals/cations, anions, and DOC analyses were stored on ice for transport to the University of Montana for analysis.

Table 6: Water sample collection and preservation					
Analyte	Bottle type	Bottle rinse	Sample type	Preservation	Storage
Hydrogen peroxide	HDPE	None	Unfiltered	None	Dark
Dissolved sulfide	HDPE	None	Unfiltered	None	None
Alkalinity	HDPE	None	Unfiltered	None	Ice
Soluble, ferrous iron	HDPE	3 times	Filtered	None	None
Cations/metals	HDPE	3 times	Filtered	Nitric acid	Ice
Anions	HDPE	3 times	Filtered	None	Ice
DOC	Glass with teflon septa	None	Filtered	HCL	Ice

Water and microbial mats for laboratory experiments on hydrogen peroxide formation and decay were collected at Chocolate Pots[1]. Water samples were collected by dipping 1-liter plastic bottles into the pool. Six liters of unfiltered water and three liters of filtered water (0.2μm sterile Gelman acrodisc filters with a glass fiber pre-filter) were collected in separate sterile glass bottles. Four mat samples were collected from the run-off channels using a 1-cm diameter plastic mold cutting the samples to a uniform size. Each mat with 300ml of unfiltered spring water was placed in a darkened, sterile glass dish. All samples were stored at room temperature in darkened containers[2].

---

[1] The water from Chocolate Pots contains 4 organism types (B. Pierson, personal communication, 1997). Two organism types die almost immediately after removal from the system while a third type survives for longer periods. Little is known about the fourth type.

[2] Storage of hot spring water samples at room temperatures reduces microbial metabolic activity while maintaining a viable microbial population for <7 days (B. Pierson, personal communication, 1997).

Analytical Methods and Materials

Analytical methods, locations, and completion times are summarized in Table 7.

Table 7: Analytical methods, locations, and completion times			
Analyte	Method	Location	Time
Hydrogen peroxide	Fluorescence	Near site	< 1 hr
Dissolved sulfide	Hach kit	Site	< 30 min
Alkalinity	Titration	Site/Univ MT	<3 days
Total, ferrous iron	Ferrozine	Site	< 30 min
Metals/cations	ICAPES	Univ MT	<75 days
Anions	IC	Univ MT	<14 days
DOC	TOC	Univ MT	<21 days

Hydrogen peroxide analysis

Hydrogen peroxide was analyzed by the scopoletin horseradish peroxidase fluorescent decay method within one hour of collection using a Turner Designs Model 111 fluorometer (Holm et al., 1987). The excitation filter was a Corning 7-60 (range: 320-390nm, primary wavelength: 365nm). The emission filter was a Wratten 65A (range: 460-540nm, primary wavelength: 495nm) coupled with a Wratten 2A (sharp cut-off below 415nm). This filter combination gives the highest sensitivity for scopoletin in distilled water (Holm et al., 1987). The light source was a general purpose ultraviolet lamp (range: 340-380nm). Cuvettes were borosilicate glass test tubes that had similar blank fluorescence readings with distilled water. A stirrer incorporated into the sample compartment provided continuous sample mixing. To speed mixing, test tubes were slowly inverted once after the addition of each reagent.

Reagents: De-ionized water for solutions and dilutions was stored in darkened containers for at least 48 hours prior to usage. Water and reagents were weighed in the lab with solutions prepared in the field. Reagents and solutions were refrigerated or stored on ice in darkened containers. Scopoletin solution (5×10^{-5} M) was made every 24 hours by adding 2 mg of scopoletin crystals (Sigma) to 200 ml of de-ionized water. The pH 7 phosphate buffer solution was prepared with de-ionized water and commercial buffer

salts (pHydrion Buffers). Horseradish peroxidase (HRP) solution was made by dissolving 10 mg of HRP (Sigma P8125, type II, 150-200 purpogallin units / p mg of solid) and 1.5 mg of NaN_3 (antimicrobial agent) in 2.5 ml of pH 7 phosphate buffer. HRP solution was made every 12 hours and it was used over a 9-10 hour period with no apparent loss of activity. Stock hydrogen peroxide solution (10^{-4} M) was made from commercial reagent grade hydrogen peroxide (VWR Scientific 30% solution reagent ACS) with the concentration determined by iodometric titration with sodium thiosulfate solution (Christian, 1977). Initially, hydrogen peroxide standard (10^{-6} M) was made prior to the field work. The standard was divided between four bottles with each bottle used for 20 to 40 hours. Although analysis of the standard after the sampling period did not indicate hydrogen peroxide deterioration, it was decided to take stock hydrogen peroxide solution to the field for the August sampling periods with fresh standard made every 20 hours.

Procedure: The method is based on the principle that scopoletin fluorescence is quenched in the reaction with hydrogen peroxide in the presence of horseradish peroxidase (Holm et al., 1987). The reaction is most efficient at pH 7 and therefore requires the addition of buffers to the samples (Sigma). The generalized procedural steps are shown in Figure 3. Reagent volumes varied for each site and sampling period. The amount of buffer added ranged from 35 µl for near neutral pH water to 300 µl for acidic pH water (pH 3.3). Scopoletin was added keeping the fluorescence below 100% with volumes ranging from 20-60 µl. Ten microliters of HRP was always added. Fluorescence was recorded after the addition of each reagent.

```
┌─────────────────────────┐                      ┌─────────────────────────┐
│ Add 5 ml  sample        │ ───────────────────▶ │ Read fluorescence       │
└─────────────────────────┘                      └─────────────────────────┘

┌─────────────────────────┐                      ┌─────────────────────────┐
│ Add buffer (to get pH ~7)│ ──────────────────▶ │ Read fluorescence       │
└─────────────────────────┘                      └─────────────────────────┘

┌─────────────────────────┐                      ┌─────────────────────────┐
│ Add scopoletin (keeping │ ───────────────────▶ │ Read fluorescence       │
│ fluorescence below      │                      └─────────────────────────┘
│ 100%)                   │
└─────────────────────────┘

┌─────────────────────────┐                      ┌─────────────────────────┐
│ Add HRP (10µl)          │ ───────────────────▶ │ Read fluorescence       │
└─────────────────────────┘                      └─────────────────────────┘

┌─────────────────────────┐                      ┌─────────────────────────┐
│ Add H₂O₂ standard       │ ───────────────────▶ │ Read fluorescence       │
└─────────────────────────┘                      └─────────────────────────┘

┌─────────────────────────┐                      ┌─────────────────────────┐
│ Add H₂O₂ standard       │ ───────────────────▶ │ Read fluorescence       │
└─────────────────────────┘                      └─────────────────────────┘

┌─────────────────────────┐                      ┌─────────────────────────┐
│ Add H₂O₂ standard       │ ───────────────────▶ │ Read fluorescence       │
└─────────────────────────┘                      └─────────────────────────┘
```
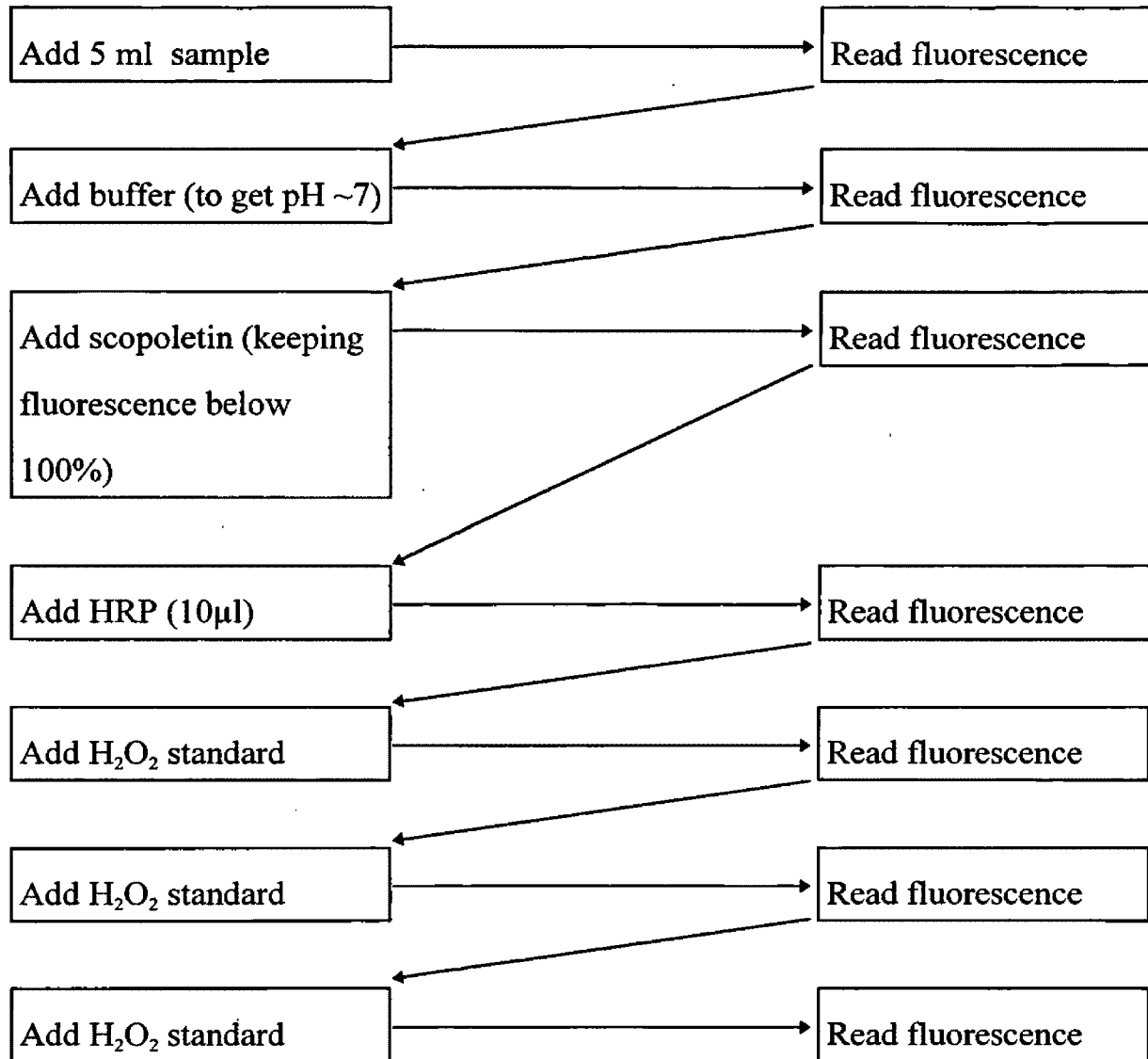
Figure 3: Schematic diagram of hydrogen peroxide analysis by the scopoletin horseradish peroxidase fluorescence decay method.

The hydrogen peroxide concentration of the sample was calculated by the method of standard additions (Holm et al., 1987; Larsen et al., 1973). Three spikes (35-70 µl) of hydrogen peroxide standard were added to the sample with the fluorescence measured and recorded after the addition of each spike. The percent fluorescence after the addition of each spike was plotted versus the total hydrogen peroxide added to the sample (Figure 4) with the sample hydrogen peroxide concentration determined by regression analysis. Each sample was analyzed in duplicate with the final hydrogen peroxide concentration determined as the mean value and the standard deviation estimated from the range of the concentrations (Dean and Dixon, 1951).
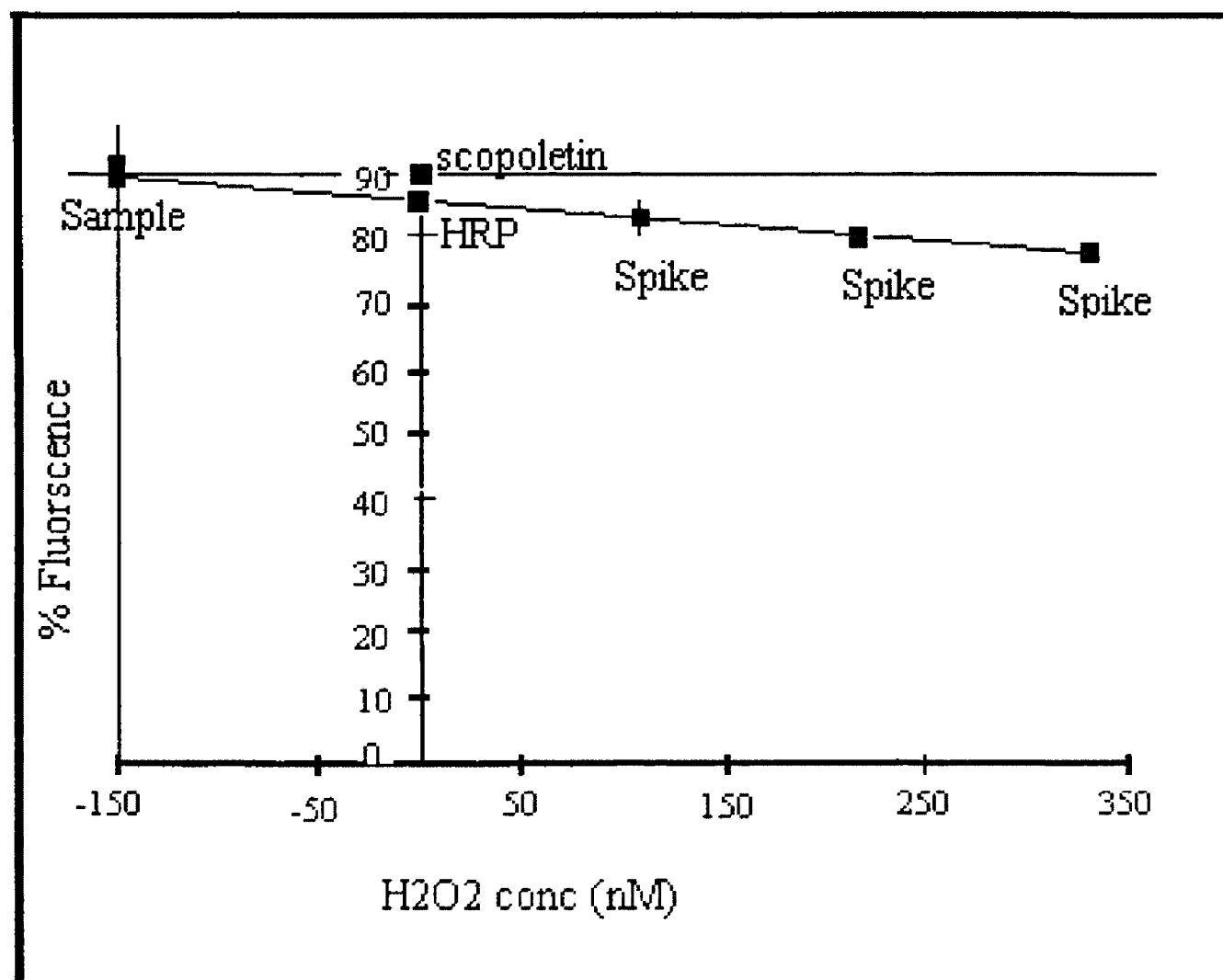
Figure 4: Hydrogen peroxide standard additions calibration curve.

Replicate analyses of the same sample were within +/-15% for concentrations less than 40 nM and +/-10% for concentrations greater than 40 nM. The method precision was +/-12% at a concentration of 25 nM and +/-7% at a concentration of 170 nM.

Because delayed analysis may produce analytical errors, hydrogen peroxide concentrations in two samples were measured over two hours. Hydrogen peroxide concentrations in both a low concentration sample (50 nM) and a high concentration sample (250 nM) were statistically the same for the immediate analysis and for the 2-hour delayed analysis. Another source of analytical errors is hydrogen peroxide in the de-ionized water used for dilutions. To reduce the hydrogen peroxide in de-ionized water, all water was stored in darkened containers for at least 48 hours prior to usage. The hydrogen peroxide concentration in the water was measured ten times obtaining a mean hydrogen peroxide concentration. The mean hydrogen peroxide concentration plus three standard deviations was the method detection limit (MDL) for that sampling period. The MDL was 32.6 nM in May, 24.8 nM in July, and 25.4 nM in August.

Field analysis

Dissolved sulfide analysis was completed within 30 minutes of sample collection using a Hach sulfide kit. Absorbence at 665nm was measured with a Hach Spectrophotometer model DR/2000. Sample sulfide concentrations were determined from standard calibration curves developed each sampling time. The standards were made fresh each time from a 1000mg/l stock standard and ranged from 0-1mg/l. Replicate analyses of the same sample were within +/- 10%.

Dissolved (< 0.45μm) ferrous and total dissolved iron analyses were completed within 30 minutes of sample collection by a modified Ferrozine method (Brown, 1997; Stockey, 1970). Ferrous iron was analyzed by adding 10 ml of Ferrozine solution (1g/l of Ferrozine in 50mM of HEPES buffered to pH 7) to 2 ml of sample. After a 2-minute color development, absorbence at 562 nm was measured with a Hach Spectrophotometer

model DR/2000. For total iron analysis, ferric iron in solution was reduced to ferrous iron by adding 1 ml of 0.25M hydroxyamine in 0.1N HCl solution to 1 ml of sample. Next, 10 ml of Ferrozine solution was added to the sample with the absorbence measured as for ferrous iron analysis.

Sample iron concentrations were determined from standard calibration curves developed each sampling time by analyzing five iron standards. The standards were made fresh each time from a 1000 mg/l stock standard (Buck Scientific) and ranged from 0-10 mg/l. Replicate analyses of the same sample were within +/-6% (Brown, 1997). Ferric iron concentrations were calculated as the difference between total and ferrous iron concentrations.

Alkalinity was determined by titration with 1.6N HCl to the bromcresol green-methyl red endpoint (pH 4.5). All samples from a 40-hour sampling period were analyzed at the same time. Replicate analyses for duplicate samples were within +/-5%.

Laboratory analysis

Water samples for dissolved organic carbon (DOC), dissolved metals/cations, and anions were analyzed at the University of Montana. Samples were refrigerated after collection with the samples warmed to room temperature prior to analysis.

DOC analyses were completed within 21 days of collection with a Shimadzu total organic carbon analyzer model TOC-5000A. The samples were purged with helium prior to analysis to remove volatile organic components. DOC concentrations were calculated from a standard calibration curve generated by analyzing 3 standards ranging from 0.5 - 5 mg/l. Samples with concentrations greater than the highest standard were diluted with de-ionized water and reanalyzed. The method precision was +/- 6% and method accuracy was +/- 10%.

Dissolved metals/cations (Al, As, B, Ca, Cr, Cu, Fe, K, Li, Mg, Mn, Mo, Na, S, Si) analyses were completed within 75 days of collection by inductively coupled argon plasma emission spectrophotometer (ICAPES) using a Jarrel Thermo Ash model IRIS. The method detection limit (MDL) for each analyte was determined by analyzing de-ionized water 10 times. The average value plus 3 times the standard deviation was the MDL (Table 8). The method precision was +/- 4% and method accuracy was +/- 15%.

Table 8: ICP cation method detection limits (mg/l)							
Al	0.06	Cr	0.011	Li	0.008	Na	0.075
As	0.07	Cu	0.008	Mg	0.198	P	0.111
B	0.041	Fe	0.032	Mn	0.003	S	0.207
Ca	0.026	K	0.518	Mo	0.017	Si	0.12

Anion (Cl, F, SO_4) analyses were completed within 14 days of collection by ion chromatography (IC) using a Dionex IC (ED40 Electrochemical detector and GP40 gradient pump) with an AS4A column. Sample analyte concentrations were calculated from a standard curve generated by analyzing 3 standards ranging from 1-10 mg/l for fluoride and chloride and 6-60 mg/l for sulfate. Samples with concentrations greater than the highest standard were diluted with de-ionized water and reanalyzed. The method precision was +/-10% and method accuracy was +/-10%.

Field measurements and observations

Temperature and pH were measured at each site with an Orion combination pH/temperature electrode model 91-57BN and meter model 230A that automatically corrects the pH for the measured temperature. The electrode was recalibrated at each hot spring by measuring the pH/temperature of buffer solutions heated to the hot spring water temperature. Electrode calibrations were checked each sampling time.

Dissolved oxygen (DO) was measured in the channels and the pool at Chocolate Pots with an Orion oxygen electrode and meter model 820. The DO electrode was recalibrated in its water-saturated sleeve with the calibration checked each sampling time.

The skies were generally clear during sampling except for brief periods of scattered clouds (Table 9). However, skies were overcast during sampling at Chocolate Pots in August. Additionally, all sites experienced periods of steam throughout the night and early morning.

Table 9: Meteorological conditions		
Location	July 1996	August 1996
Black Sand Pool	clear skies, mild winds scattered clouds the afternoon of July 11 steam at night and early morning run-off channel shaded in the morning channel site shaded until mid-morning	clear skies, mild winds steam at night and early morning run-off channel shaded in the morning channel site shaded until mid-morning

Chocolate Pots	clear skies, mild winds
	July 10: cloudy in the afternoon
	intermittent shading throughout period
	
	steam at night and early morning
		overcast skies, moderate winds
		August 18:
		    atmospheric lightning 0330 - 0500
		    rain 0500 - 0600
		steam at night and early morning

Nymph Lake	clear skies, no wind steam at night and early morning	August 6: rain until ~7AM, cloudy until ~11AM clear skies, no wind rest of period steam at night and early morning

Sunlight intensity was measured with a Sunfleck Ceptometer model SF-80 and/or a foot-candle meter. The Sunfleck Ceptometer has 80 light sensors at one-centimeter intervals that measure photosynthetically active radiation (PAR) (400-700nm). The foot-candle meter measures light intensity in foot-candles. After development of a comparison curve for light readings between the two meters, the foot-candle meter was used to measure light intensity when the Ceptometer was unavailable (Appendix B).

Sunlight intensity at Nymph Lake was measured with the Sunfleck Ceptometer during both sampling periods. On June 30, 1996, light intensity was measured manually every 30 minutes at each site. Because light readings at the three sites agreed except for minor variations, light measurements on subsequent days (July 1 and August 6-7, 1996) were taken at a central location with the Ceptometer in the automatic mode.

Sunlight intensity at Chocolate Pots and Black Sand Pool was measured with the foot-candle meter during sampling in July. At Chocolate Pots, light readings were taken every 30 minutes at the pool and mid-day at the channel. At Black Sand Pool, light readings were taken every 30 minutes at each site. Due to unavailability of either light meter in mid-August, light readings were not taken the last sampling period at either location.

Vegetation at each location produced intermittent shading throughout sampling. At Black Sand Pool, trees near the run-off channel shaded the channel most of the day with the channel site shaded until mid-morning. At Chocolate Pots, small trees and bushes surrounding the pool resulted in intermittent shading of the pool and the run-off channel throughout the day. The sampling sites at Nymph Lake were free of shading from vegetation.

Laboratory hydrogen peroxide formation and decay study

The hydrogen peroxide formation and decay studies were conducted in late-October 1997 and late-April 1998. Water and mats collected from Chocolate Pots in mid-October and in mid-April were kept at room temperature in darkened containers until testing. Experiments with mats and unfiltered water were conducted within 7 days of sample collection. In April, the experiments were run in duplicate.

The formation study consisted of 4 sets of hot spring water samples exposed to different wavelengths of mid-day sunlight. Each set of samples consisted of 250 ml of unfiltered, filtered (0.2 μm), or unfiltered-autoclaved hot spring water placed in each of 4 wide-mouthed (4-inch diameter) glass dishes wrapped with duct tape. A fourth set of samples consisted of a microbial mat and 250ml of unfiltered water in each of 4 dishes. The samples, covered with glass lids and cardboard, were placed in a water bath (48°C) in an area that received mid-day sunlight. The samples were heated for one hour before replacing the cardboard and the lids with specific light passing filters (Table 10). The

heated samples were then exposed to 4-hours of mid-day sunlight. At the end of 4 hours, the samples were covered with glass lids and cardboard for the decay study.

Table 10: Light passing filters		
Filter	Light passing	Cut-off wavelength
Cellulose diacetate	UVB-UVA-PAR	<300 nm
Polyester	UVA-PAR	< 320 nm
UF-5	PAR	<400 nm
Opaque	None	All light

Hydrogen peroxide analysis was conducted by removing 5ml aliquots from the samples. To determine hydrogen peroxide formation, hydrogen peroxide concentrations were measured prior to heating and after 4 hours exposure to sunlight. To determine hydrogen peroxide decay, hydrogen peroxide concentrations were measured every 2 hours in unfiltered water samples and every 4 hours in filtered and autoclaved water samples. Analysis continued for a maximum of 24 hours or until concentrations decreased by 50%.

The controlled light experiments were conducted in a cabinet equipped with fluorescent lamps. A Westinghouse fluorescent lamp (peak radiation 310nm) provided UVB radiation and a Sylvania black light fluorescent lamp (peak radiation 365nm) provided UVA radiation. The Westinghouse fluorescent lamp was replaced prior to the experiments conducted in late April 1998. Separate experiments were conducted to determine hydrogen peroxide formation with different regions of the solar spectrum (UVB, UVA, UVB-UVA). 250 ml of unfiltered hot spring water was placed in wide-mouthed (4-inch diameter) glass dishes wrapped with duct tape. The samples, covered with glass lids and cardboard, were placed in a water bath (48ºC) in the cabinet. The cover on one sample was replaced with a light-attenuating filter and the fluorescent lights were turned on for 4 hours. After 4 hours, the samples were covered with glass lids and cardboard. Hydrogen peroxide concentrations were measured prior to heating and after 4 hours exposure to the fluorescent light.

CHAPTER 3: RESULTS

Field Study

General observations

Sunlight intensity, measured as photosynthetically active radiation (PAR) (400-700nm), varied between locations and between the July and August sampling periods (Figure 5). PAR levels were highest at Nymph Lake and Black Sand Pool where the areas were relatively open with sparse vegetation. The sampling sites at Nymph Lake were free of shading from vegetation while the channel site at Black Sand Pool was shaded until mid-morning. The lower PAR levels at Chocolate Pots were due to the position in the Gibbon River valley and the surrounding vegetation that resulted in intermittent shading of the pool and the channel throughout the day. PAR levels were higher in July (maximum ~400 watts/m²/sec) than in August (maximum ~370 watts/m²/sec) (Figure 5b). Calculated UVA (320-400nm) and UVB (290-320nm) were 6.12 % and 0.31 % of PAR respectively[1].

Several redox-reactive components (hydrogen peroxide, dissolved oxygen (DO), dissolved iron (total, ferrous, and ferric) (<0.45μm), and dissolved sulfide)) and dissolved organic carbon were monitored in the pool and channel of 4 hot springs (Appendix B). Concentrations of these components varied between hot springs, between sites at a given hot spring, and between the July and August sampling periods (Table 11). Most component concentrations exhibited diel cycling during both sampling periods. However, variations in DOC concentrations did not follow a predictable pattern.

---

[1] UV:PAR ratios were calculated from readings obtained in Missoula in April 1998. Lighting conditions were similar to those observed in Yellowstone during the summer of 1996 with a maximum PAR level ~375 watts/m²/sec.
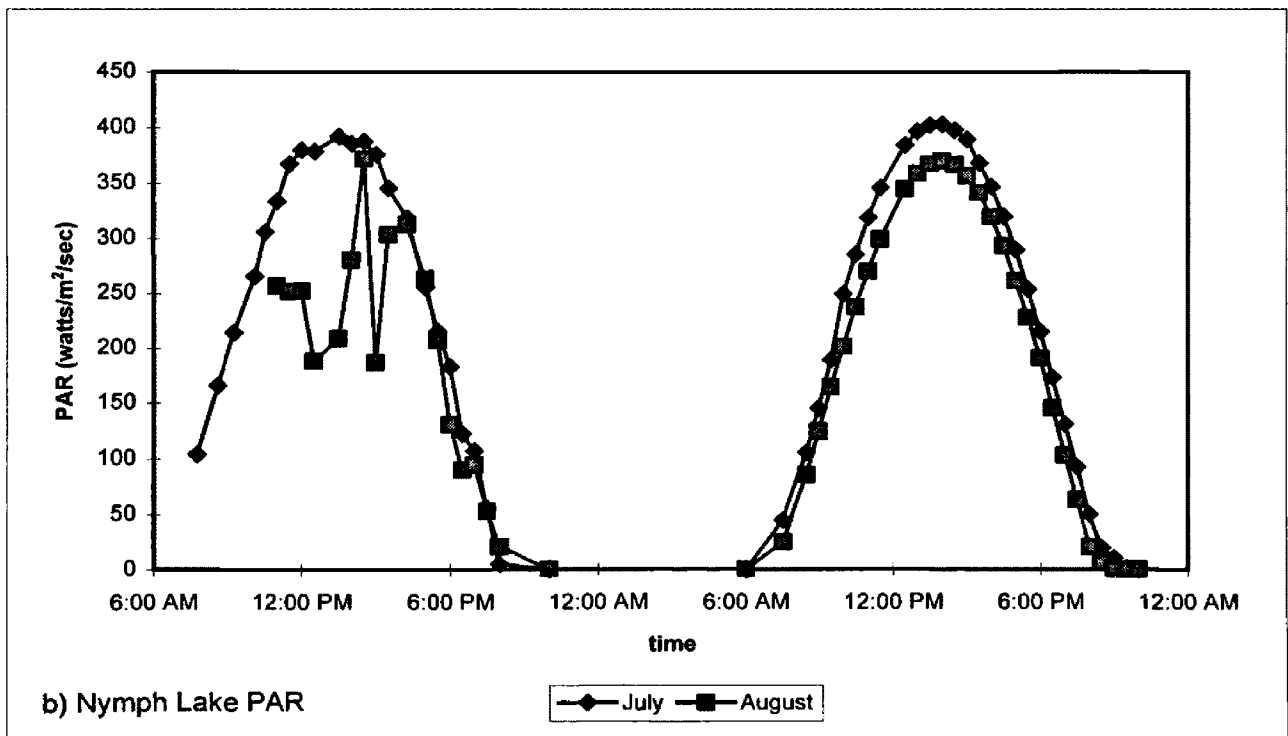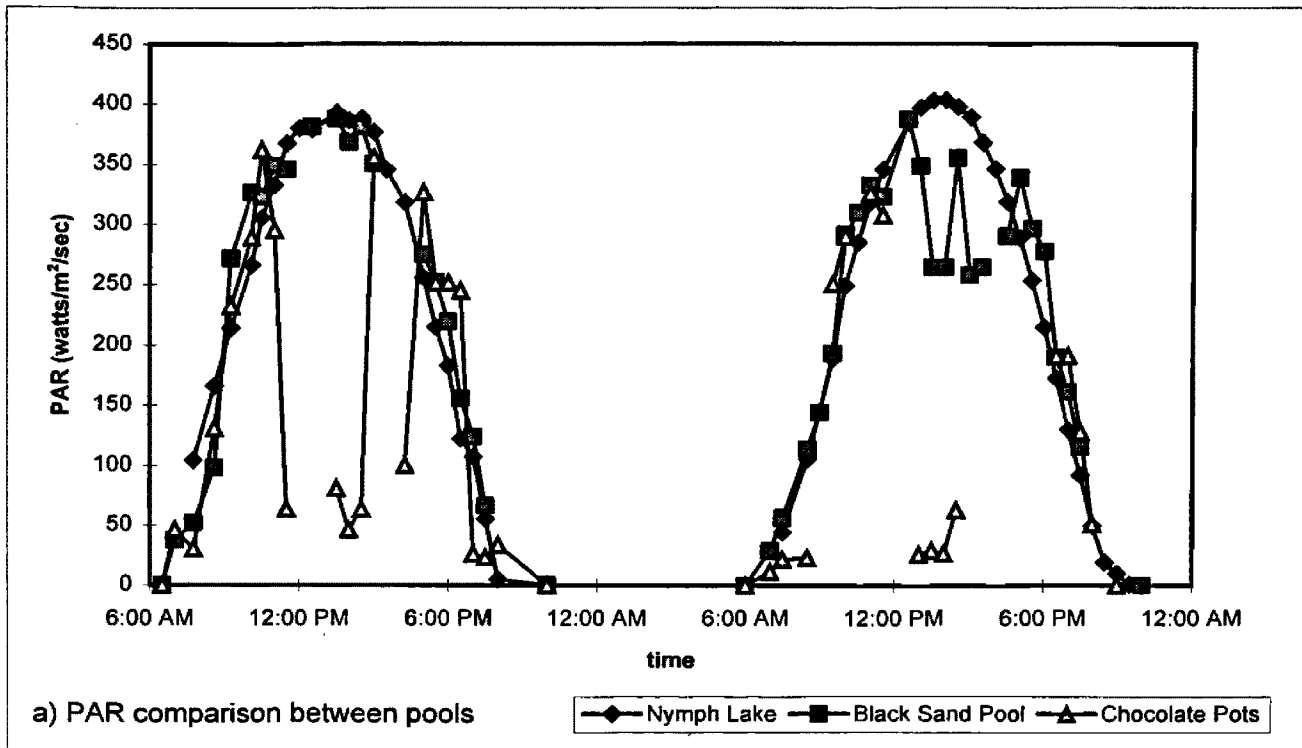
Figure 5: PAR comparison a) between pools in July, low PAR levels at Chocolate Pots are due to shading; b) between the months at Nymph Lake, flucuating PAR levels the first day in August are to due clearing skies.

Table 11: Highest water component concentrations (A = higher in August, J = higher in July)						
	Black Sand Pool		Chocolate Pots		Nymph Lake		
	pool	channel	pool	channel	Sulfur pool	Iron pool	Iron channel
H2O2	A	A	A	A	J	J	J
DOC	J	J	J	A	J	A	A
S^{-2}	J	J	SAME	SAME	SAME	SAME	SAME
DO	-	A	J	J	-	-	J
Fe total (ferrozine)	-	-	A	-	-	J	J

Diel cycling of hydrogen peroxide and oxygen coincided with variations in PAR levels. Concentrations reached maximum levels in the afternoon and dropped to minimum levels in the early morning. Average hydrogen peroxide concentrations were higher in August than in July except at Nymph Lake (Table 11). Since the DO probe could only be used at temperatures less than 60°C, DO measurements were limited to channel sites of all springs and to the pool at Chocolate Pots. Average DO concentrations were higher in July than in August except at Black Sand Pool (Table 11).

Diel cycling of dissolved iron (total, ferrous, and ferric) was observed in the pool and channel at the Nymph Lake-iron spring and in the pool at Chocolate Pots where it cycled inversely to hydrogen peroxide, DO and PAR cycles. Dissolved iron was not detected by the Ferrozine method at the other hot springs (Table 11). The ferrous iron cycle had smaller amplitude than the ferric iron cycle which resulted in a relative increase in ferrous iron concentrations during the day and a relative decrease in ferrous iron concentrations during the night.

While dissolved sulfide was detected at all sites, diel sulfide cycling was only observed at Black Sand Pool and the Nymph Lake-iron pool where sulfide cycled inversely to hydrogen peroxide, DO and PAR cycles. Average sulfide concentrations in July were higher or equal to concentrations in August at all hot springs (Table 11).

Site specific observations

Black Sand Pool

Hydrogen peroxide concentrations varied from less than 50 nM at night to as much as 495 nM during the afternoon with higher concentrations in the pool than in the channel (Figures 6,7). In addition, concentrations at both sites were higher in August than in July. Higher average DO concentrations were also observed in August (Table12). In contrast, sulfide and DOC concentrations were higher in July than in August at both sites.

Hydrogen peroxide and DO concentrations cycled with greater amplitude in August than in July (Figure 8). Additionally, there was a positive correlation between hydrogen peroxide and DO concentrations ($r^2 = 0.72$, n=22). In contrast, while hydrogen peroxide cycled opposite sulfide cycling (Figures 9,10), there was no correlation between hydrogen peroxide and sulfide concentrations in the pool ($r^2 = -0.37$, n=22) or in the channel ($r^2 = -0.11$, n=22). Sulfide concentrations and cycling were greater in the pool than in the channel with higher amplitude in July.

Table 12: Black Sand Pool component concentrations (DOC in mg/l) (sulfide, H_2O_2 ,iron, and oxygen in μM)				
	July		August	
	Pool	Channel	Pool	channel
H_2O_2 ave	0.159	0.122	0.219	0.136
min	0.051	<0.025	0.040	<0.025
max	0.311	0.417	0.495	0.345
amplitude	0.260	0.280	0.300	0.320
DOC ave	1.24	1.42	<0.5	0.90
S^{-2} ave	3.44	0.62	2.19	<0.32
min	2.28	0.32	1.14	<0.32
max	4.00	0.86	3.43	<0.32
amplitude	1.72	0.54	1.25	-
DO ave	-	150	-	160
min	-	90	-	70
max	-	190	-	310
amplitude	-	110	-	140
Fe total (ferrozine)	-	-	-	-
Fe (ICP)	2.9	3.1	3.0	3.1

Figure 6: Diel variations in hydrogen peroxide concentrations and photosynthetically active radiation (PAR) at the pool at Black Sand Pool, Yellowstone National Park
a) July 1996: low hydrogen peroxide concentrations mid-day on July 14 coincide with fluctuating PAR levels, b) August 1996: PAR was not measured. UVB ~0.31% PAR, UVA ~6.12% PAR.

a) July 1996
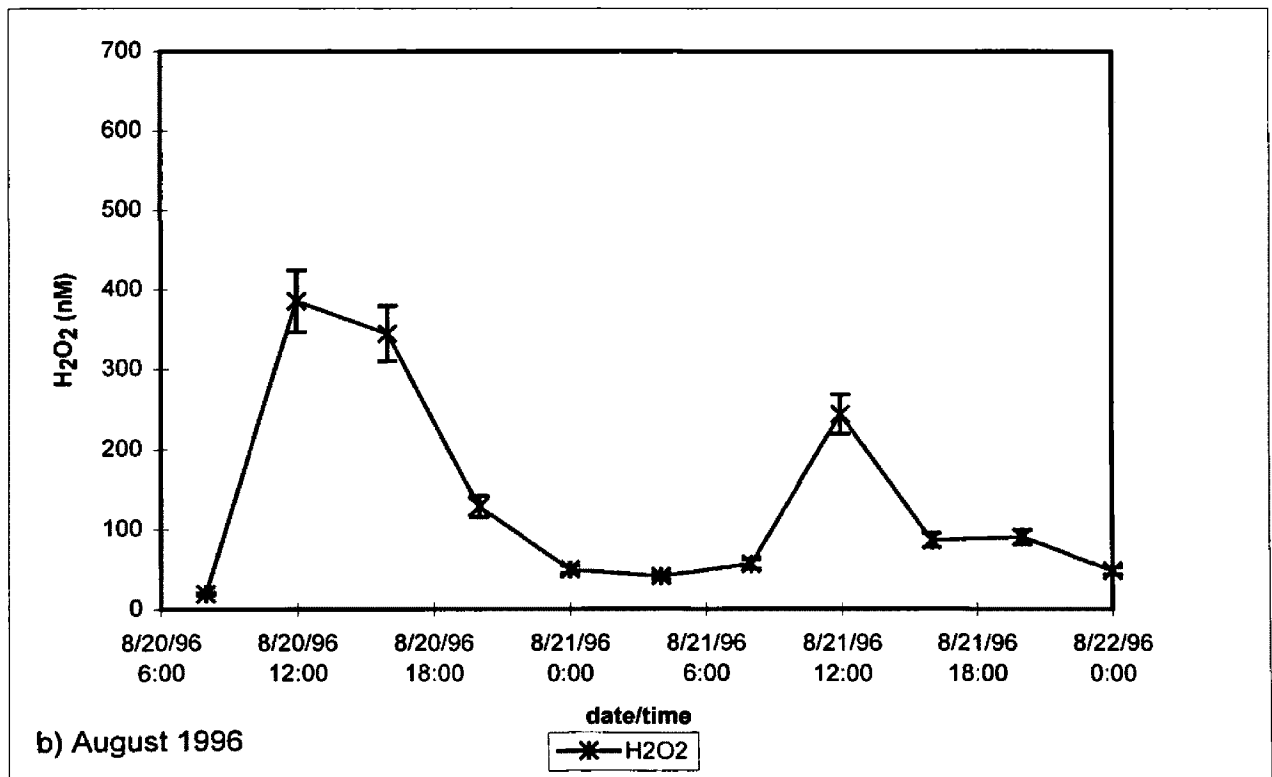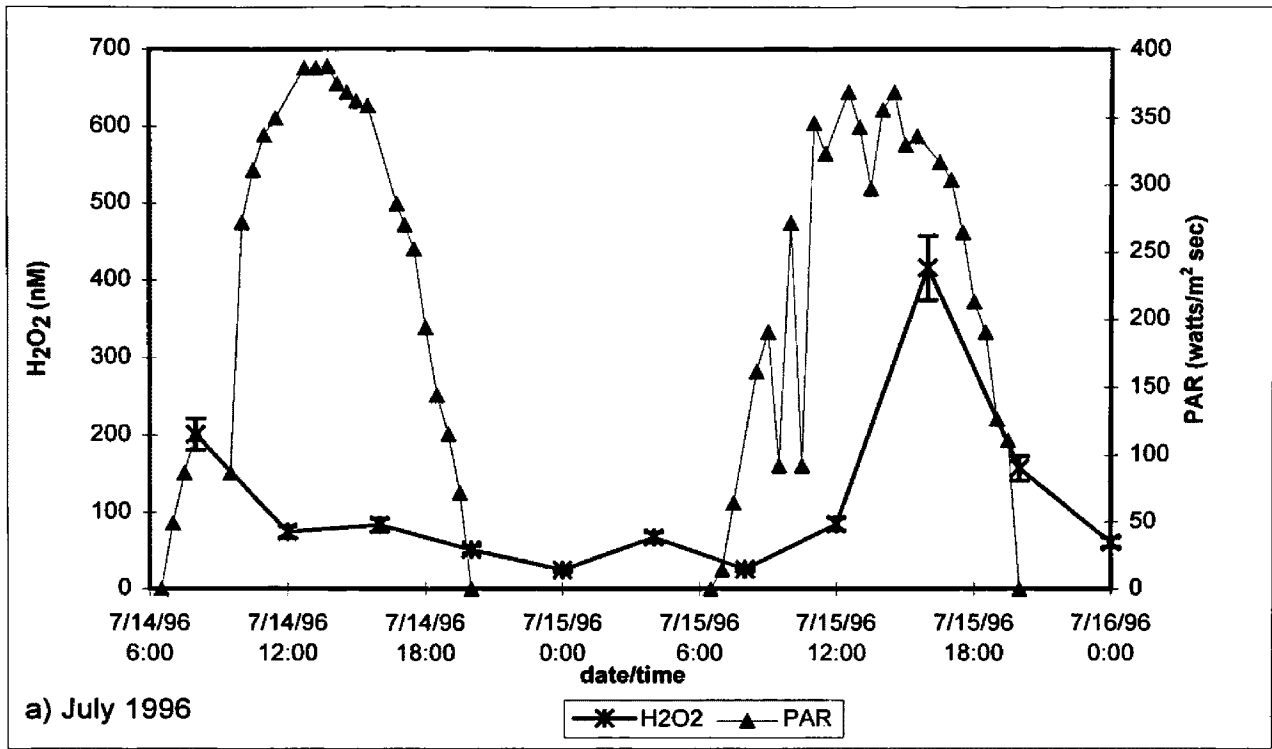
b) August 1996

Figure 7: Diel variations in hydrogen peroxide concentrations and photosynthetically active radiation (PAR) at the channel at Black Sand Pool, Yellowstone National Park a) July 1996, b) August 1996: PAR was not measured. UVB ~0.31% PAR, UVA ~6.12% PAR.
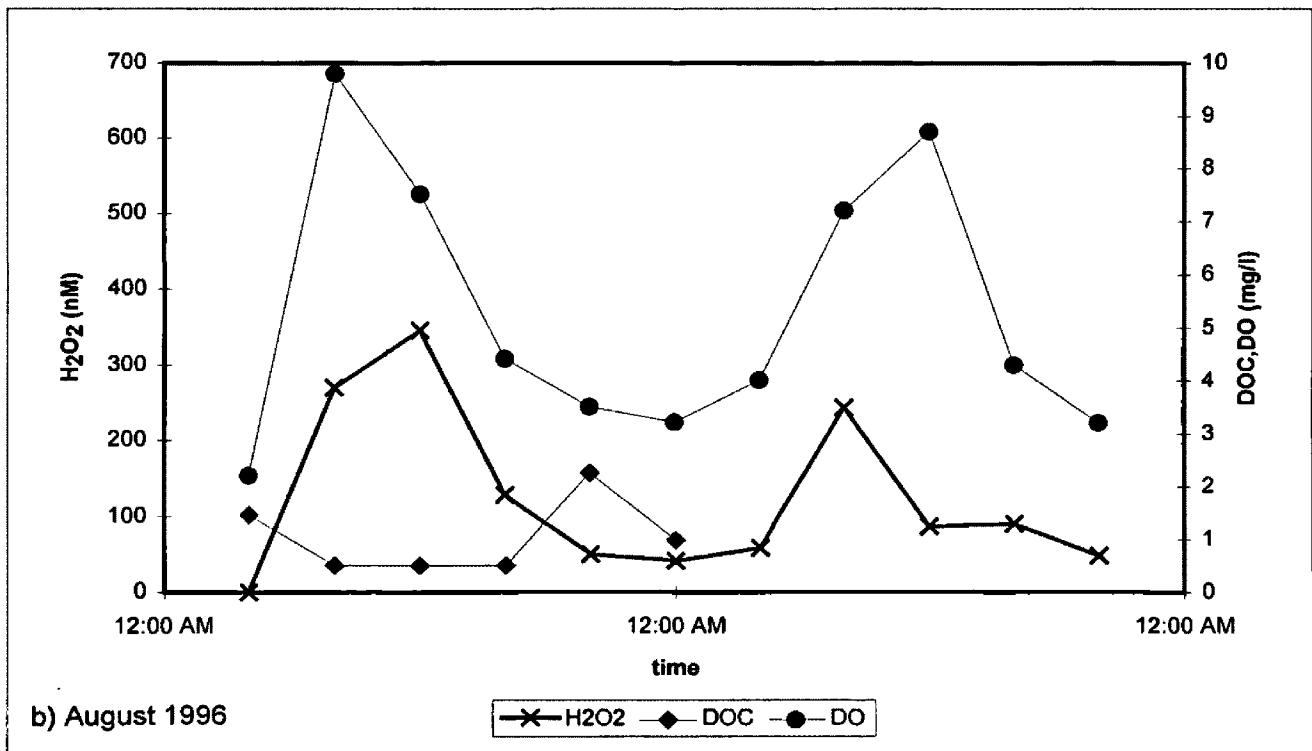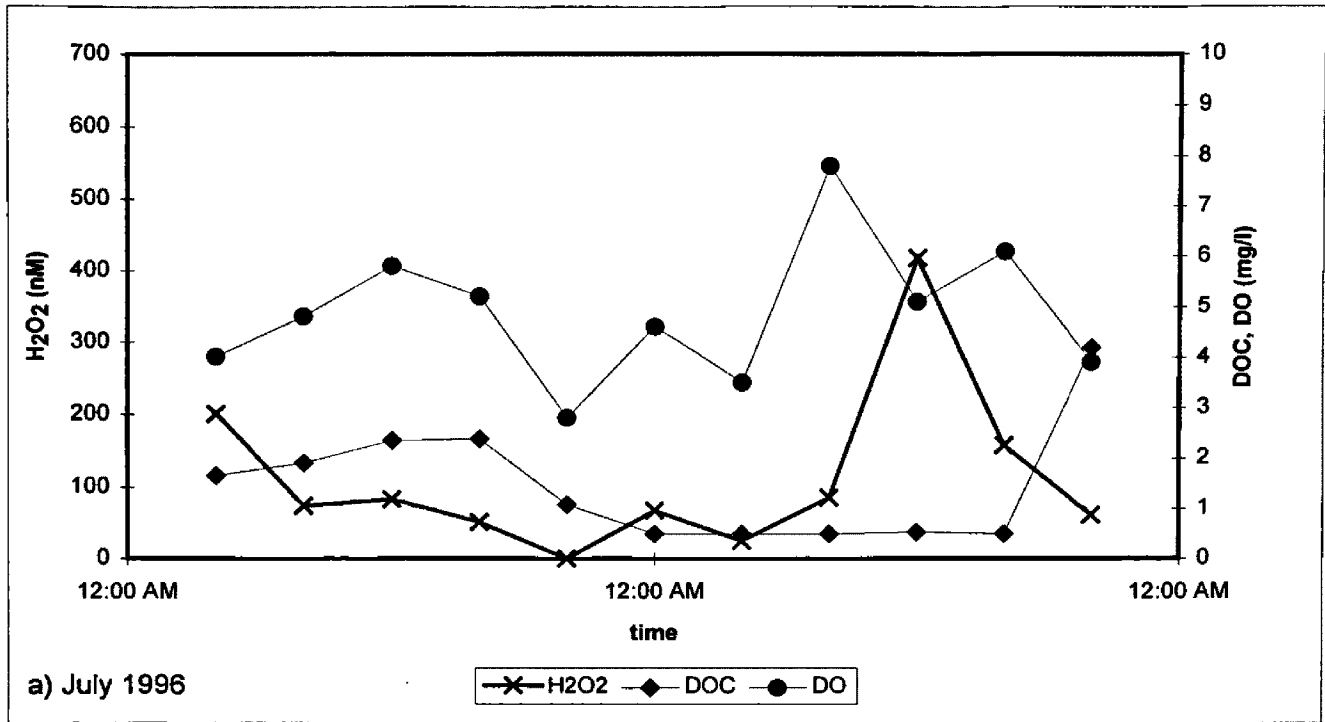
Figure 8: Variations in dissolved organic carbon (DOC), dissolved oxygen (DO), and hydrogen peroxide concentrations at the channel at Black Sand Pool, Yellowstone National Park (a) July 1996 (b) August 1996.
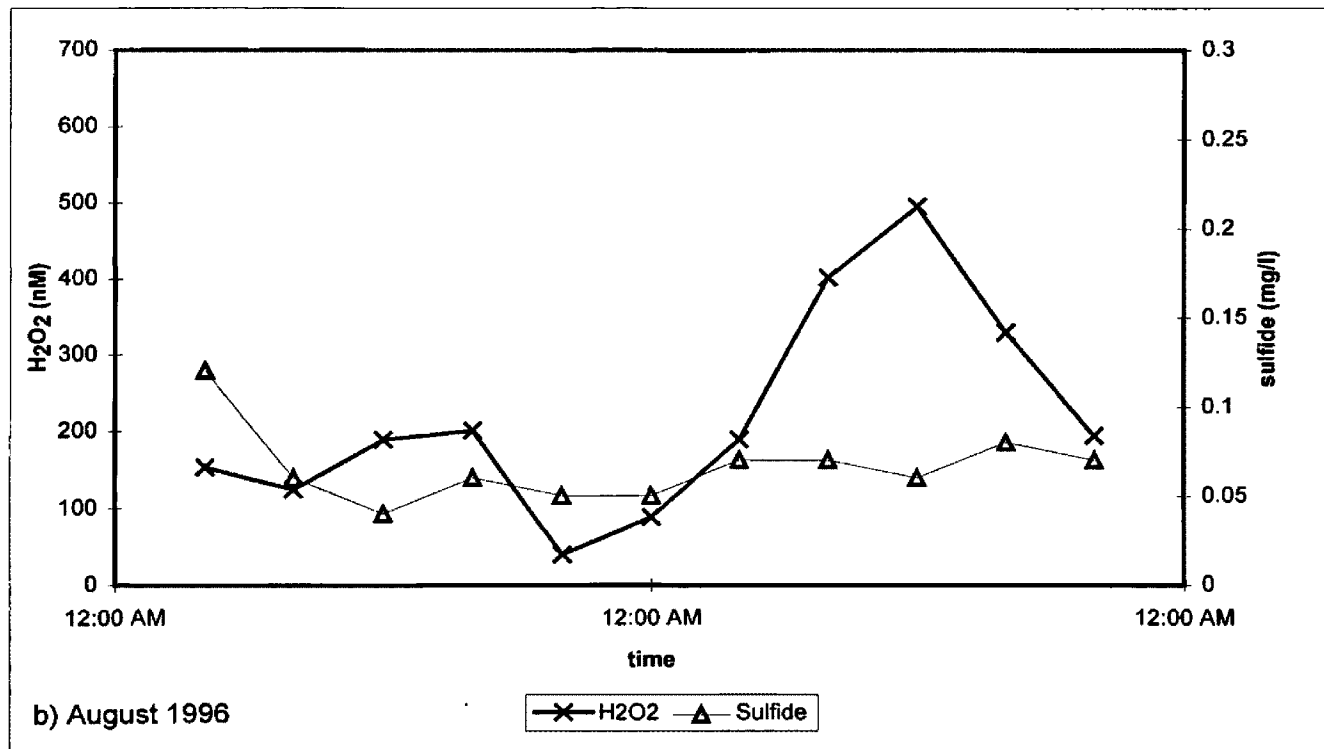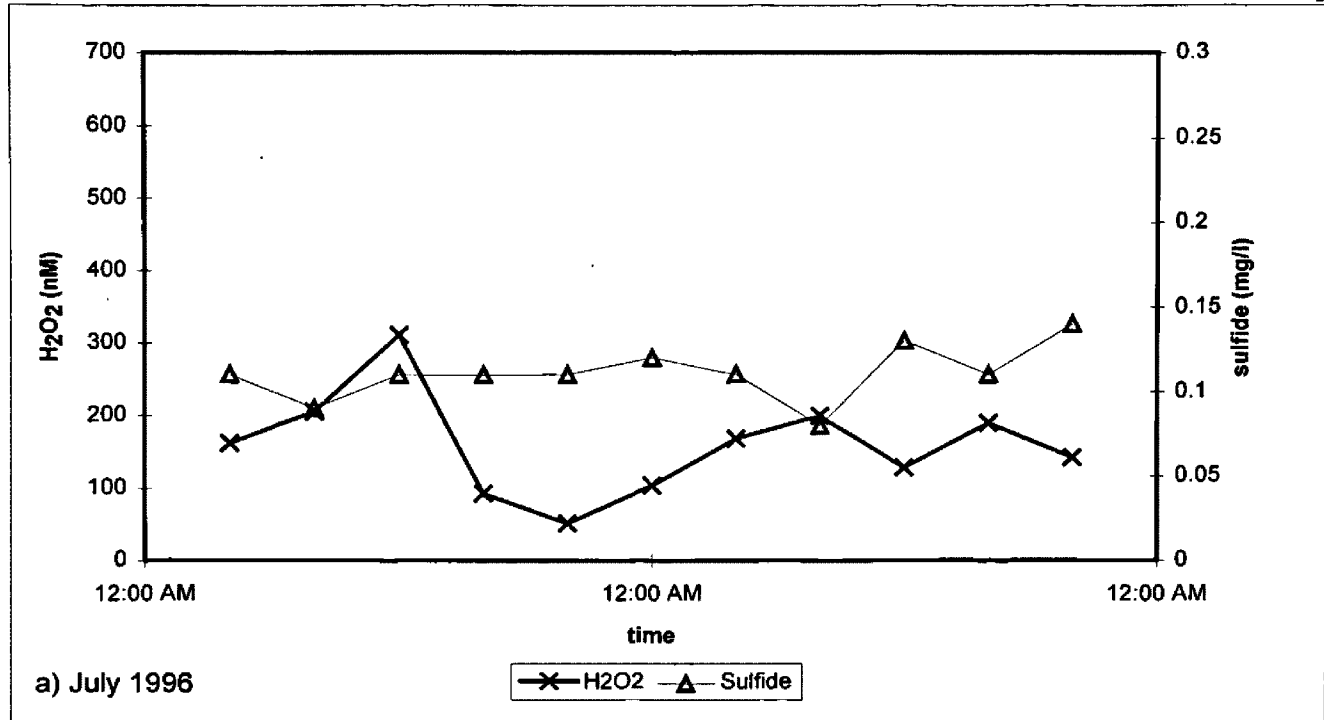
Figure 9: Variations in sulfide and hydrogen peroxide concentrations at the pool at Black Sand Pool, Yellowstone National Park (a) July 1996 (b) August 1996.
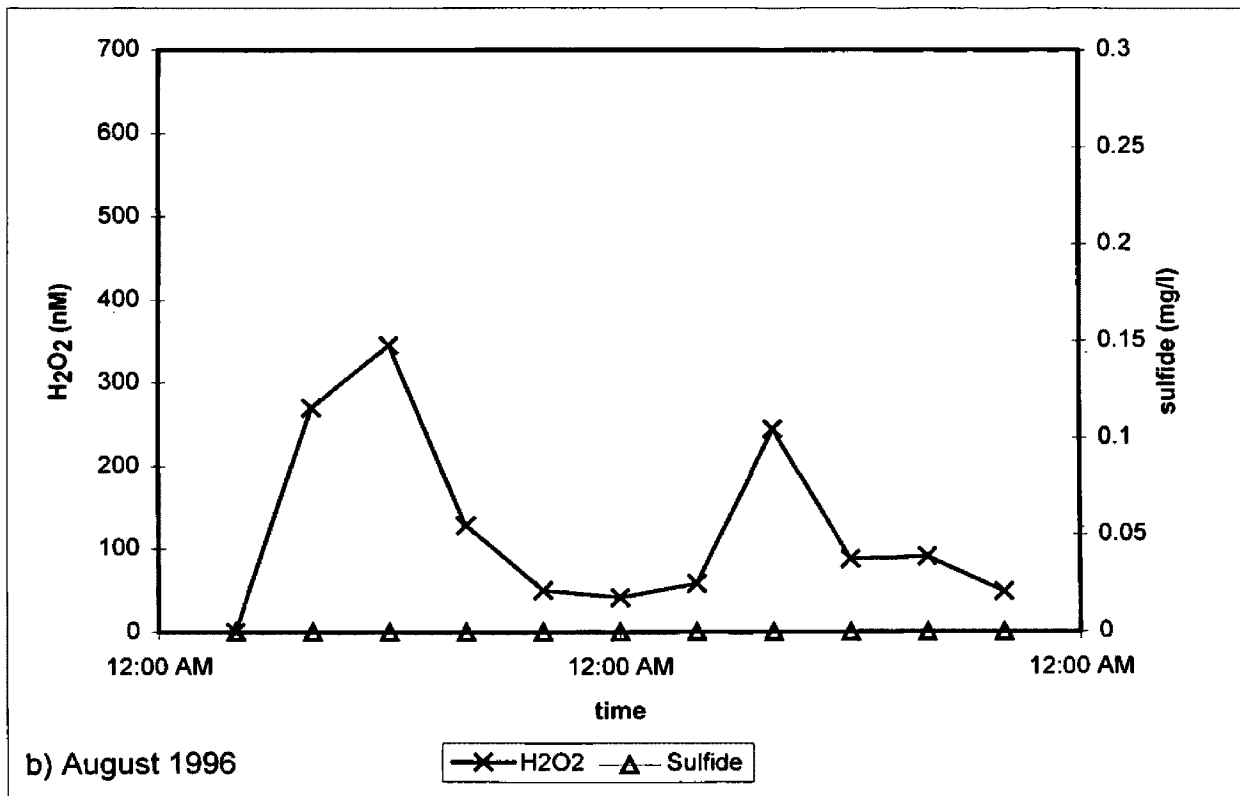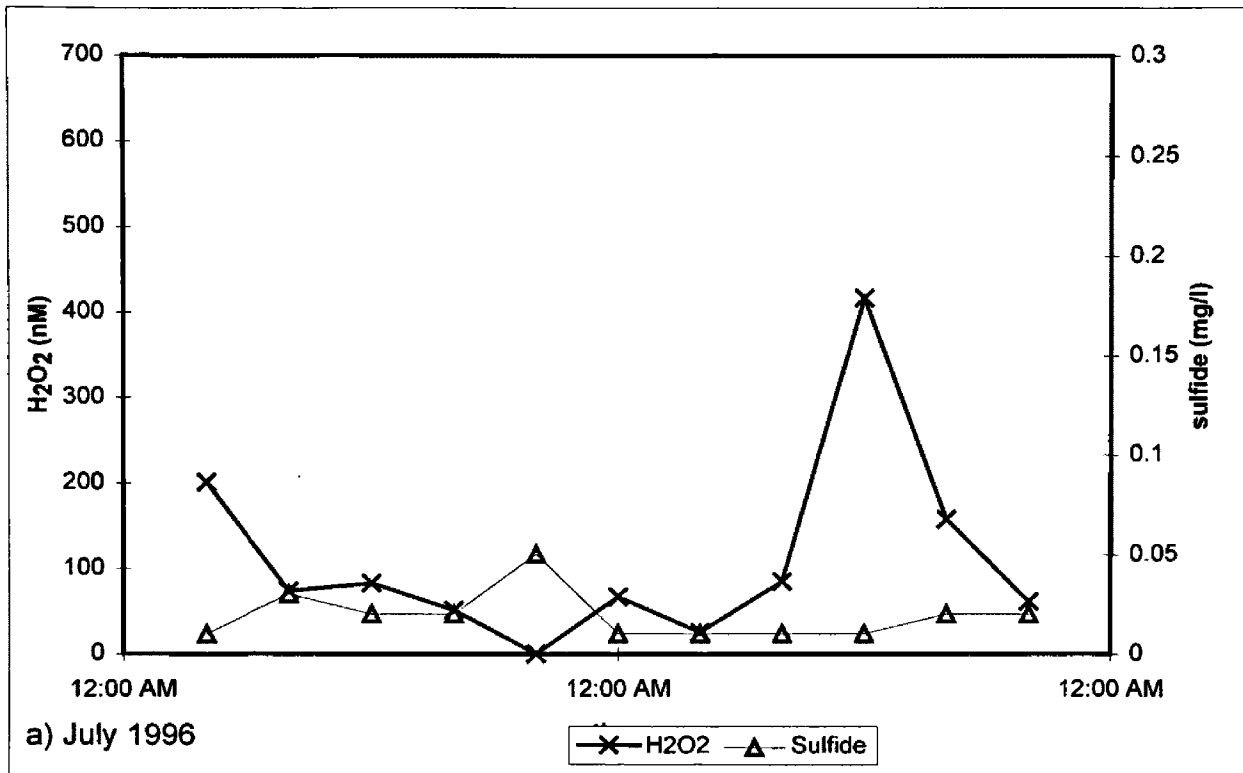
Figure 10: Variations in sulfide and hydrogen peroxide concentrations at the channel at Black Sand Pool, Yellowstone National Park, (a) July 1996 (b) August 1996.

Chocolate Pots

Hydrogen peroxide concentrations ranged from less than 50nM in the early morning to as much as 630nM in the late afternoon with higher concentrations in the channel than in the pool (Figures 11,12). Hydrogen peroxide concentrations at both sites were higher in August than in July despite overcast skies in August. In contrast, average DO and sulfide concentrations were lower at both sites in August than in July. DOC concentrations in the pool were higher in July than in August while DOC concentrations in the channel were higher in August than in July (Table 13). Total dissolved iron was not detected by Ferrozine analysis in the channel but it was detected in the pool where concentrations were higher in August than in July (Table 13).

Hydrogen peroxide concentrations cycled with greater amplitude in August than in July (Figures 13,14). In the pool, the hydrogen peroxide cycle preceded the DO cycle by 4-8 hours. In the channel, the hydrogen peroxide cycle lagged the DO cycle by 4-8 hours. There was a positive correlation ($r^2 = 0.68$, n=11) between hydrogen peroxide and DO concentrations in the pool but no correlation ($r^2 = -0.20$, n=11) between hydrogen peroxide and DO concentrations in the channel. While sulfide cycling was not observed at either site (Figures 15,16), there was a negative correlation ($r^2 = -0.64$, n=21) between hydrogen peroxide and sulfide concentrations in the pool but no correlation ($r^2 = 0.21$, n=21) between hydrogen peroxide and sulfide concentrations in the channel. In the pool, there was a negative correlation ($r^2 = -0.63$, n=21) between hydrogen peroxide and total dissolved iron concentrations but a positive correlation ($r^2 = 0.58$, n=21) between hydrogen peroxide and relative ferrous iron concentrations (Figure 17).
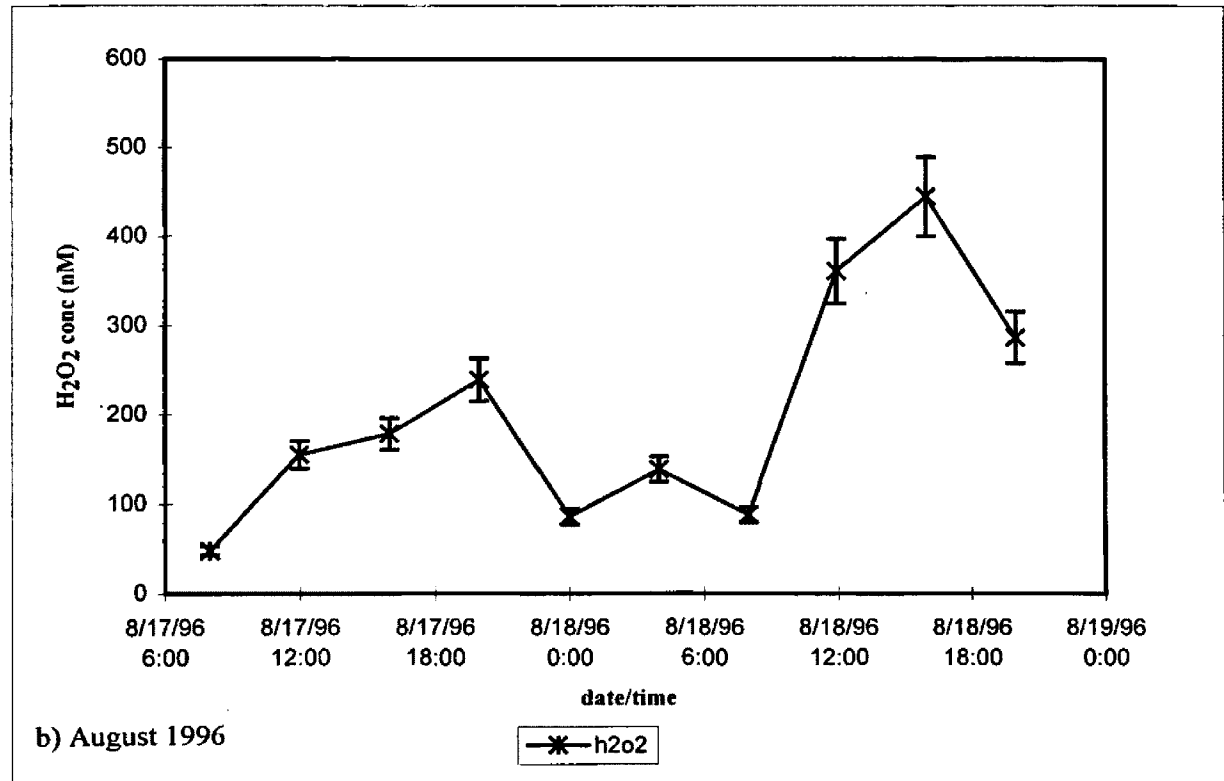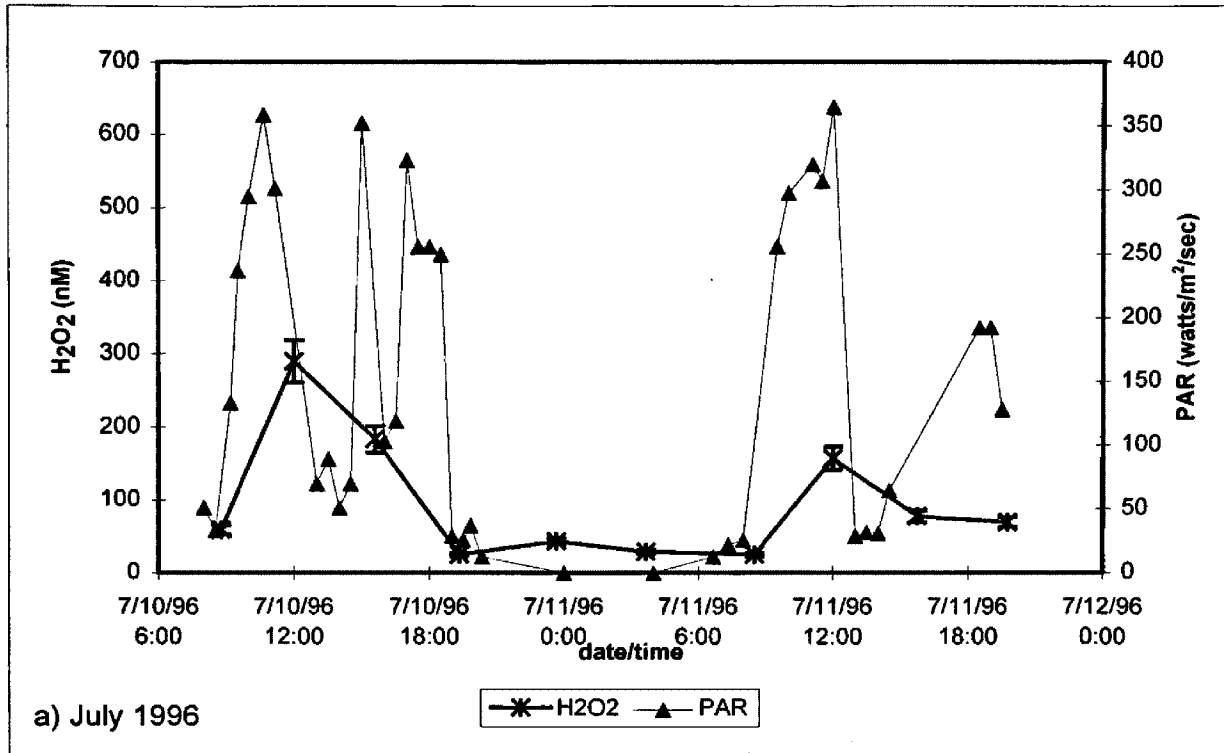
Figure 11: Diel variations in hydrogen peroxide concentrations and photosynthetical active radiation (PAR) at the pool at Chocolate Pots, Yellowstone National Park a) July 1996, b) August 1996: PAR was not measured. UVB ~0.31% PAR, UVA ~6.12% PAR.
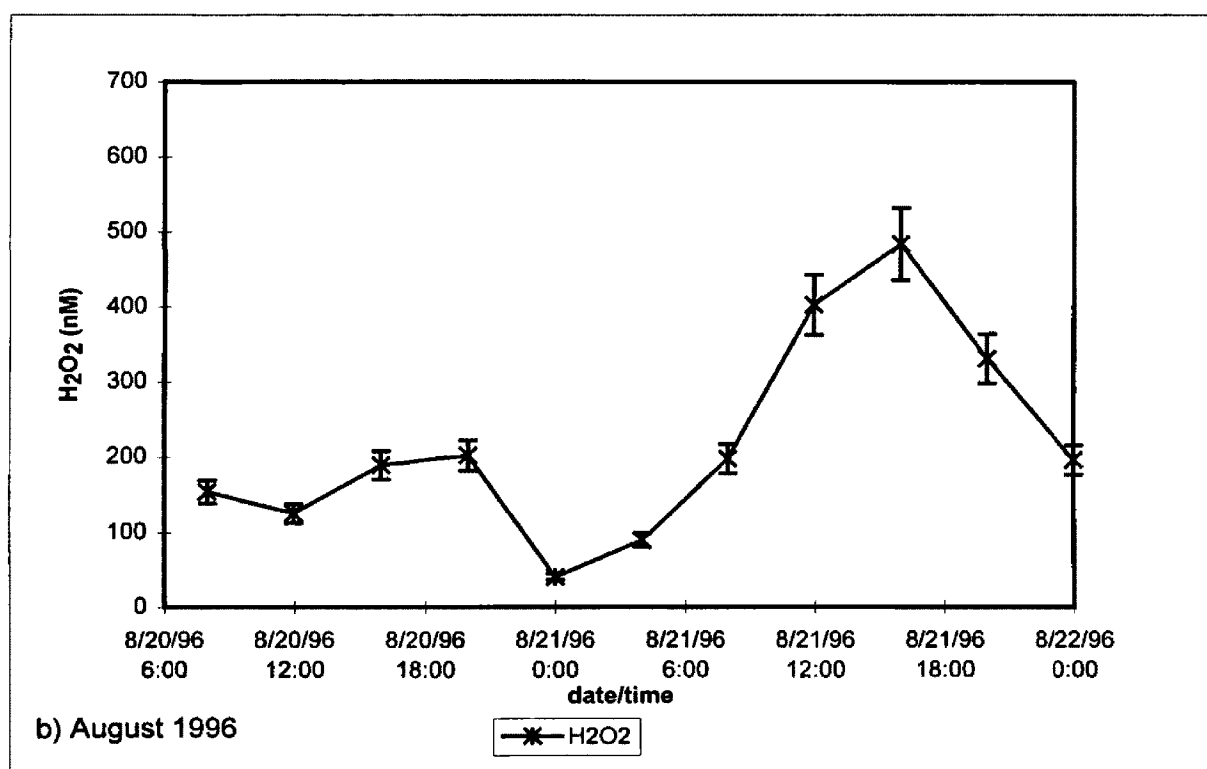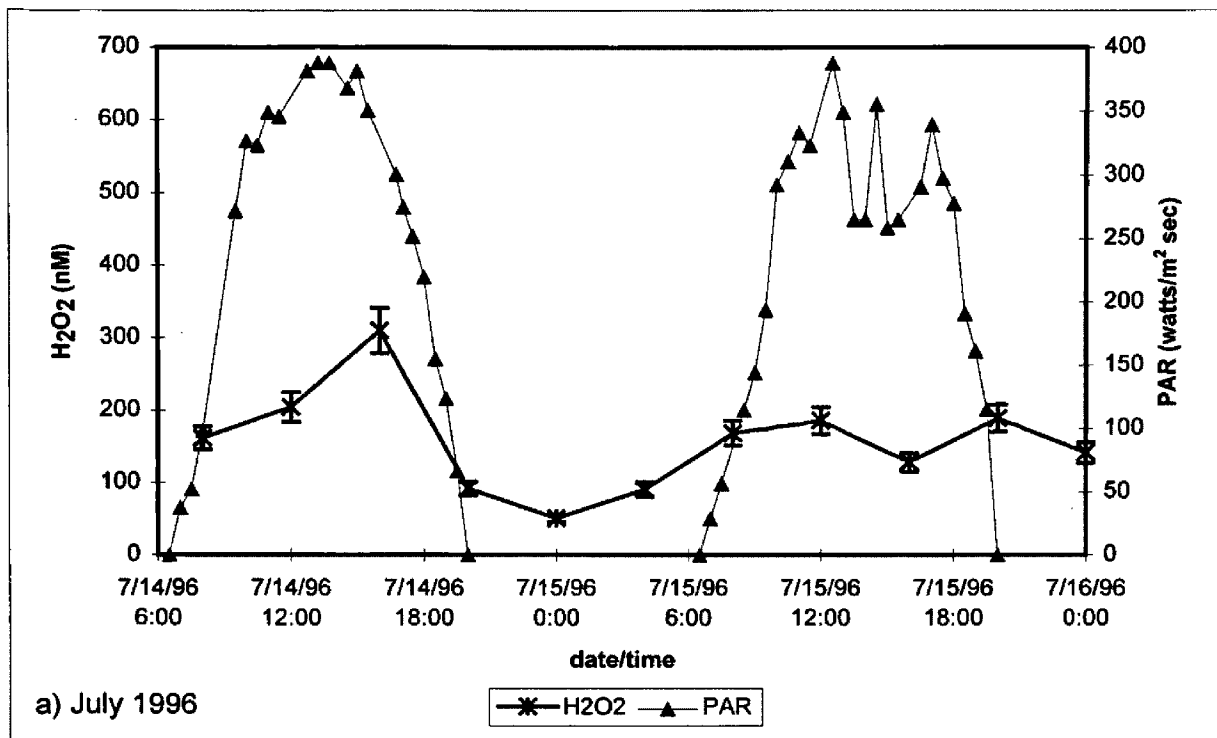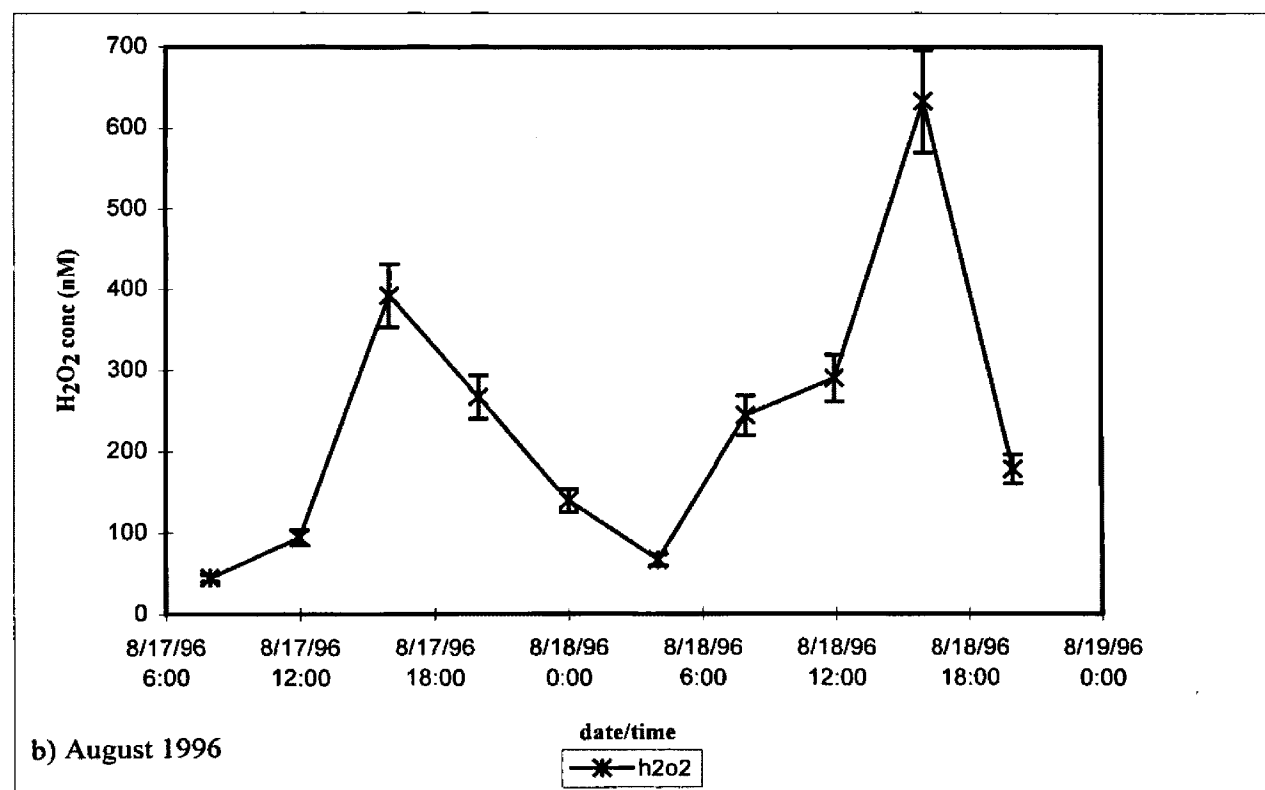
Figure 12: Diel variations in hydrogen peroxide concentrations and photosynthetically active radiation (PAR) at the channel at Chocolate Pots, Yellowstone National Park a) July 1996, b) August 1996: PAR was not measured. UVB ~0.31% PAR, UVA ~6.12% PAR.

Figure 13: Variations in dissolved organic carbon (DOC), dissolved oxygen (DO), and hydrogen peroxide concentrations at the pool at Chocolate Pots, Yellowstone National Park, a) July 1996, b) August 1996. DO was not monitored in August.

a) July 1996
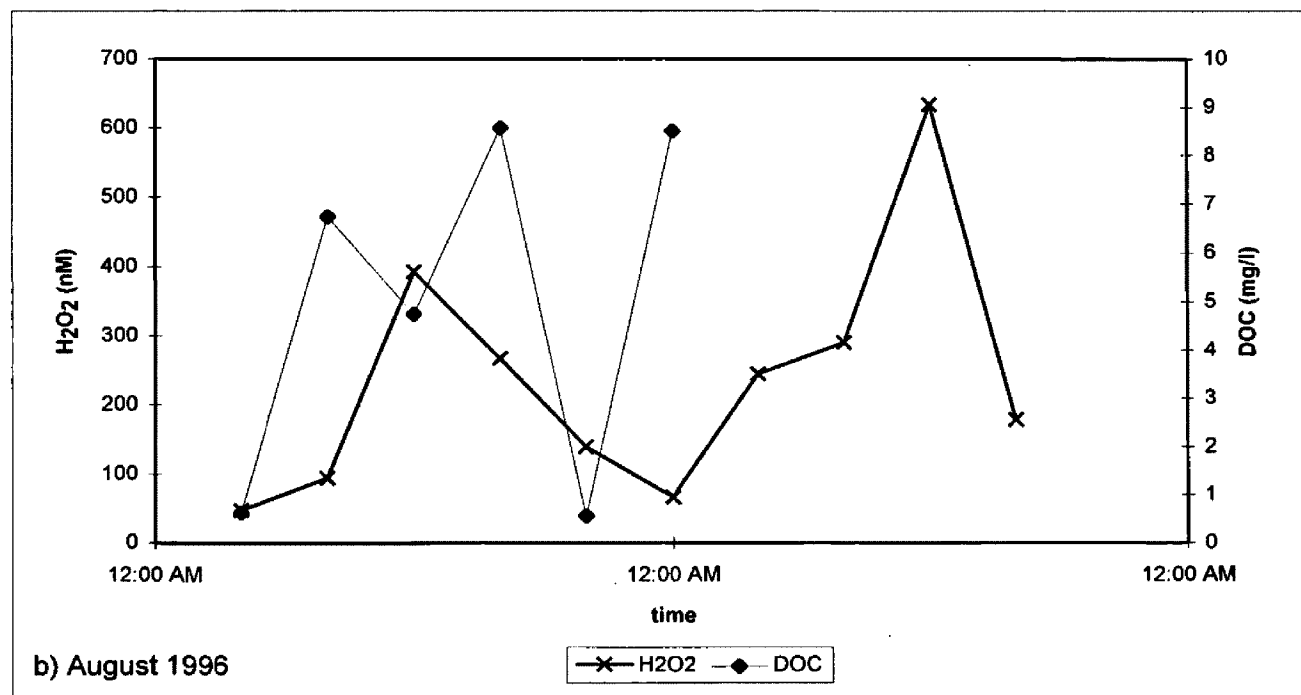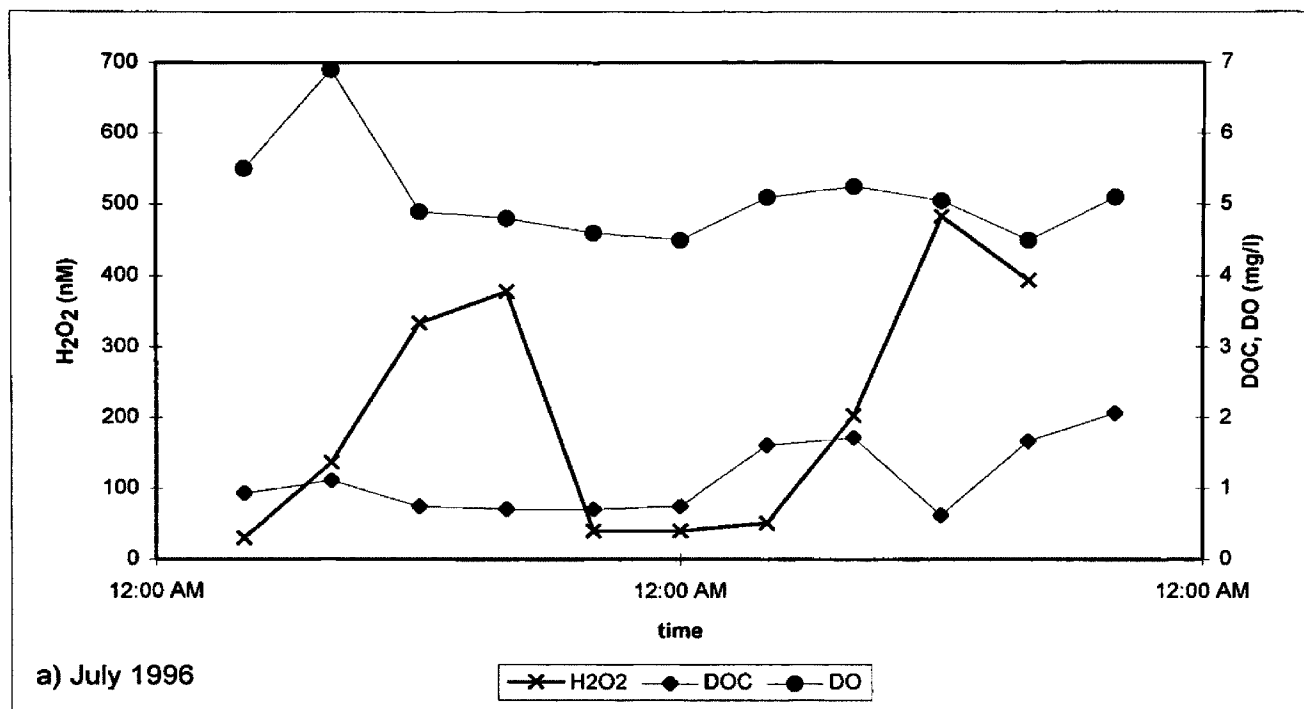
b) August 1996

Figure 14: Variations in dissolved organic carbon (DOC), dissolved oxygen (DO), and hydrogen peroxide concentrations at the channel at Chocolate Pots, Yellowstone National Park a) July 1996, b) August 1996. DO was not monitored in August.
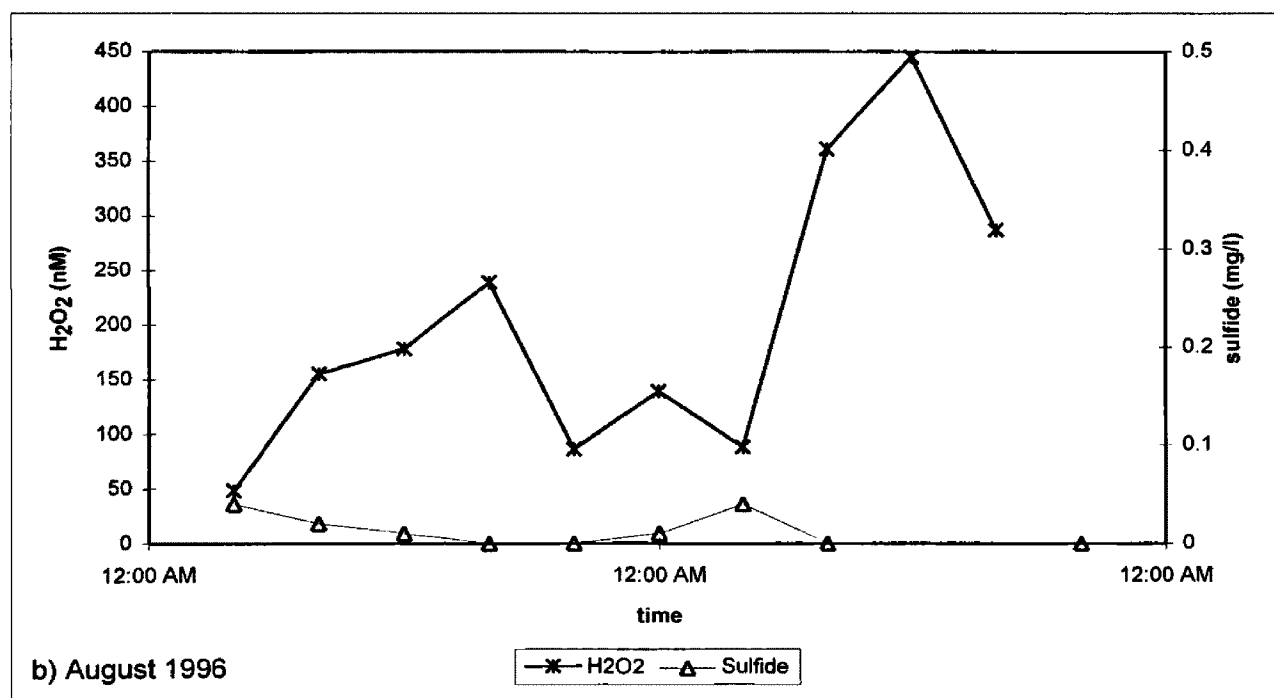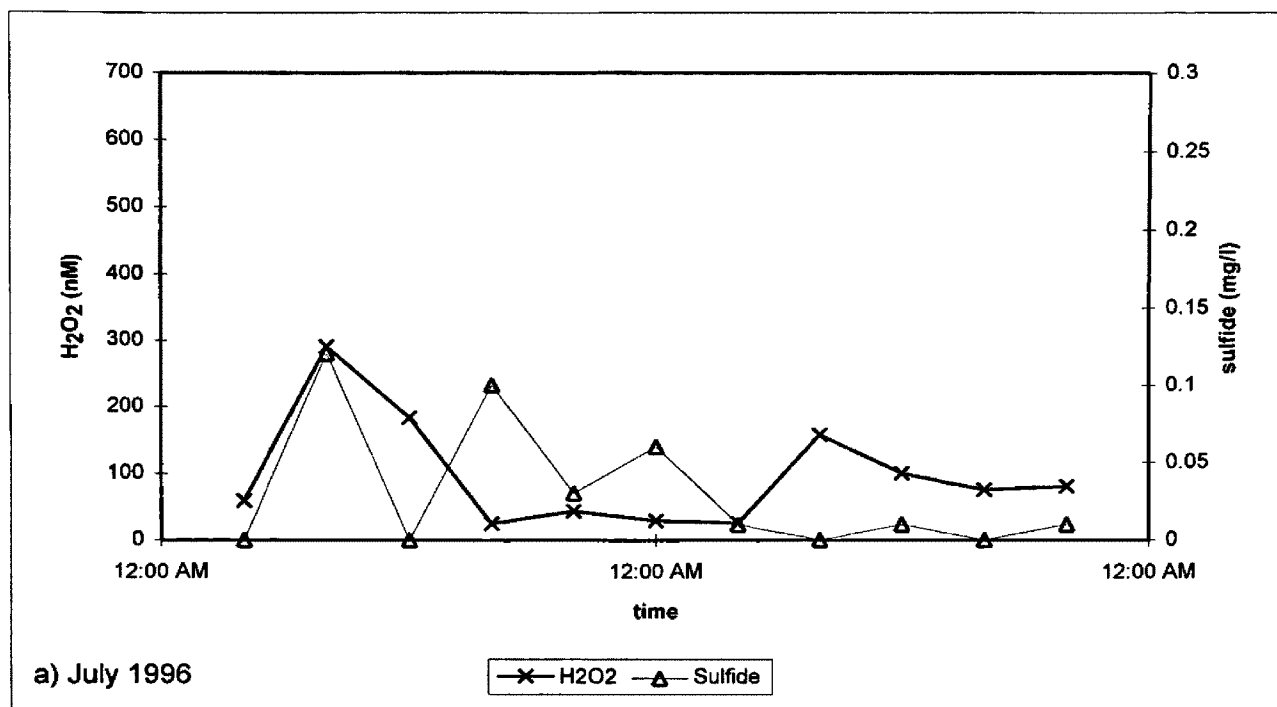
Figure 15: Variations in sulfide and hydrogen peroxide concentrations at the pool at Chocolate Pots, Yellowstone National Park (a) July 1996 (b) August 1996.
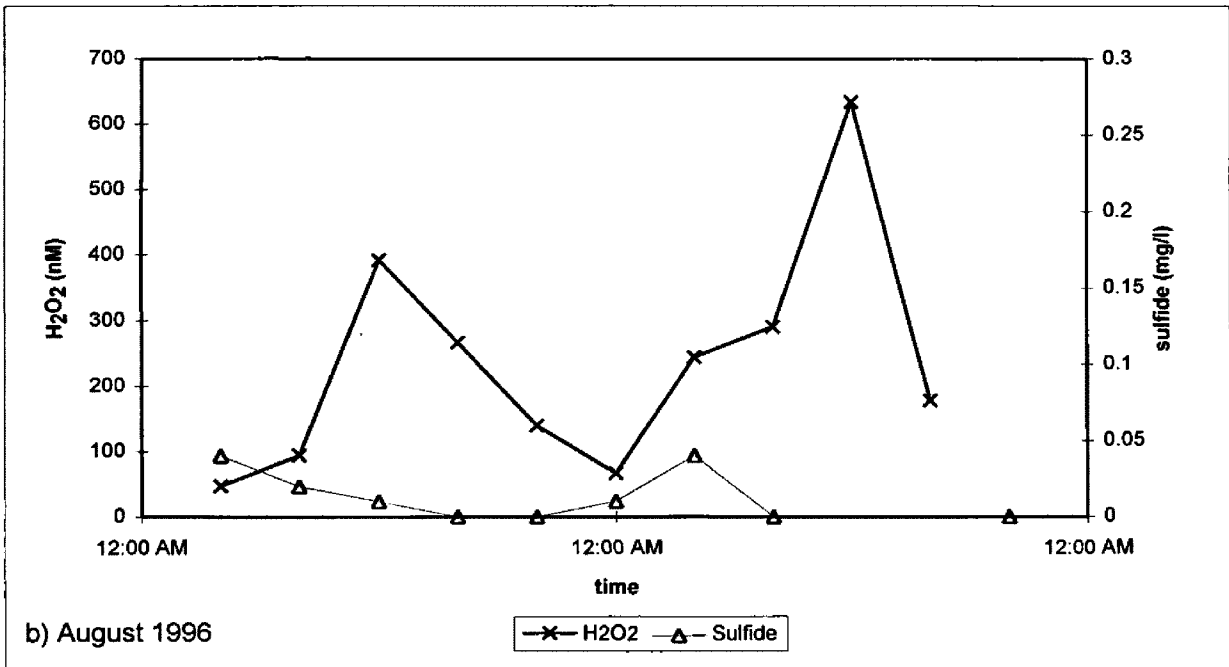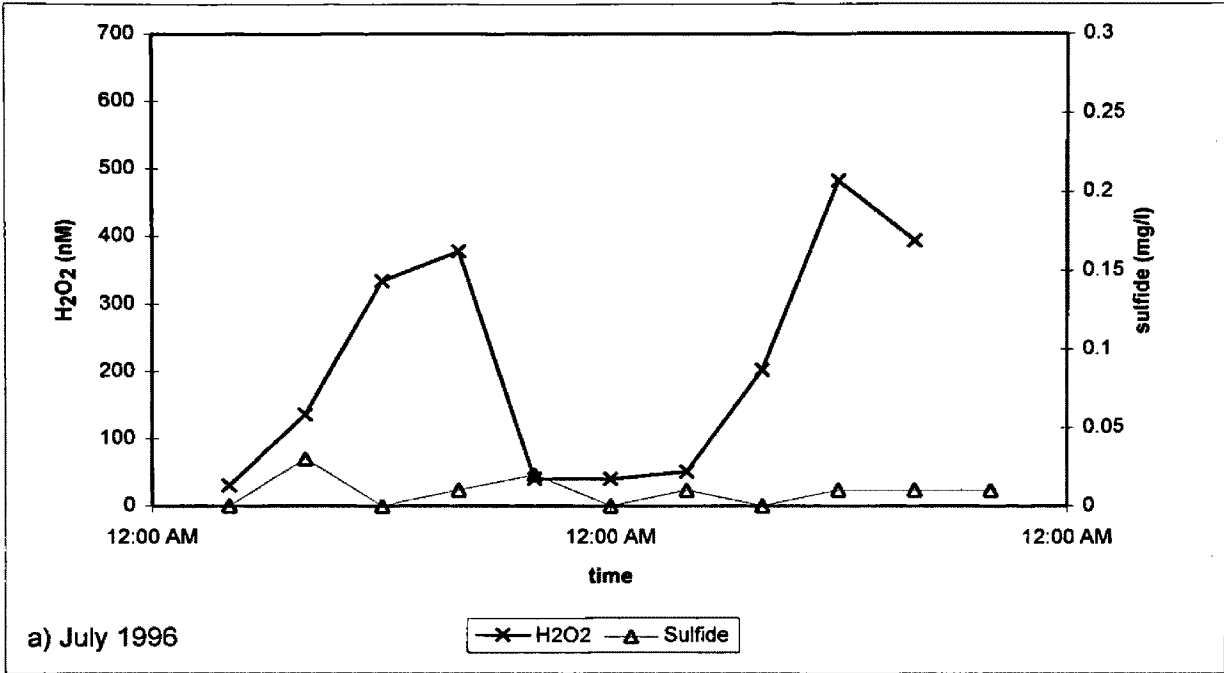
Figure 16: Variations in sulfide and hydrogen peroxide concentrations at the channel at Chocolate Pots, Yellowstone National Park (a) July 1996 (b) August 1996.

Figure 17: Diel variations in hydrogen peroxide, total soluble, ferrous and ferric iron concentrations at the Chocolate Pots pool, Yellowstone National Park.
a) July 1996, b) August 1996

c) July 1996

d) August 1996

Figure 17 cont: Diel variations in hydrogen peroxide, ferrous and ferric iron as percent total iron at the Chocolate Pots pool, Yellowstone National Park. c) July 1996, d) August 1996

Table 13: Chocolate Pots component concentrations (DOC in mg/l, sulfide, H_2O_2, iron, and oxygen in µM,)				
	July		August	
	Pool	Channel	Pool	channel
H_2O_2 ave	0.113	0.209	0.203	0.235
Min	<0.025	0.040	0.086	0.066
Max	0.290	0.483	0.445	0.633
Amplitude	0.180	0.290	0.275	0.370
DOC ave	2.27	1.15	0.9	4.95
S^{-2} ave	0.86	0.32	0.32	0.32
Min	<0.32	<0.32	<0.32	<0.32
Max	3.43	0.86	1.14	1.14
Amplitude	1.50	0.54	0.80	0.60
DO ave	17.8	160	<6.0	143
Min	<6.0	140	<6.0	141
Max	73.4	215	<6.0	147
Amplitude	37.5	42.0	-	-
Fe total (ferrozine)	142	-	174	-
Min	115	-	150	-
Max	167	-	188	-
Amplitude	52	-	33	-
Fe total (ICP)	99.7	33.9	107	27.6

Nymph Lake

Hydrogen peroxide concentrations ranged from less than 50nM in the early morning to 500nM in the late afternoon. Hydrogen peroxide concentrations were higher in July than in August and coincided with higher PAR levels in July (Figures 18,19). Average sulfide concentrations were similar for the two months with higher concentrations in the pools than in the iron channel. Higher hydrogen peroxide concentrations in the sulfur pool in July coincided with higher DOC concentrations in July. In contrast, average DOC concentrations in the iron pool and channel were higher in August. Higher average DO concentrations were observed in the iron channel in July than in August. Using Ferrozine analysis, total dissolved iron concentrations in the iron pool and channel were higher in July than in August. Iron was not detected in the sulfur pool by Ferrozine analysis.

Hydrogen peroxide concentrations in the sulfur pool and the iron channel cycled with greater amplitude in August whereas hydrogen peroxide concentrations in the iron pool cycled with greater amplitude in July (Figures 18,19). DO concentrations in the iron channel did not cycle (Figure 20). In the iron pool, there was no correlation between hydrogen peroxide and sulfide concentrations (r^2 = -0.44, n=20) (Figures 21-23). Sulfide cycling was not observed in the sulfur pool or the iron channel. In the iron pool and channel, hydrogen peroxide cycled inversely to total dissolved iron cycling (Figures 24, 25). There was a negative correlation between hydrogen peroxide and total dissolved iron in the iron pool channel (r^2 = -0.70, n=20) but no correlation between hydrogen peroxide and total dissolved iron in the channel (r^2 = -0.48, n=20). There was a positive correlation between hydrogen peroxide and relative ferrous iron concentrations in the pool and in the channel (r^2= 0.58, n=20).

| Table 14: Nymph Lake component concentrations (DOC in mg/l, sulfide, H_2O_2, iron, and oxygen in µM,)						
		July			August		
		Sulfur Pool	Iron Pool	Iron channel	Sulfur Pool	Iron Pool	Iron channel
H_2O_2	ave	0.156	0.119	0.198	0.119	0.113	0.152
	min	0.079	0.050	<0.025	0.032	0.027	0.029
	max	0.443	0.381	0.394	0.298	0.244	0.500
	Amplitude	0.230	0.275	0.345	0.250	0.220	0.365
DOC	ave	2.56	1.05	1.13	1.70	3.78	2.75
S^{-2}	ave	4.00	2.00	0.86	3.71	1.71	0.32
	min	2.00	1.71	0.57	2.86	<0.32	<0.32
	max	6.86	3.43	1.43	5.71	3.14	0.32
	Amplitude	4.86	1.72	0.86	2.85	2.82	-
DO	ave	-	-	169	-	-	138
	min	-	-	168	-	-	128
	max	-	-	171	-	-	147
	Amplitude	-	-	3	-	-	19
Fe total (ferrozine)		-	73.5	58.2	-	55.6	42.0
	min	-	52.9	42.4	-	32.0	23.8
	max	-	86.4	65.1	-	73.5	54.4
	amplitude	-	33.5	22.7	-	41.6	30.6
Fe total (ICP)		2.4	53.3	45.6	2.6	42.3	33.1
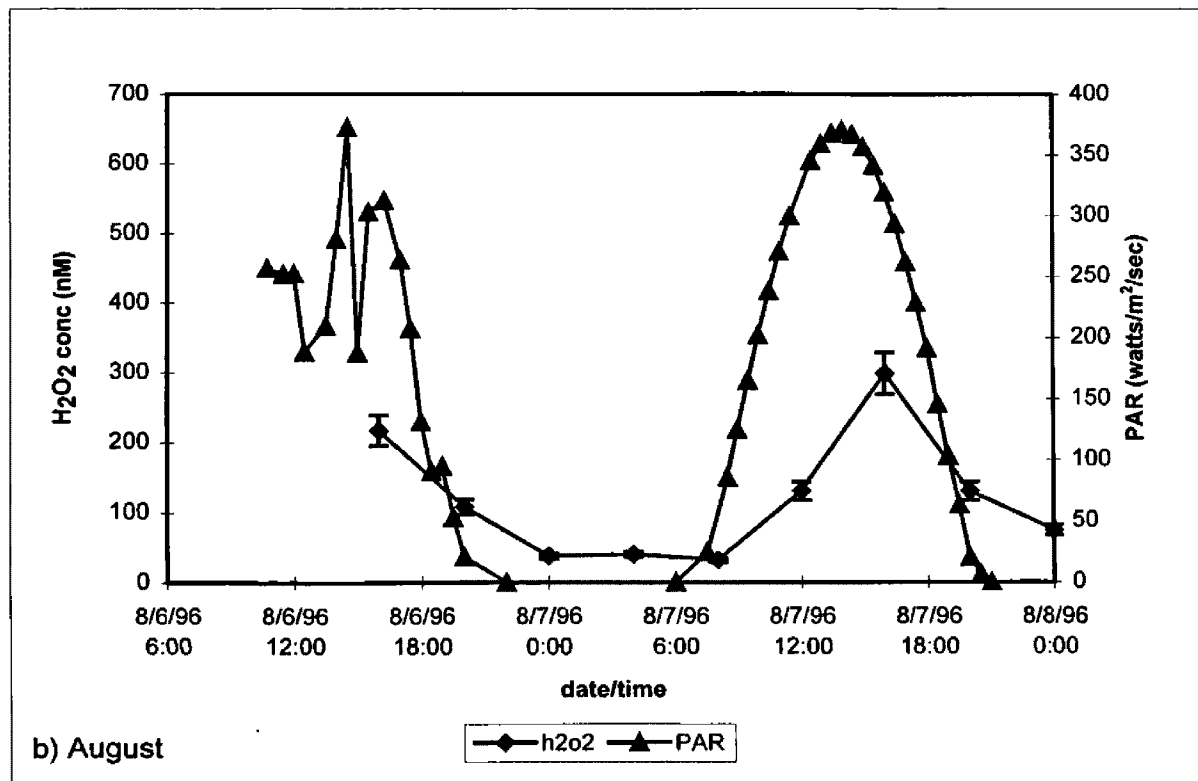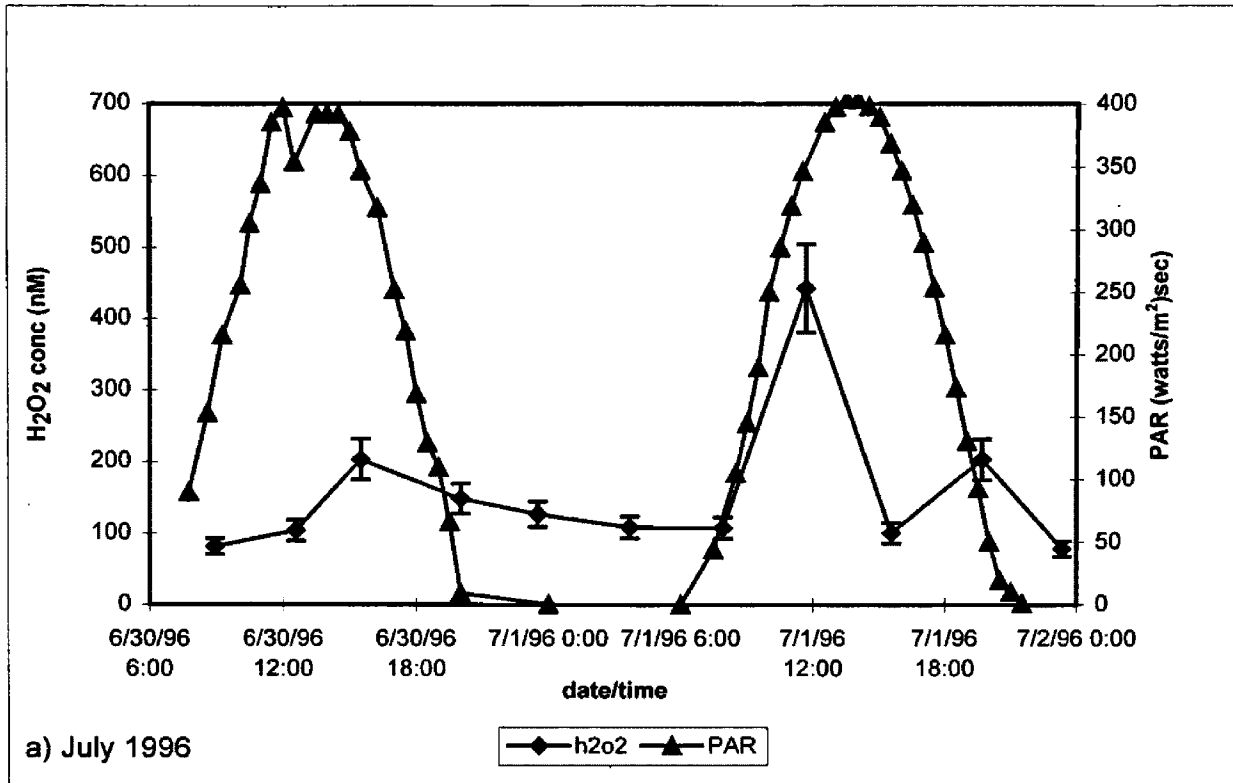
Figure 18: Diel variations in hydrogen peroxide concentrations and photosynthetically active radiation (PAR) at the Nymph Lake-sulfur pool, Yellowstone National Park
a) July 1996, b) August 1996 fluctuating PAR are due to clearing skies.
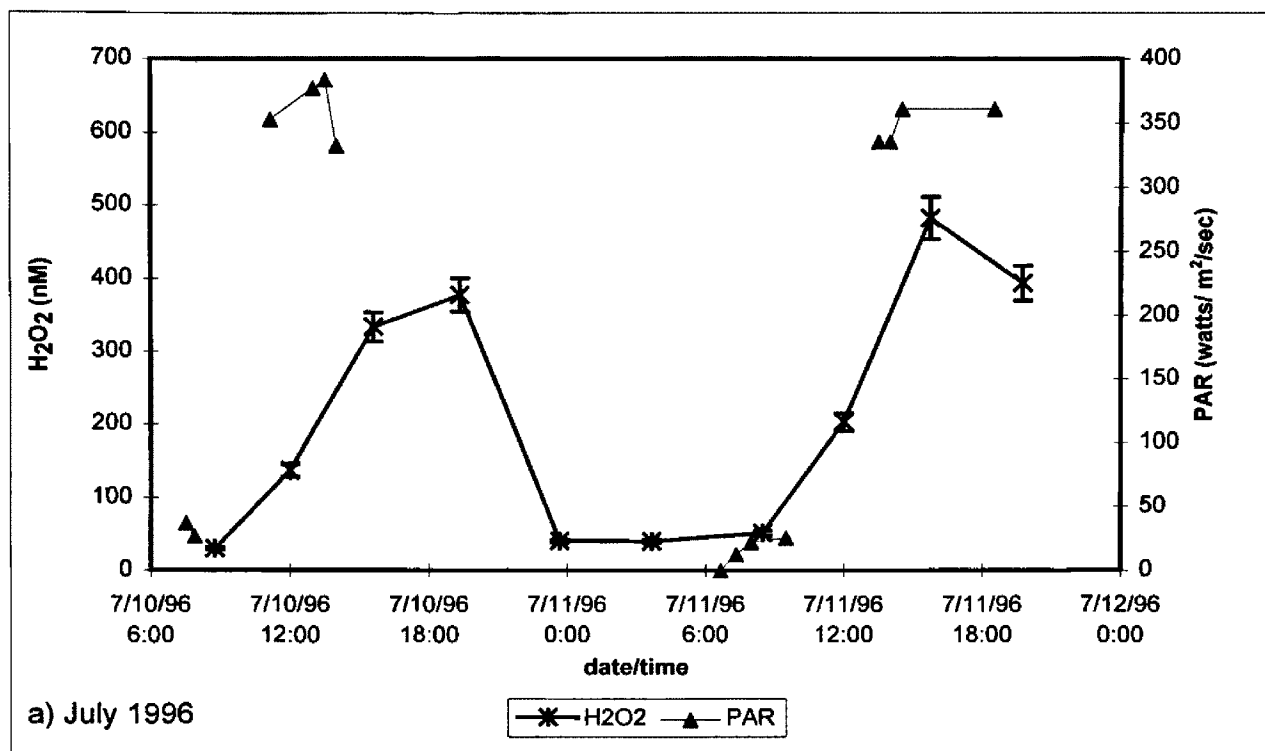UVB ~0.31% PAR, UVA ~6.12% PAR.
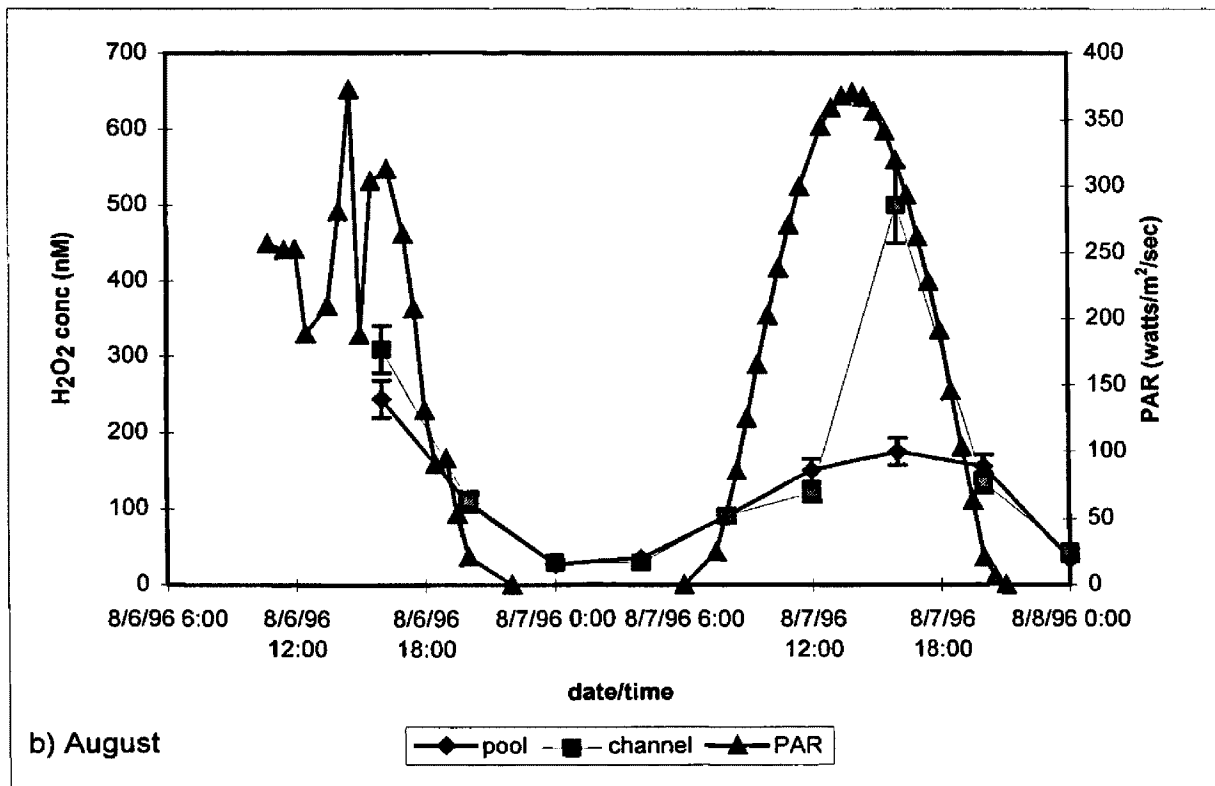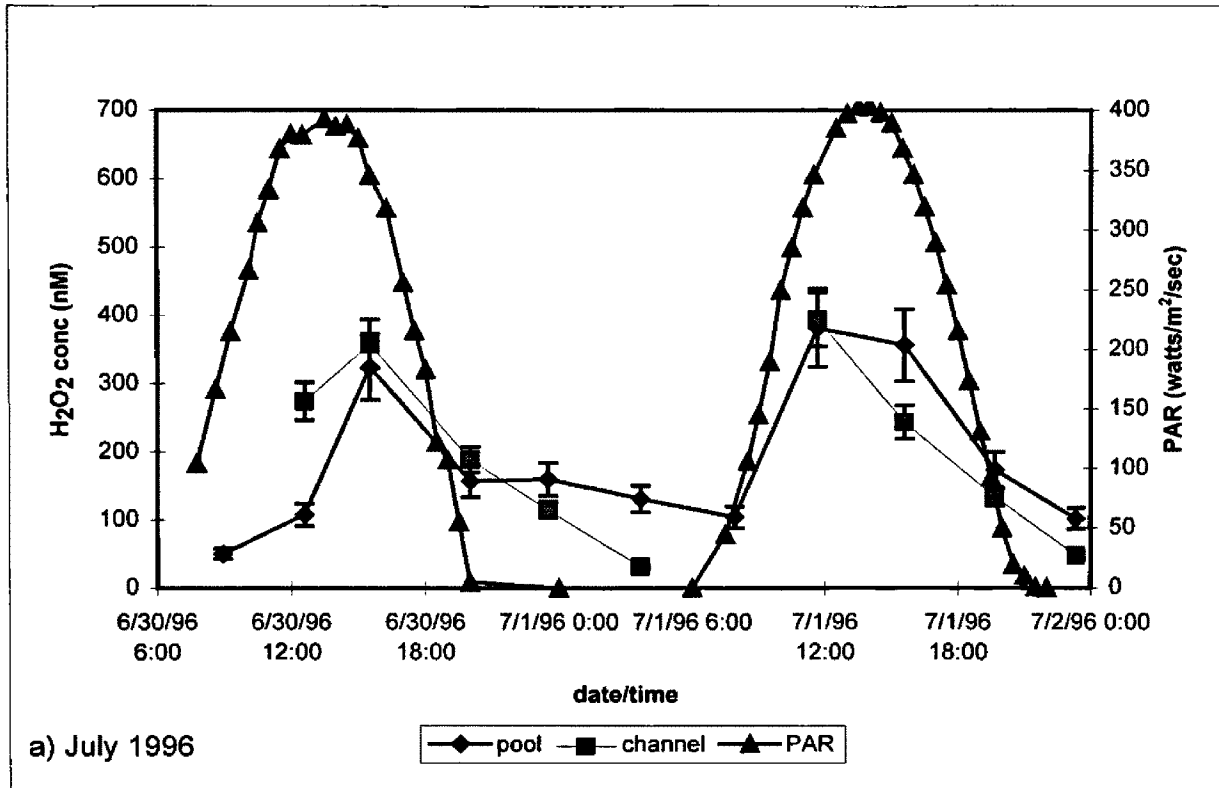
Figure 19: Diel variations in hydrogen peroxide concentrations and photosynthetically active radiation (PAR) at the Nymph Lake-iron spring, Yellowstone National Park a) July 1996, b) August 1996 fluctuating PAR are due to clearing skies.
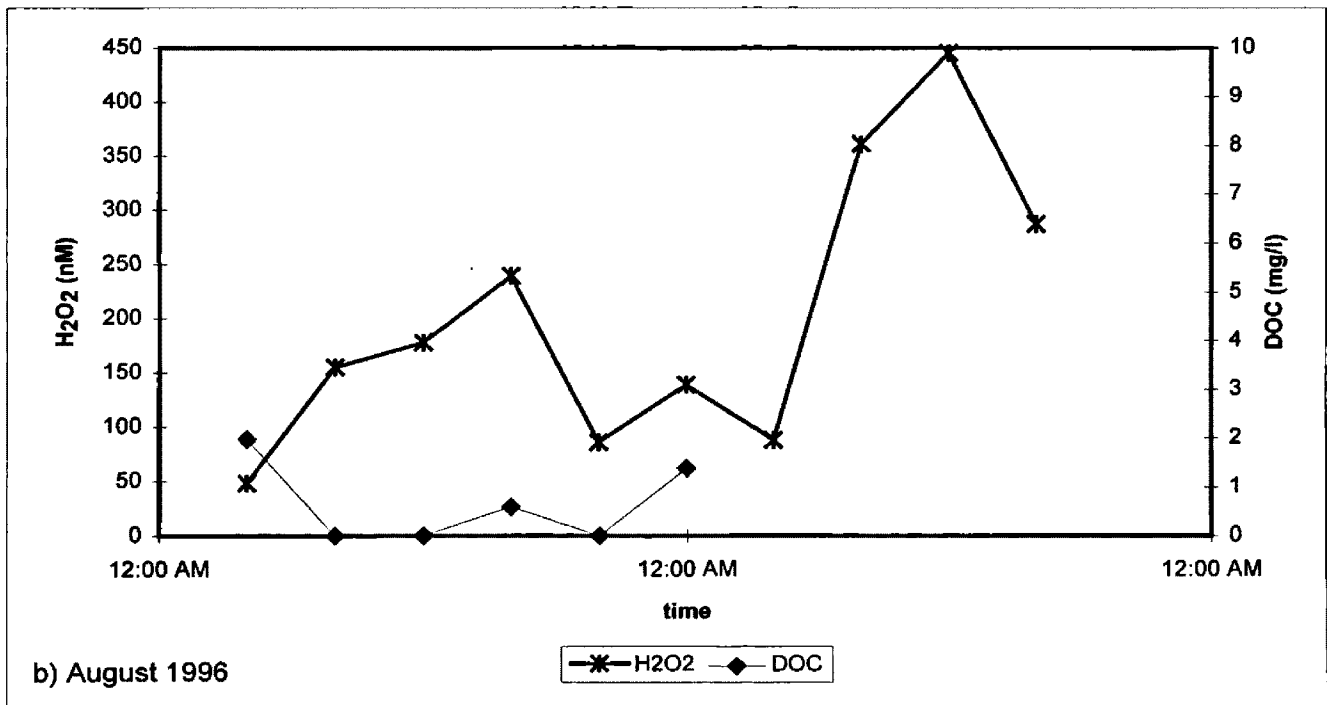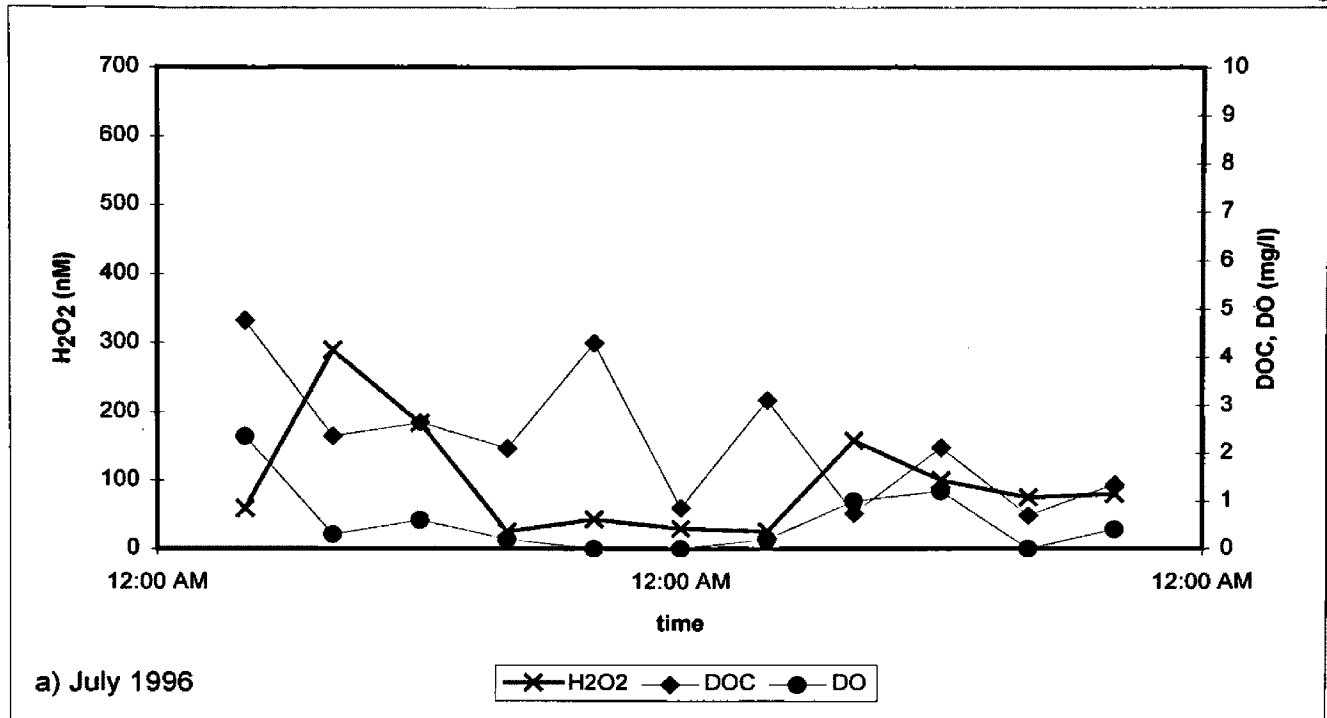UVB ~0.31% PAR, UVA ~6.12% PAR.
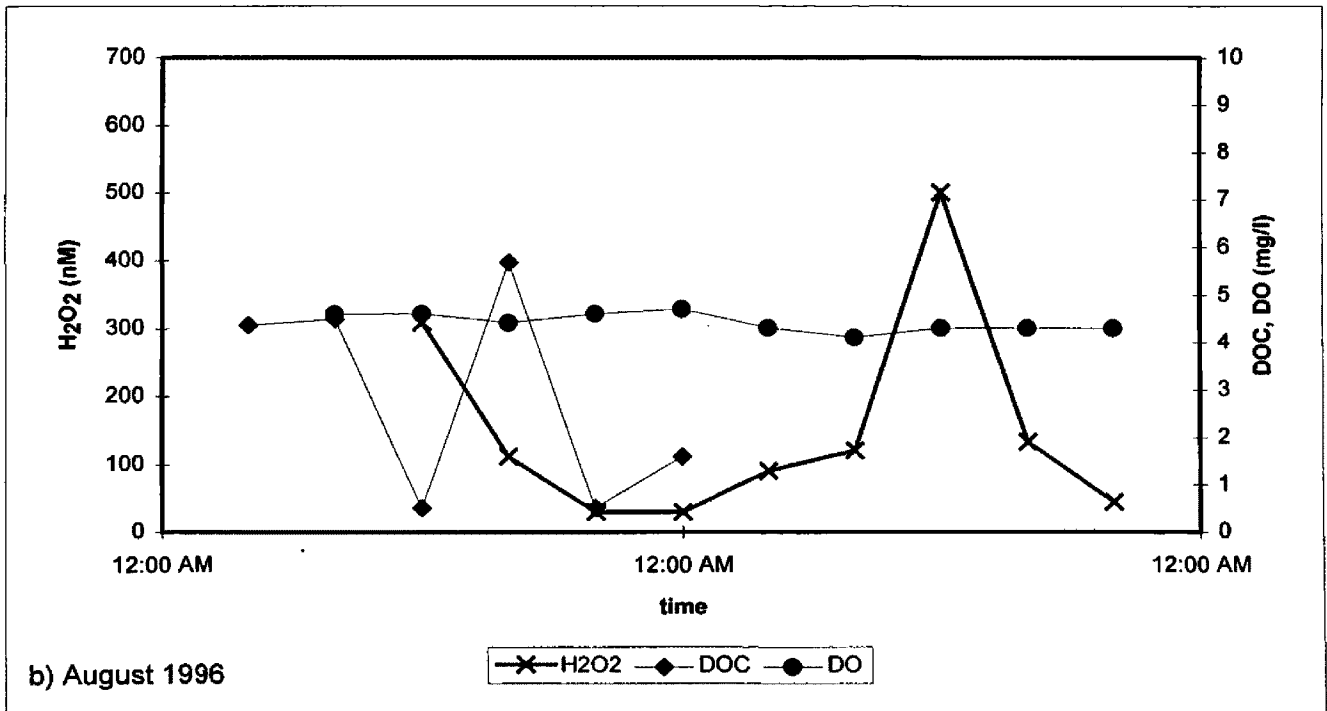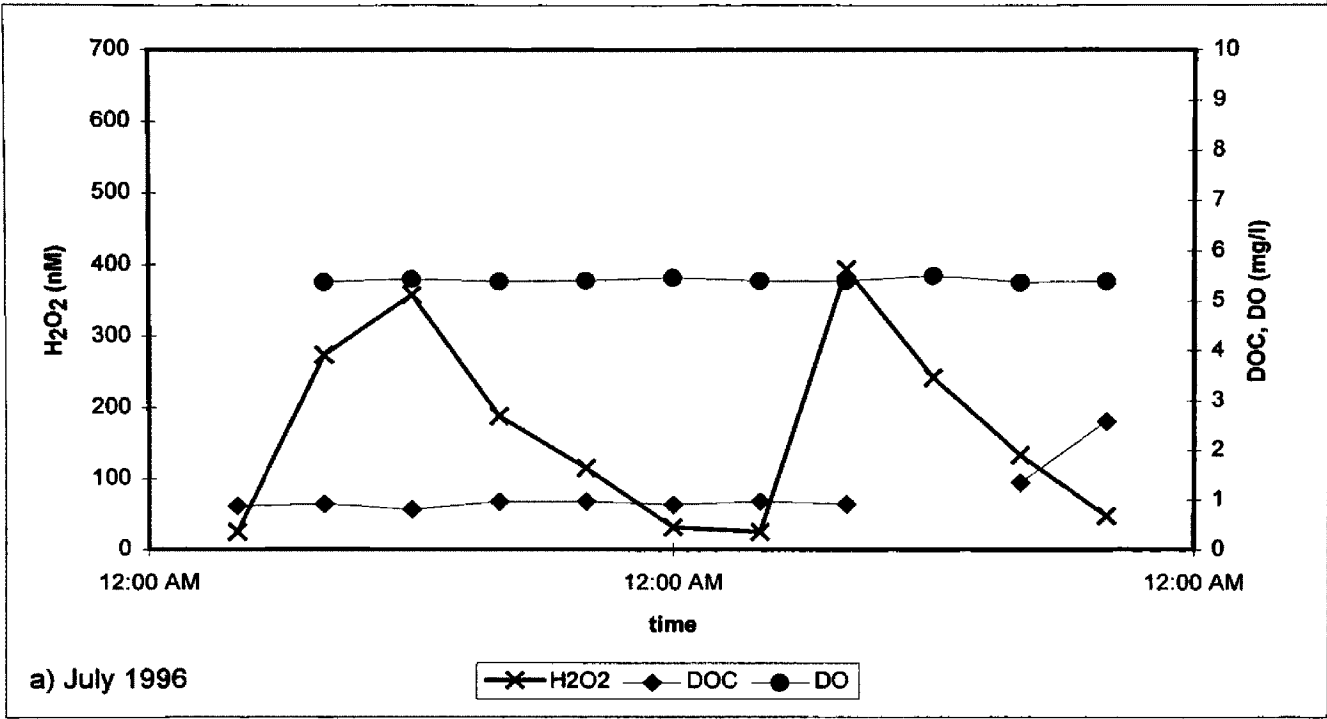
Figure 20: Variations in dissolved organic carbon (DOC), dissolved oxygen (DO), and hydrogen peroxide concentrations at the Nymph Lake-iron channel, Yellowstone National Park a) July 1996, b) August 1996.
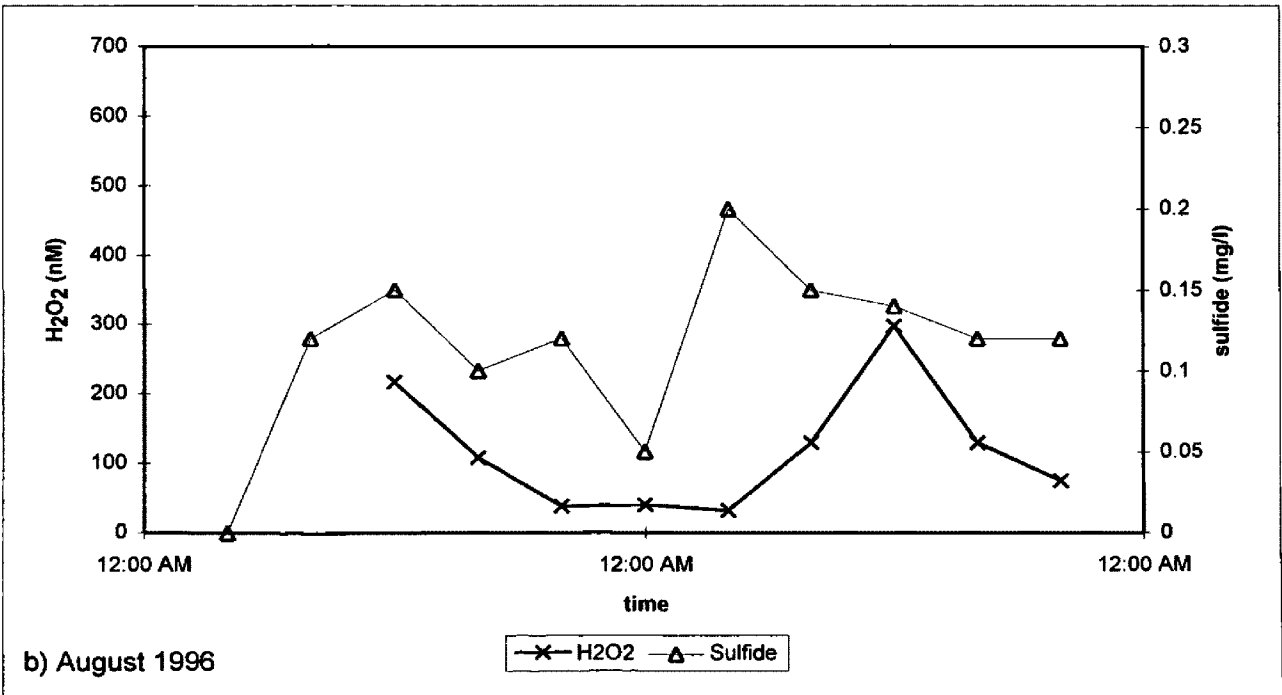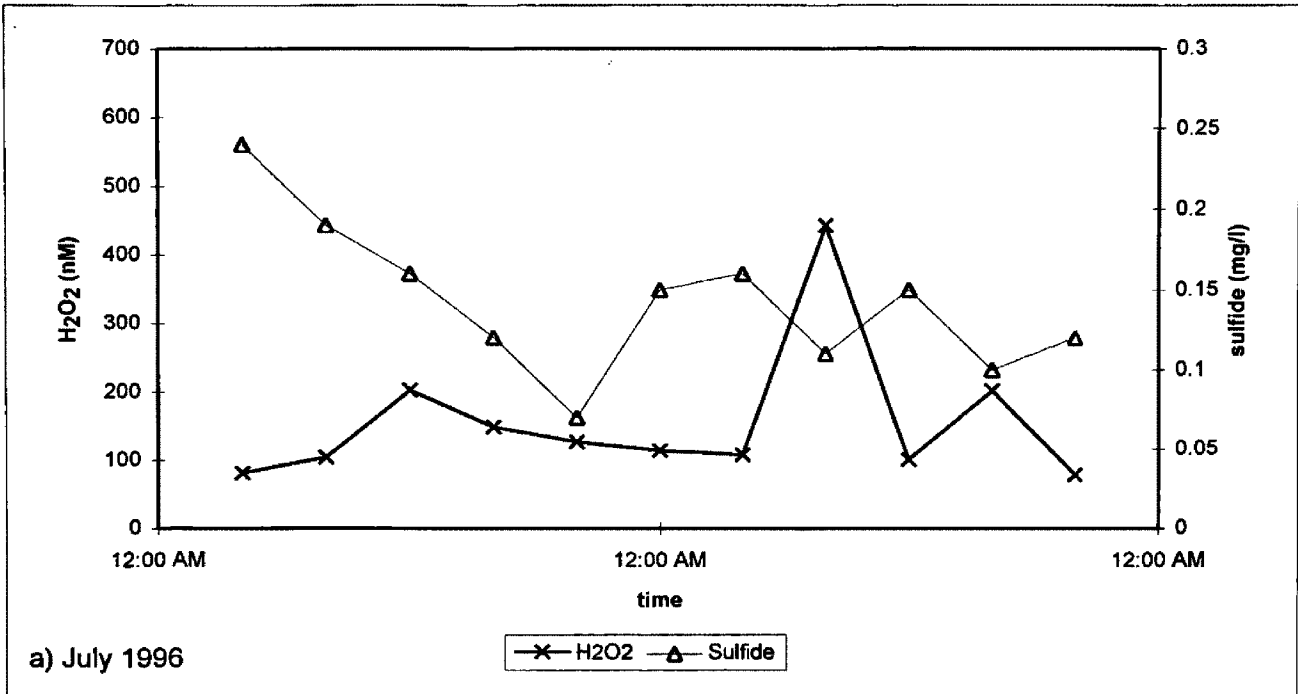
Figure 21: Variations in sulfide and hydrogen peroxide concentrations at the Nymph Lake-sulfur pool, Yellowstone National Park (a) July 1996 (b) August 1996.
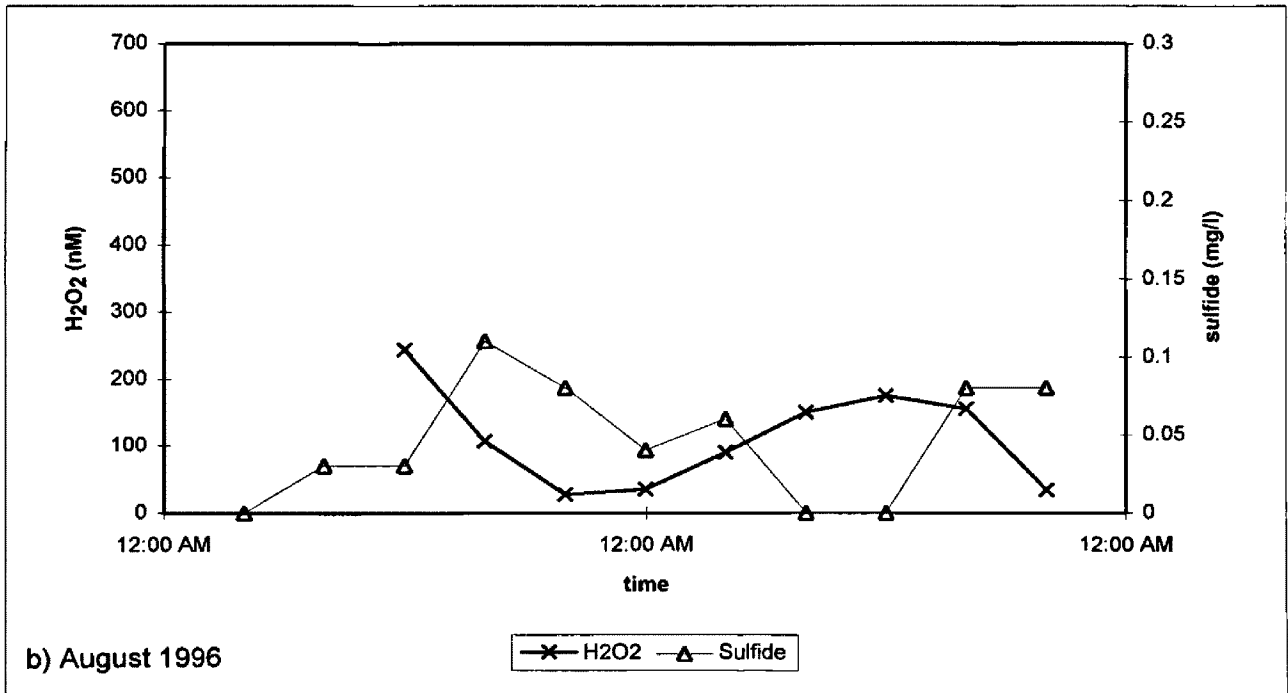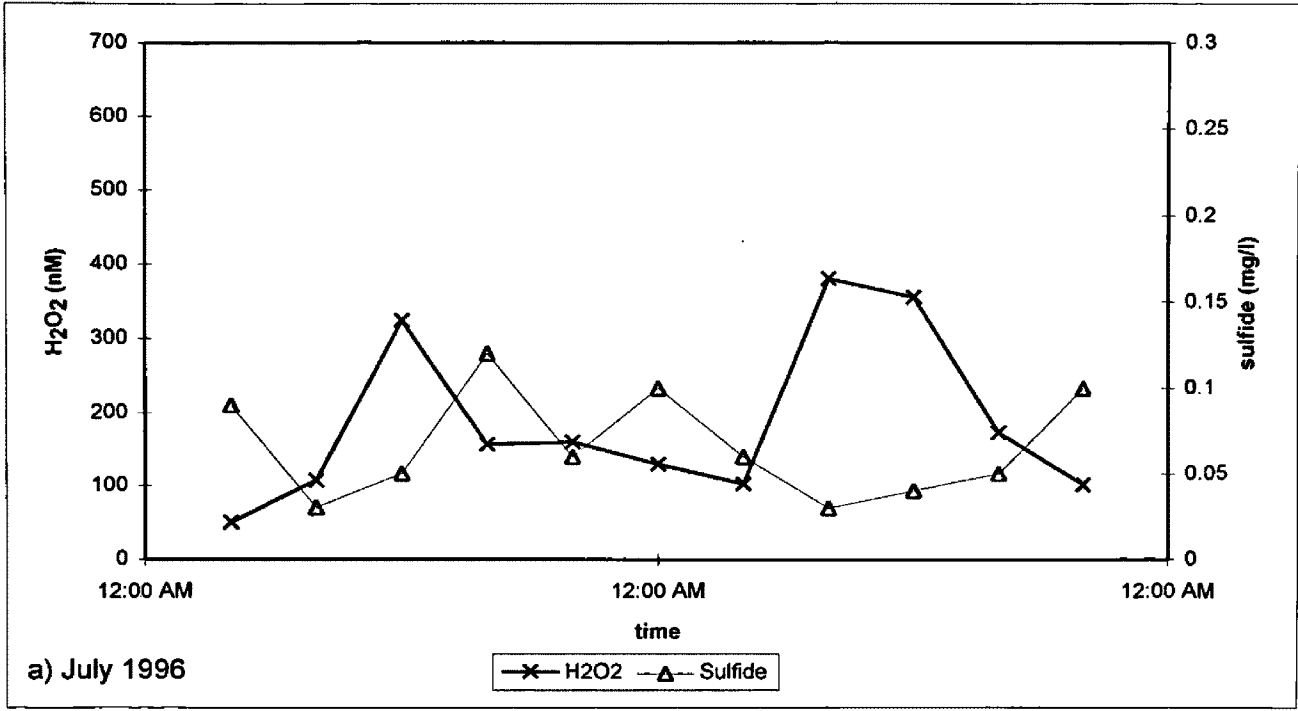
Figure 22: Variations in sulfide and hydrogen peroxide concentrations at the Nymph Lake-iron pool, Yellowstone National Park (a) July 1996 (b) August 1996.
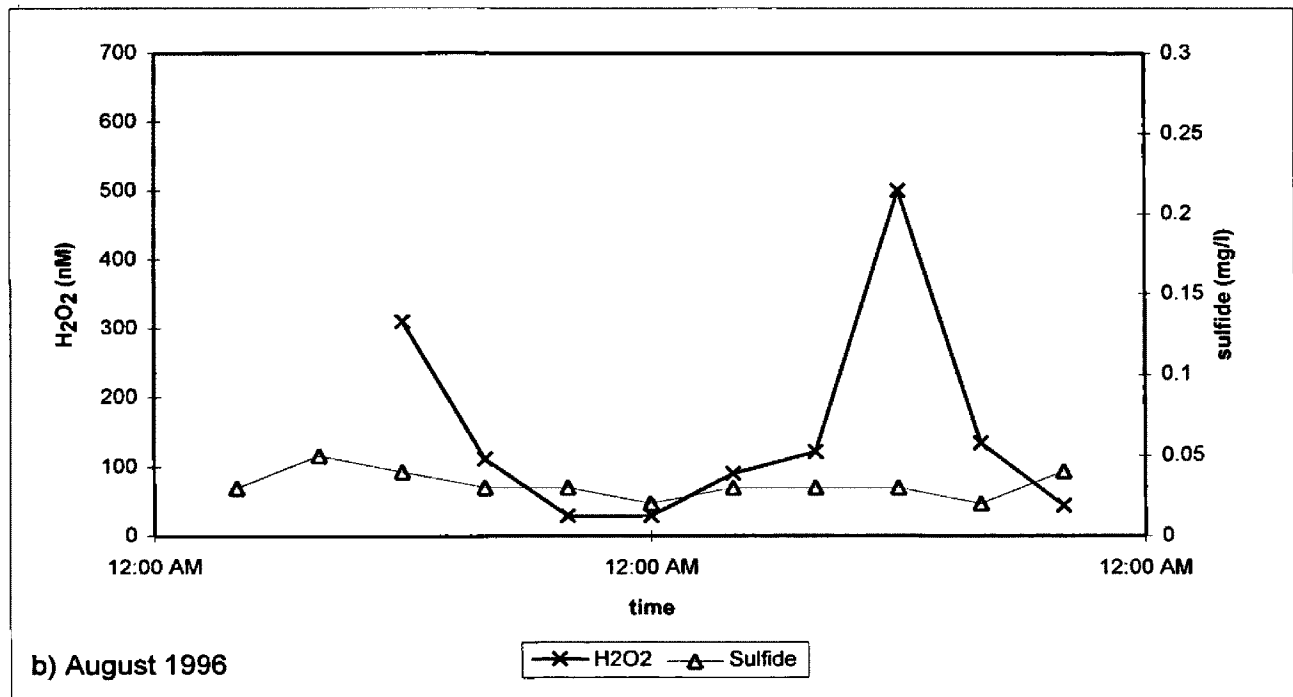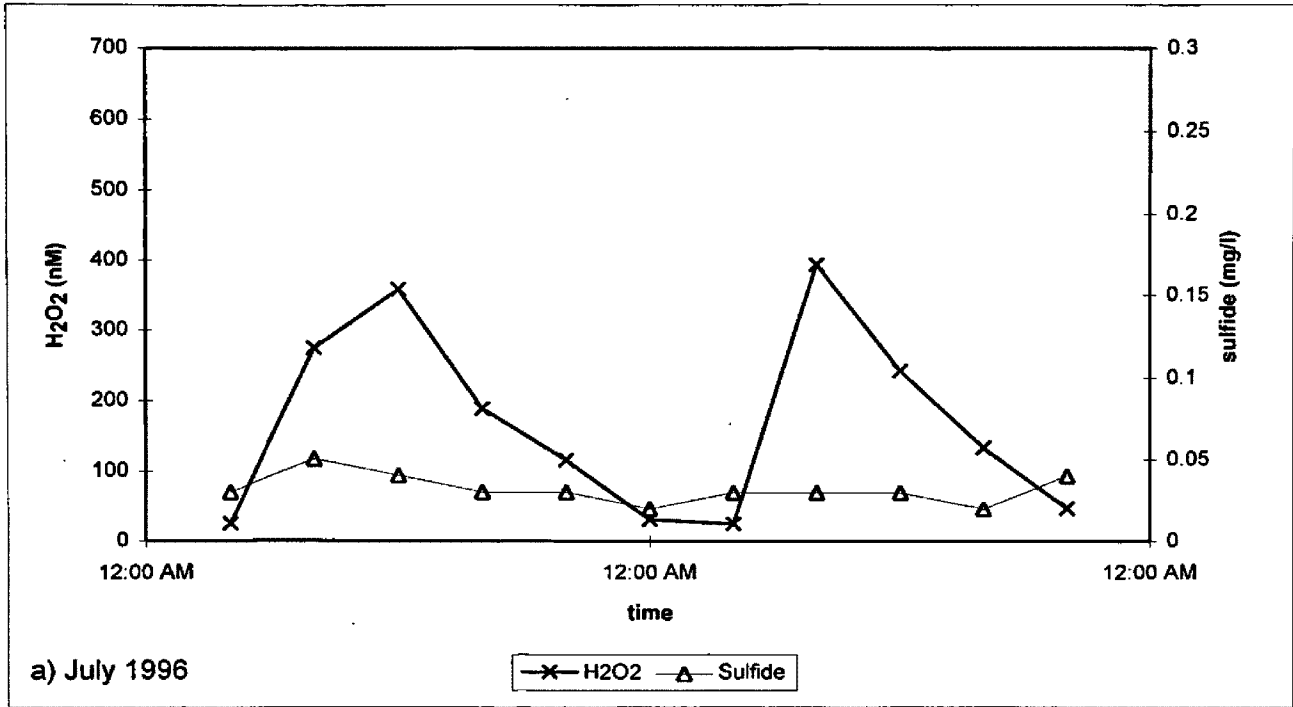
Figure 23: Variations in sulfide and hydrogen peroxide concentrations at the Nymph Lake-iron channel, Yellowstone National Park (a) July 1996 (b) August 1996.
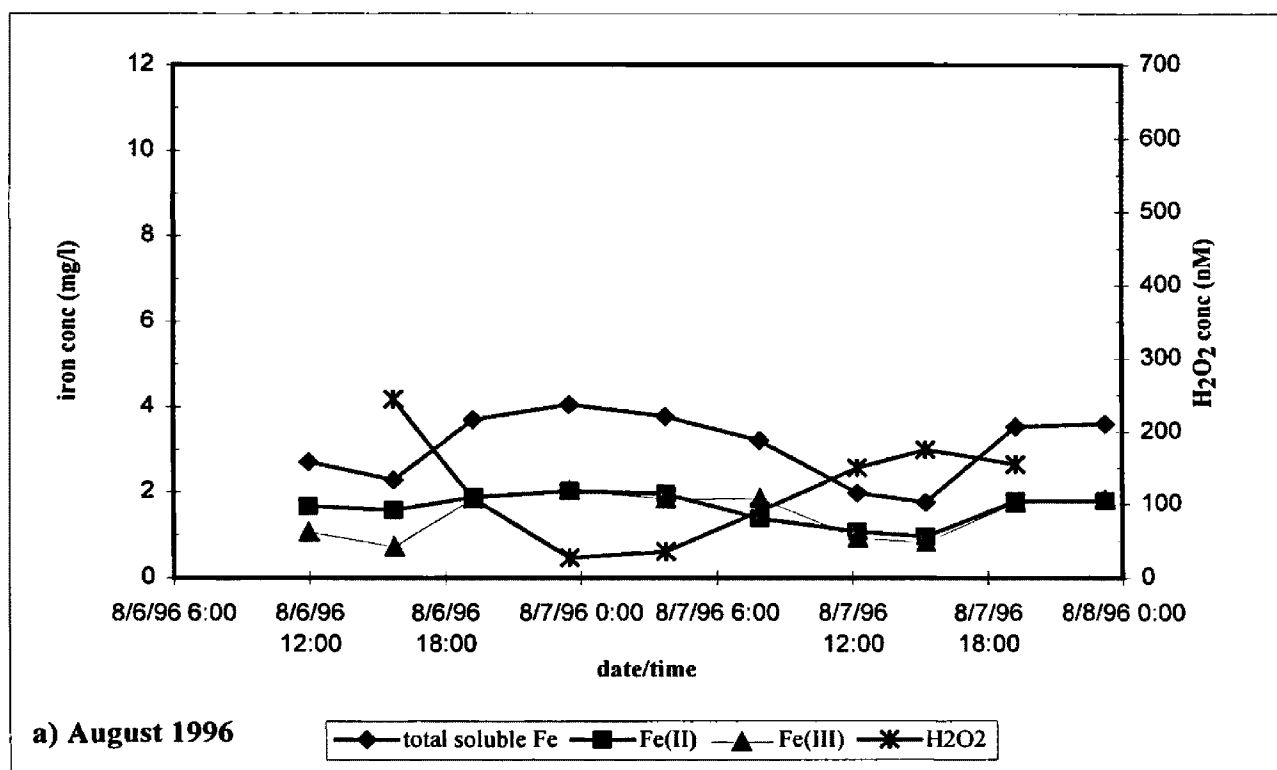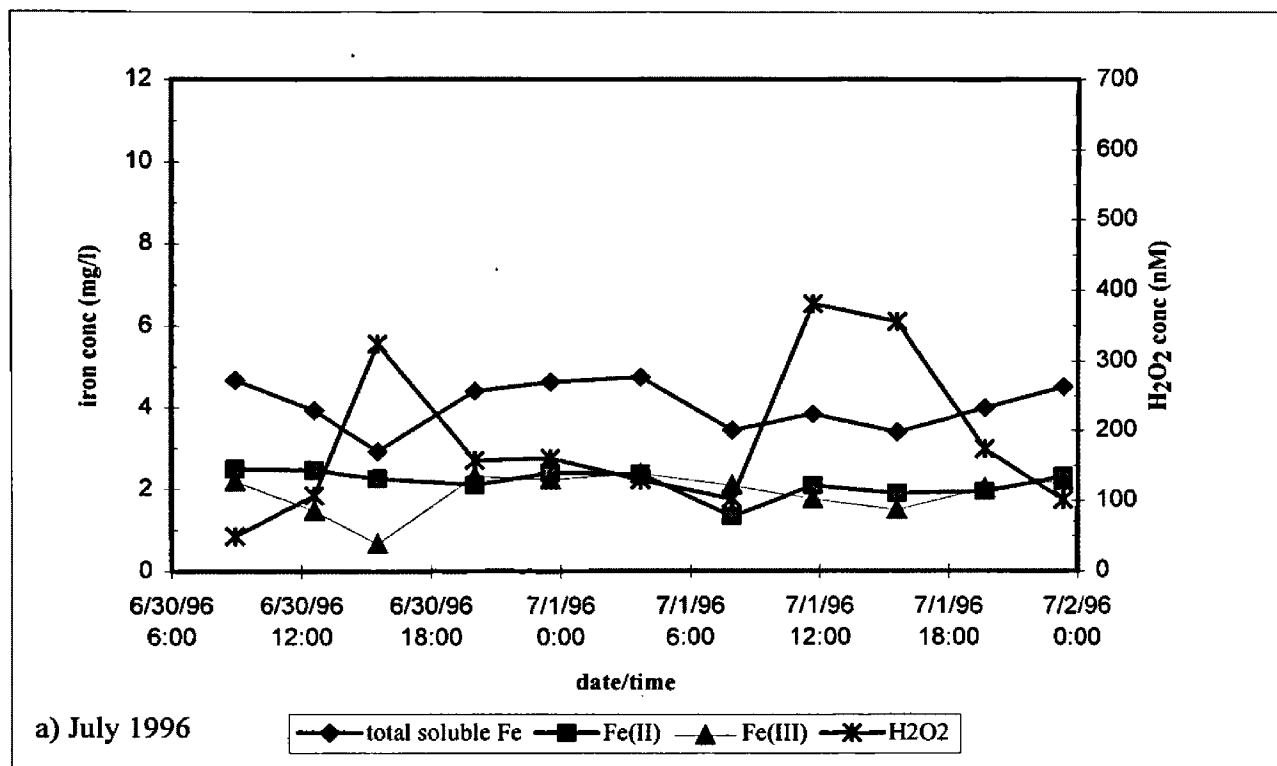
Figure 24: Diel variations in hydrogen peroxide, total soluble, ferrous and ferric iron concentrations at the Nymph Lake-iron pool, Yellowstone National Park.
a) July 1996, b) August 1996
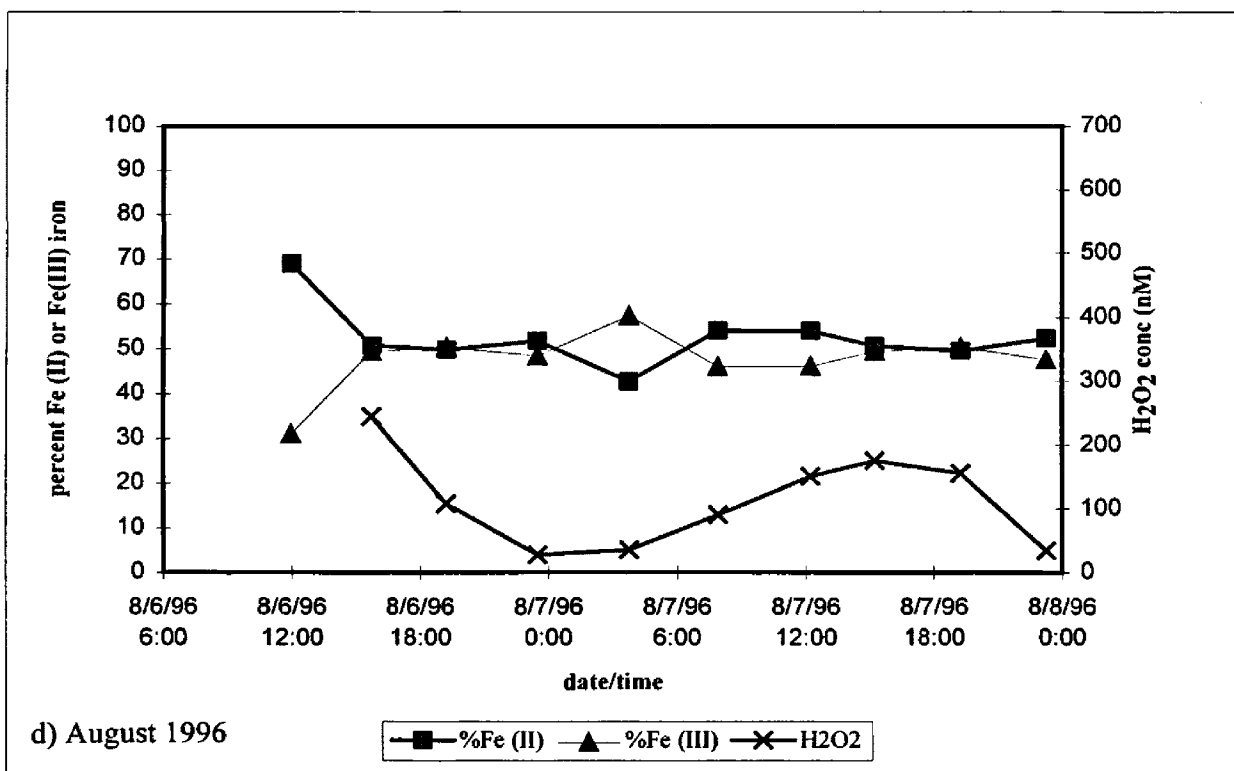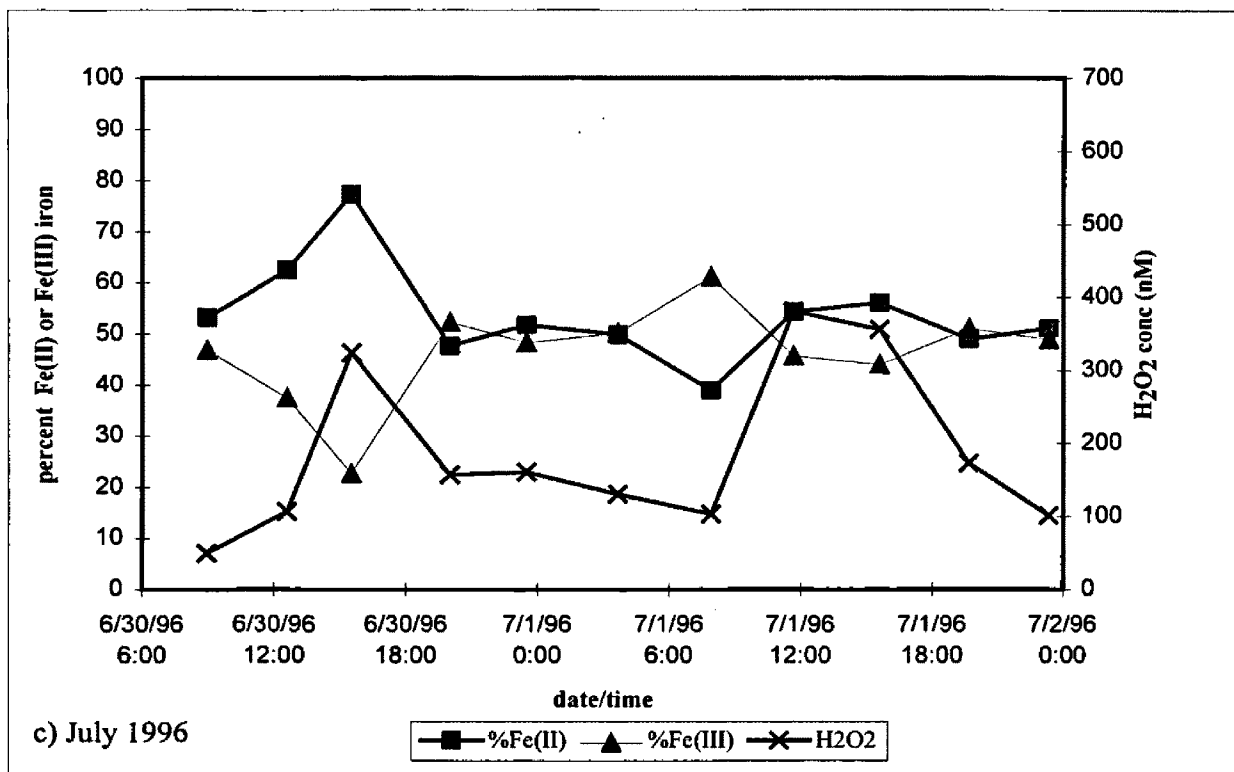
Figure 24 cont: Diel variations in hydrogen peroxide, ferrous and ferric iron as percent total iron at the Nymph Lake-iron pool, Yellowstone National Park. c) July 1996, d) August 1996

a) July 1996
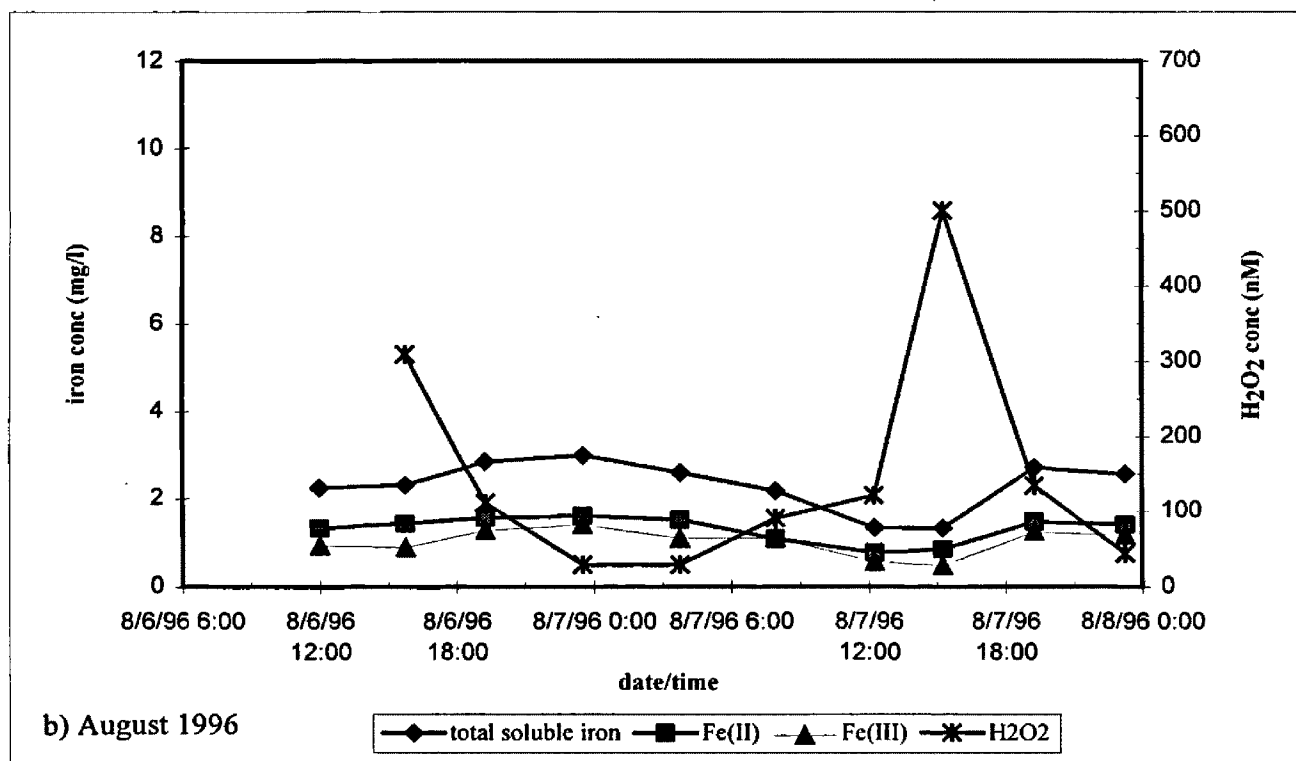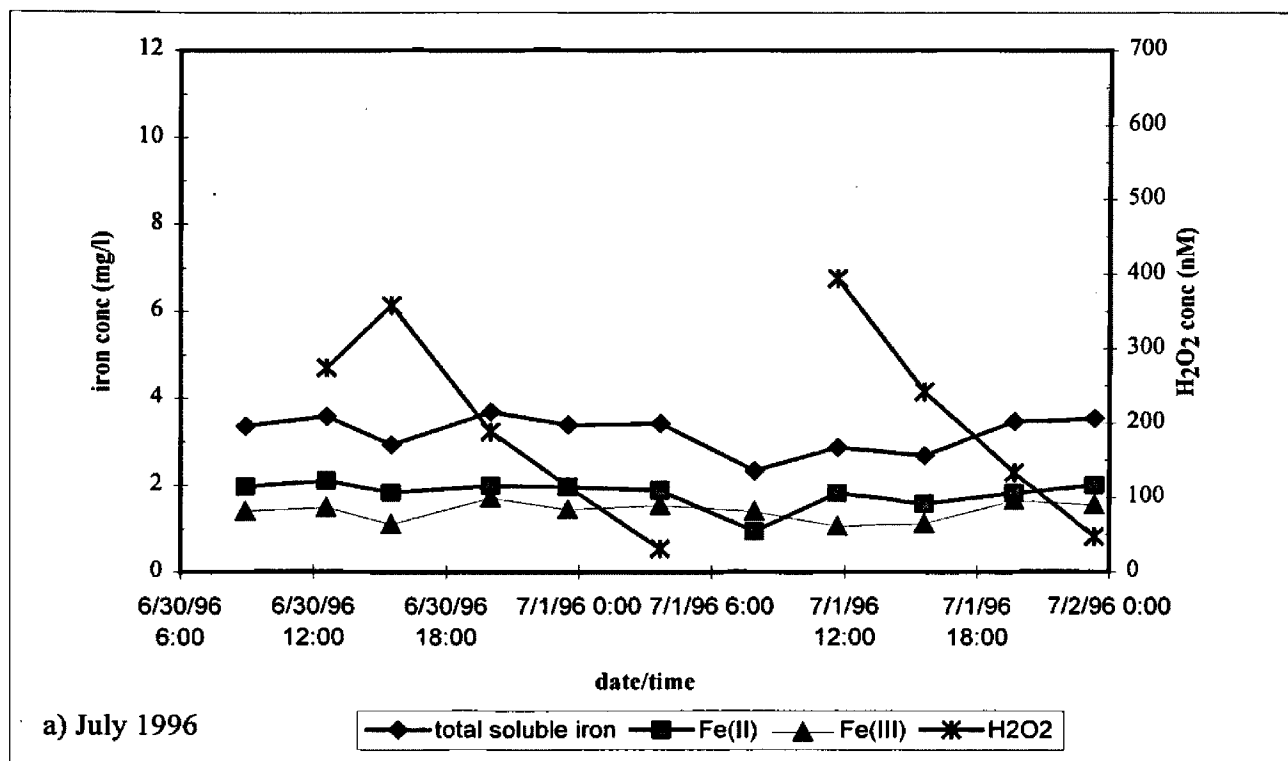
b) August 1996

Figure 25: Diel variations in hydrogen peroxide, total soluble, ferrous and ferric iron concentrations at the Nymph Lake-iron channel Yellowstone National Park.
a) July 1996, b) August 1996

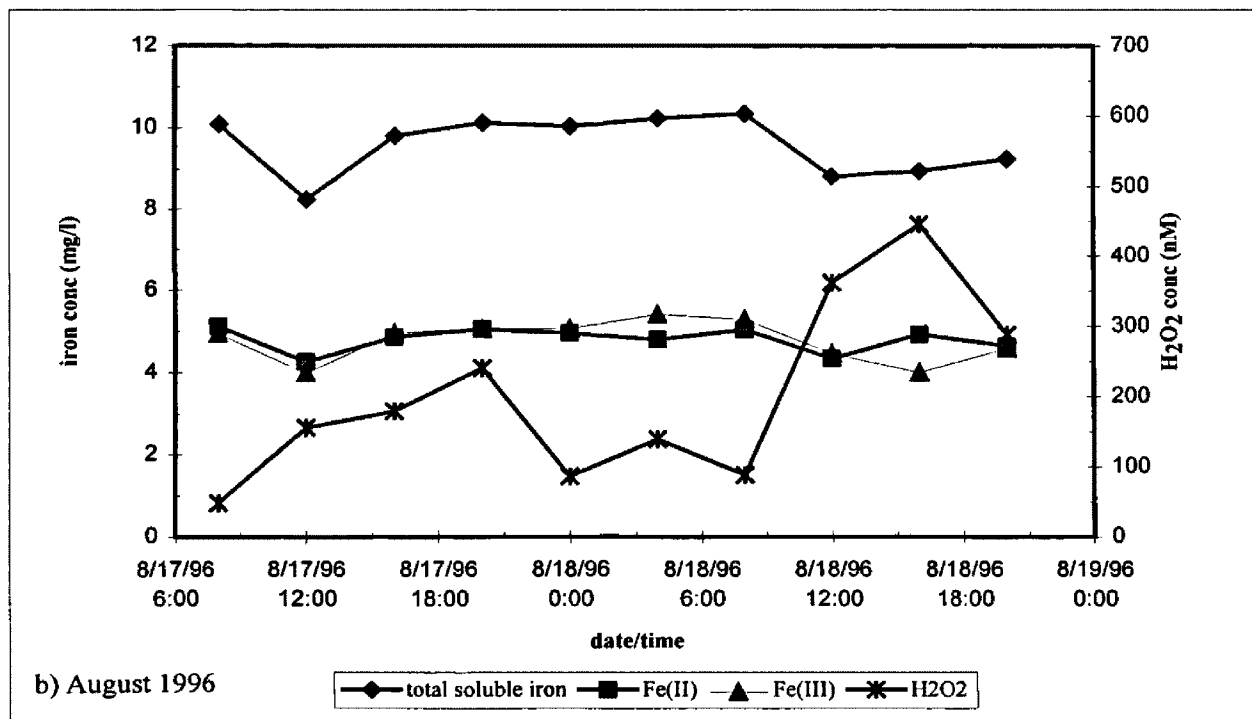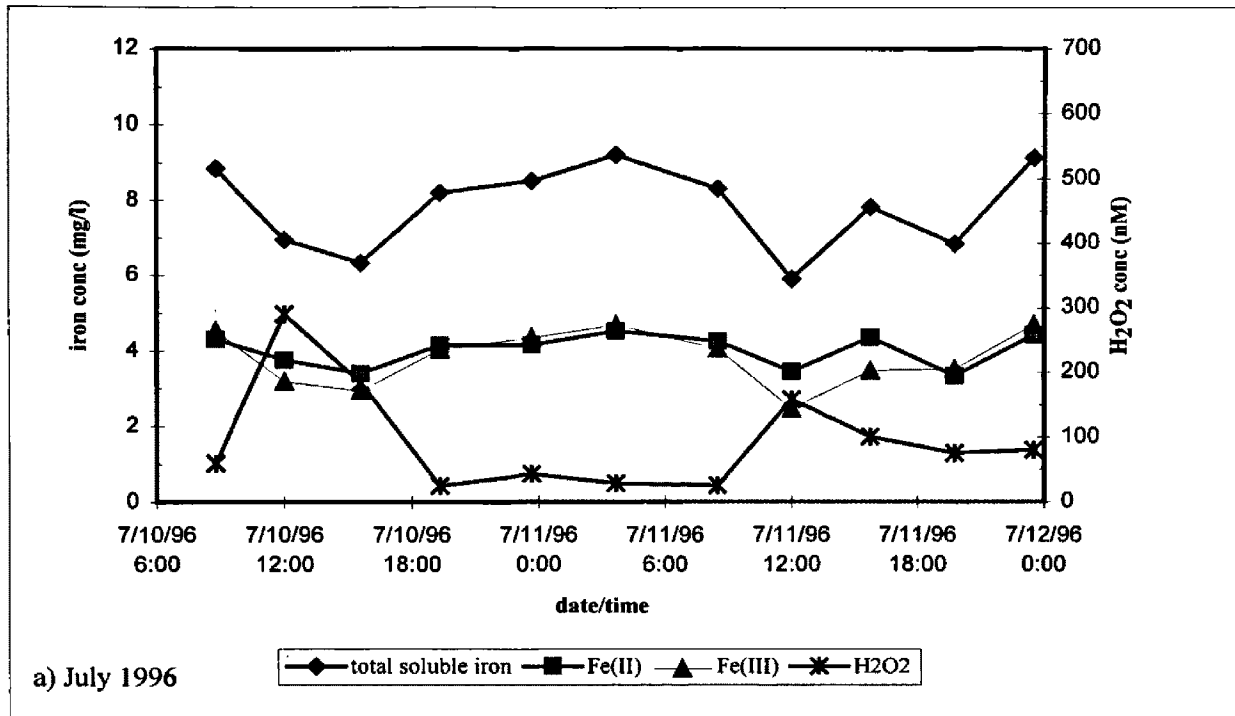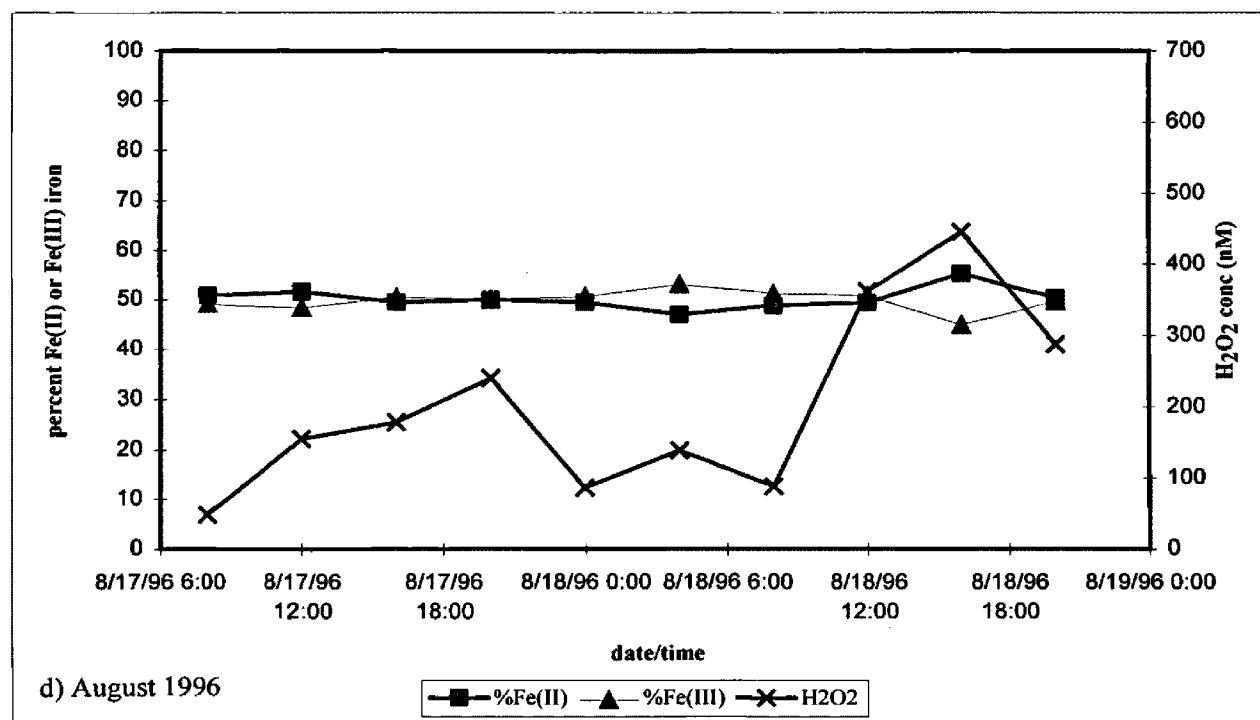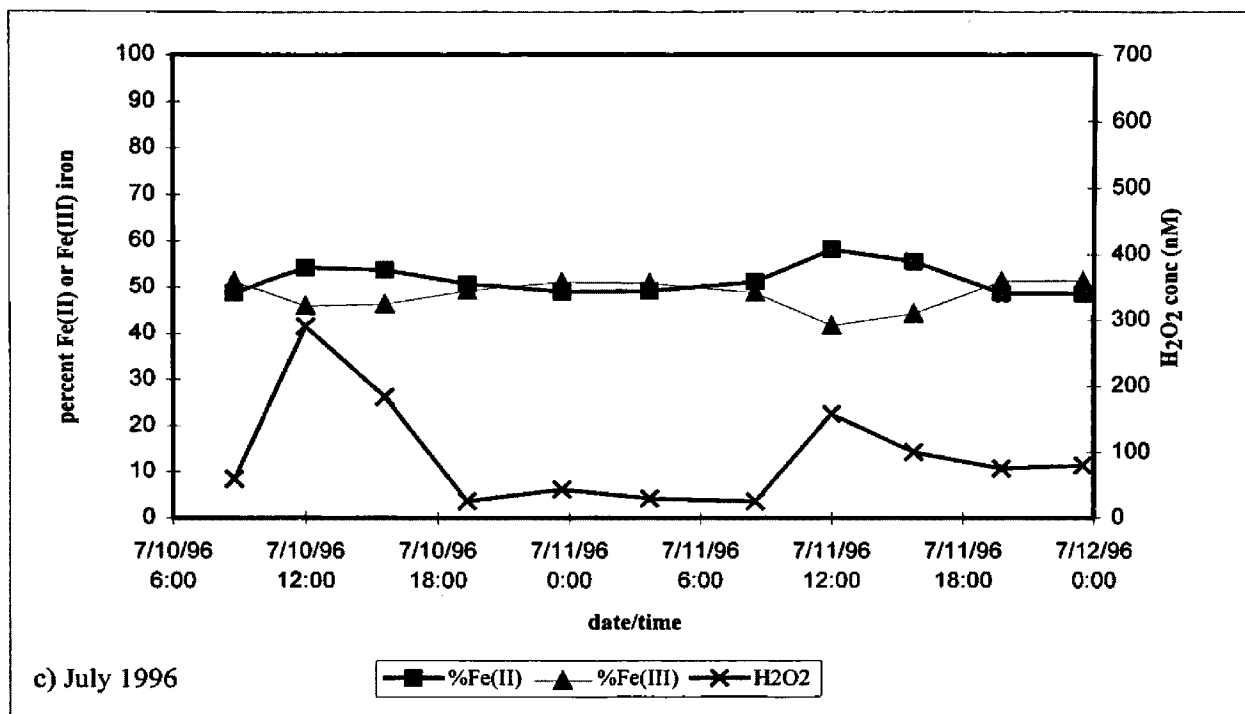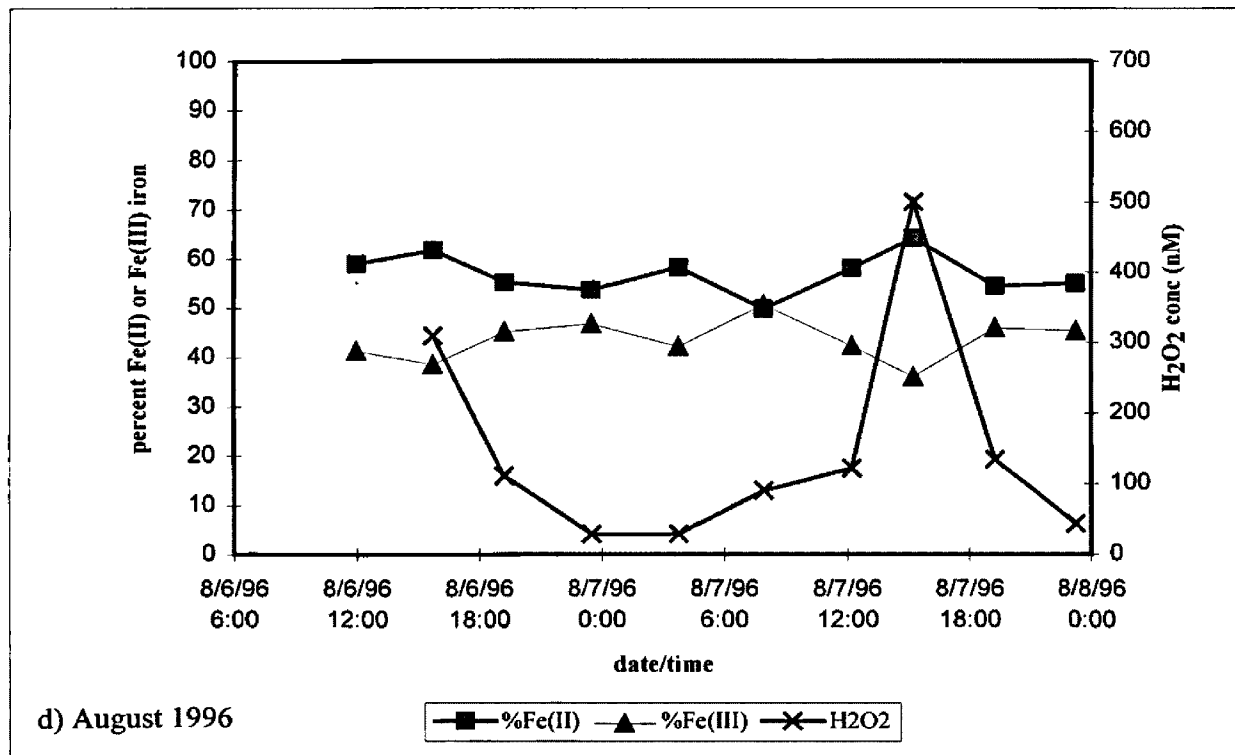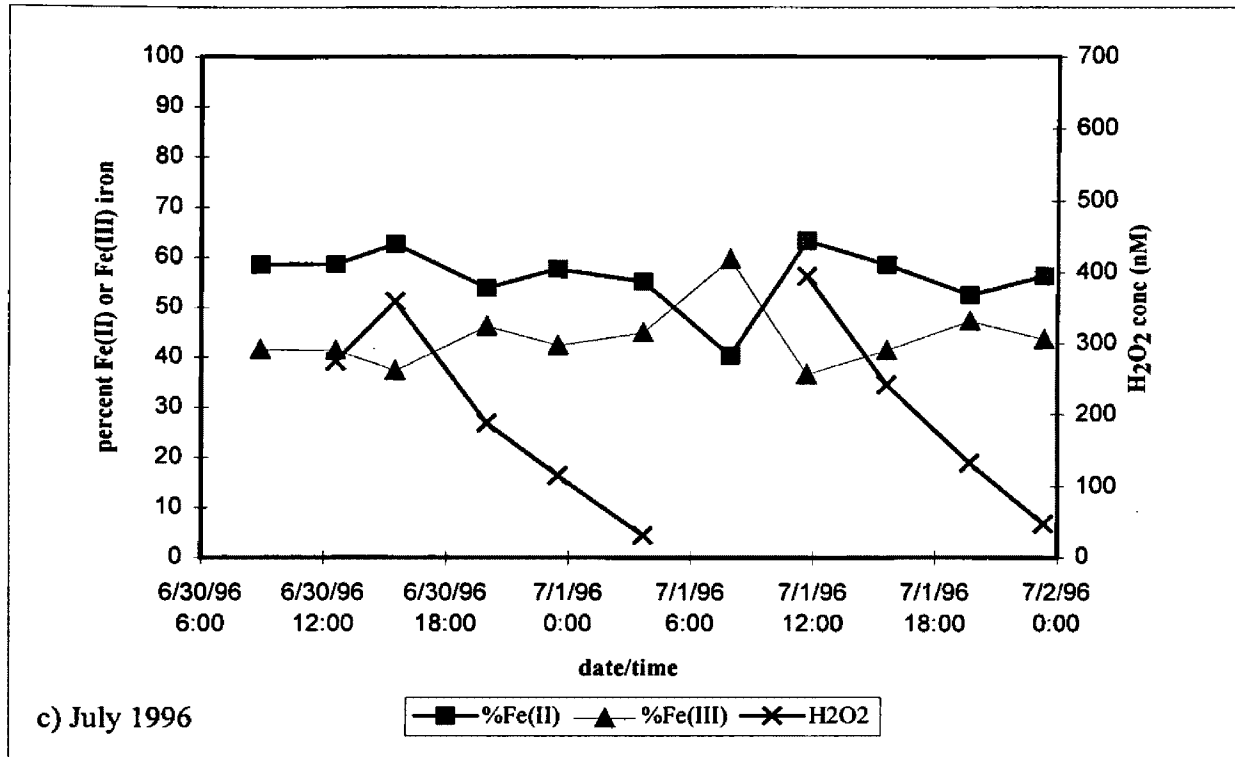Figure 25 cont: Diel variations in hydrogen peroxide, ferrous and ferric iron as percent total iron at the Nymph Lake-iron channel, Yellowstone National Park. c) July 1996, d) August 1996

Laboratory study

The laboratory study was designed to determine 1) photochemical hydrogen peroxide formation with different regions of the solar spectra, 2) hydrogen peroxide formation and decay by particulate (unfiltered water) versus non-particulate matter (<0.20μm filtered water), and 3) hydrogen peroxide formation and decay by biotic (mats and unfiltered water) versus abiotic (autoclaved water) processes. Water from Chocolate Pots was selected for the study because the water contains high iron concentrations (5.68mg/l by ICP) and four microbial species including a photosynthetic microorganism. Microbial mats from the channel contain a photosynthetic microorganism. High iron concentrations were desirable to test the theory that metal redox cycling is involved in hydrogen peroxide formation. Microbial mats with photosynthetic microorganisms were desired to determine if hydrogen peroxide is formed through photosynthesis.

Hydrogen peroxide formation

An increase in temperature from 25°C to 48°C produced small but statistically insignificant changes in hydrogen peroxide concentrations in controls and experimental waters. The exception was autoclaved water which had a small, and apparently statistically, significant decrease in hydrogen peroxide concentrations (Table 15).

Table 15: Difference in mean hydrogen peroxide concentrations (nM) 95% confidence (α=0.05)								
	De-ionized water		Unfiltered water		Filtered water		Autoclaved water	
	Pre-heat	Post-heat	Pre-heat	Post-heat	Pre-heat	Post-heat	Pre-heat	Post-heat
Mean	20.2	21.5	33.6	36.2	41.0	43.6	55.8	48.6
Std dev	2.55	1.98	3.85	3.27	6.60	4.83	2.77	3.71
Uncertainty*	3.34		5.22		5.19		4.78	
|Pre – post|	1.30		2.60		2.60		7.20	
* if uncertainty is greater than the difference, the means are not statistically different (Ott, 1993). Experiments were repeated three times except for autoclaved water which was conducted once.								

Hydrogen peroxide photochemical formation was determined by exposing heated water samples to 4 hours of solar radiation (Table 16). Hydrogen peroxide concentrations increased when exposed to solar radiation (Figure 26). The greatest increase was observed with UVA-PAR radiation while UVB-UVA-PAR resulted in hydrogen peroxide concentrations similar to those observed with PAR radiation.

Table 16: Solar radiation levels for laboratory experiments (watts/m²/sec)			
	UVB	UVA	PAR
Natural solar radiation			
Oct 97	0.49 ± 0.04	10.98 ± 1.17	215 ± 65
Oct 97*	0.35 ± 0.06	7.41 ± 1.46	172 ± 40
April 98	0.95 ± 0.07	19.08 ± 1.13	312 ± 68
Artificial solar			
Nov 97	0.27	3.01	-
April 98#	0.41/0.48	3.09	-
*filtered and autoclaved water sample experiments			
# UVB levels were for experiments with UVB-UVA and UVB radiation respectively			

Net hydrogen peroxide formation was greatest in the region of UVA-PAR radiation (320-700 nm) except for autoclaved water (Figure 27). Hydrogen peroxide concentrations in these samples were 2-4 times greater than concentrations in the dark control (Figure 27). The other spectral regions, PAR (400-700 nm) and UVB-UVA-PAR (280-700 nm), produced lower net increases in hydrogen peroxide concentrations that were 2-3 times greater than concentrations measured in the dark control (Figure 27).

Hydrogen peroxide formation in unfiltered and filtered water was not statistically different for any region of the solar spectrum (Figure 27, Table 17). In contrast, hydrogen peroxide formation was statistically different between unfiltered and unfiltered-autoclaved water with the greatest hydrogen peroxide formation in the unfiltered water. Additionally, hydrogen peroxide formation was statistically greater in unfiltered water than in unfiltered water with microbial mats except when UVA-PAR was the energy source.
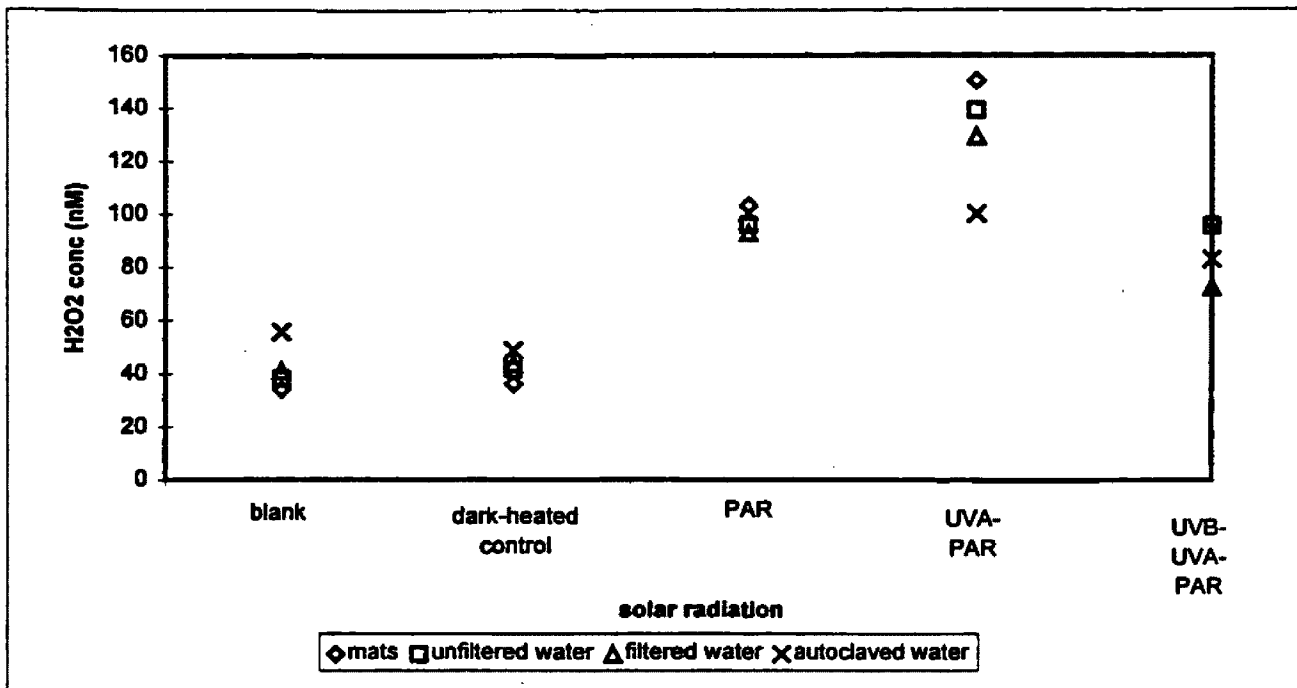
Figure 26: Net hydrogen peroxide concentrations with different regions of the solar spectra during laboratory experiments.
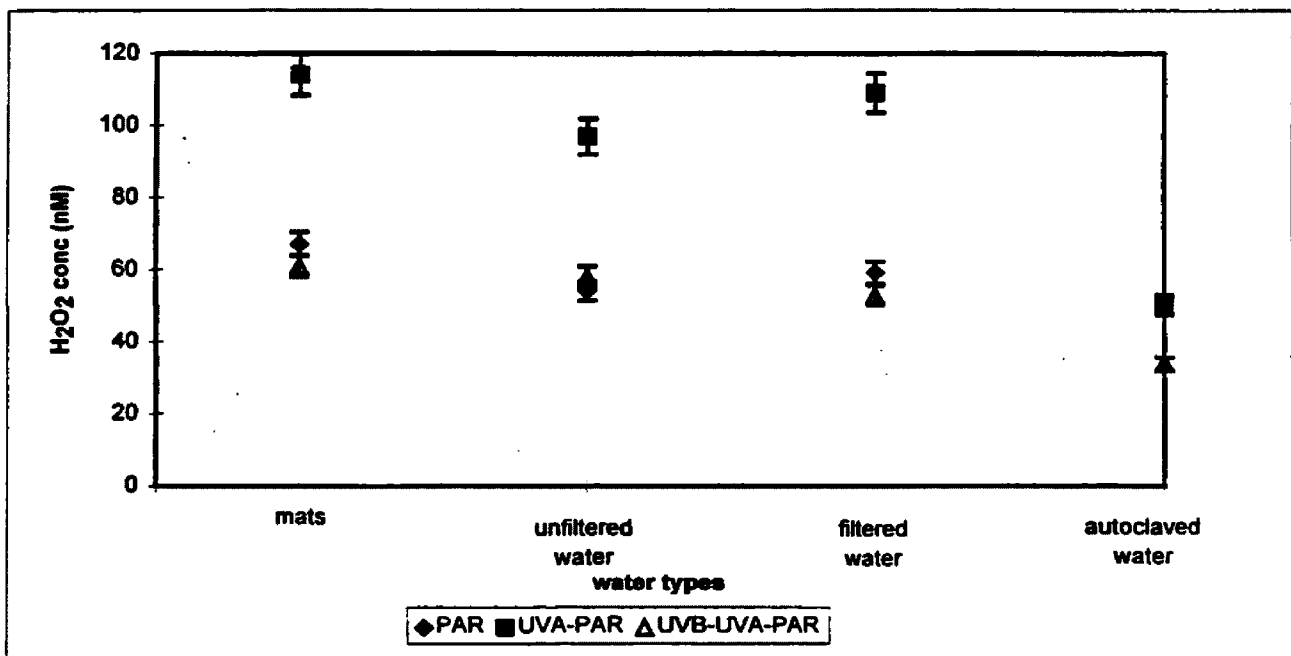
Figure 27: Net hydrogen peroxide formation in different water types exposed to selected regions of solar radiation during laboratory experiments.

Table 17: Comparison of hydrogen peroxide formation (nM) 95% confidence (α=0.05) between water types with different regions of solar spectra						
Mats with unfiltered water and unfiltered water						
	PAR		UVA-PAR		UVB-UVA-PAR	
	Mats/unfiltered	unfiltered	Mats/unfiltered	unfiltered	Mats/unfiltered	unfiltered
Mean	55	65	127	110	57	60
Std dev	15	13	21	15	15	16
Uncertainty	8		11		9	
Δ mean	10		17		13	
Unfiltered water and unfiltered-autoclaved water						
	PAR		UVA-PAR		UVB-UVA-PAR	
	unfiltered	autoclave	unfiltered	autoclave	unfiltered	autoclaved
Mean	65	50	110	50	60	45
Std dev	13	8	17	14	16	15
Uncertainty	6		7		7	
Δ mean	15		60		15	
Unfiltered water and filtered water						
	PAR		UVA-PAR		UVB-UVA-PAR	
	unfiltered	filtered	unfiltered	filtered	unfiltered	filtered
Mean	65	65	110	110	65	60
Std dev	13	7	17	10	16	7
Uncertainty	6		8		7	
Δ mean	0		0		5	
* if uncertainty is greater than the difference, the means are not statistically different (Ott, 1993). Experiments were repeated three times except for autoclaved water which was conducted once.						

Hydrogen peroxide formation in unfiltered water and unfiltered water with microbial mats varied between the tests conducted in October 1997 and the tests conducted in April 1998 (Table 18). In April, hydrogen peroxide formation was greater in the unfiltered water samples exposed to PAR and UVB-UVA-PAR but greater in the unfiltered water with mats exposed to UVA-PAR. In October, hydrogen peroxide formation was similar in the two sample types exposed to PAR and UVB-UVA-PAR but greater in unfiltered water with mats exposed to UVA-PAR. Hydrogen peroxide formation in filtered water was similar for the tests conducted in October 1997 and the tests conducted in April 1998.

Table 18: Hydrogen peroxide concentrations (nM) and formation in water exposed to 4 hrs of mid-day solar radiation					
Mats with unfiltered water					
date	control	heated	PAR	UVA-PAR	UVB-UVA-PAR
Oct-97	34 +/- 4	36 +/- 3	103+/-4	150+/-9	97+/-1
Apr-98	31 +/- 2	33 +/- 3	75+/-3	169+/-15	84+/-4
average	33	34	89	159	90
average net			~55	~125	~55
Unfiltered water					
date	control	heated	PAR	UVA-PAR	UVB-UVA-PAR
Oct-97	38 +/- 3	42 +/- 4	96+/-10	139+/-7	100+/-9
Apr-98	31 +/- 2	36 +/- 5	108+/-10	145+/-13	114+/-5
average	34	39	102	142	107
average net			~65	~110	~70
Filtered water					
date	control	heated	PAR	UVA-PAR	UVB-UVA-PAR
Oct-97	41 +/- 6	44 +/- 4	103+/-4	150+/-9	97+/-1
Apr-98	35 +/- 4	38 +/- 2	110+/-12	148+/12	104+/-7
average	38	41	104	149	100
average net			~65	~110	~60
Autoclaved water					
date	control	heated	PAR	UVA-PAR	UVB-UVA-PAR
Oct-97	56 +/- 2	49 +/- 3	100+/-7	100+/-12	83+/-13
average	56	49	100	100	93
average net			~50	~50	~45

Controlled light experiments examined hydrogen peroxide formation by UVA and UVB radiation. In these experiments, unfiltered water samples were exposed to a narrow range of the solar spectrum for 4 hours (Table 20). Hydrogen peroxide formation was greatest in water exposed to UVB-UVA radiation (Table 19) with hydrogen peroxide concentrations 6-7 times greater than concentrations observed in the control. Hydrogen peroxide formation in water exposed to UVA radiation was 4-times greater than concentrations observed in the control (Table 19) while hydrogen peroxide concentrations in water exposed to UVB radiation were only 2-times greater than those observed in the control.

TABLE 19: Hydrogen peroxide concentrations (nM) in unfiltered water exposed to 4 hours of artificial solar radiation					
Date	Initial	Heated	UVA-UVB	UVA	UVB
Nov 97	37 +/- 4	39 +/- 2	-	159 +/- 5	79 +/- 2
April 98	32 +/- 3	35 +/- 3	206 +/- 10	145 +/- 3	81 +/- 3
April 98	28 +/- 2	32 +/- 3	217 +/- 8	148 +/- 2	79 +/- 4

The amount of hydrogen peroxide formed per watt of solar energy also varied between the two solar spectral regions. In particular, UVB formed 1-2nM of hydrogen peroxide per watt/sec/m^2 and UVA formed ~0.3nM of hydrogen peroxide per watt/sec/m^2 (Table 20).

TABLE 20: Hydrogen peroxide formation per watt/sec/m^2 of incident solar radiation						
	Solar energy (watt/sec/m^2)		H$_2$O$_2$ (nM)		Formation rate (nM/ watt/sec/m^2)	
Date	UVA	UVB	UVA	UVB	UVA	UVB
Nov 97	3.01	0.27	159+/-5	79+/-2	0.37	2.03
April 98	3.09	0.41	145+/-3	81+/-3	0.33	1.37
April 98	3.09	0.48	148+/-2	79+/-4	0.33	1.14

Hydrogen peroxide decay

The dark decay study examined the degradation potential of particulate versus non-particulate components and of biotic versus abiotic processes. Samples from the formation study were used for the dark decay study. These samples were covered immediately after the 4 hours exposure to mid-day sun. Hydrogen peroxide measurements were taken every 2 or 4 hours. Hydrogen peroxide dark decay was fastest in the presence of microorganisms in microbial mats and unfiltered water (Table 21). The half-life for hydrogen peroxide in these waters was 2-4 hours with hydrogen peroxide decay fastest in the presence of microbial mats.

Hydrogen peroxide decay was slowest in the absence of particulate matter (filtered water <0.2 μm) or by abiotic processes (autoclaved water). These samples showed no net hydrogen peroxide decay after 24 hours. In fact, hydrogen peroxide concentrations continued to increase in these waters after the samples were removed from the sun.

Hydrogen peroxide concentrations in both cases reached maximum concentrations at ~4 hours.

TABLE 21: Hydrogen peroxide dark decay									
time	Mats/unfiltered water			unfiltered water			filtered water			autoclaved water
	Oct97	April98	April98	Oct97	April98	April98	Oct97	April98	April98	Oct97
initial	150	185	149	139	164	135	93	126	80	100
2 hrs	100	77	55	101	145	77		152	123	
4 hrs	68	45		72	85	45	145	177	138	148
8 hrs							135	180	140	125
12 hrs								168	128	
16 hrs							115	155	106	100
20 hrs							103	136	85	92
24 hrs							97	122	75	85

CHAPTER 4: DISCUSSION

Field Study

Hydrogen peroxide concentrations and diel cycling in the hot springs studied are consistent with observations in other surface waters (marine and freshwater) (Cooper and Lean, 1989; Cooper et al., 1989; Zika et al., 1985). The diel variability in hydrogen peroxide concentrations suggests photochemical processes are responsible for hydrogen peroxide formation. In other surface waters (fresh and marine), the primary photochemical process is the interaction of dissolved organic carbon (DOC) with UV radiation (Cooper et al., 1988; Cooper et al, 1994). If the main pathway responsible for hydrogen peroxide formation in surface geothermal waters is the same as that in fresh and marine surface waters, hydrogen peroxide concentrations should correspond with DOC concentrations.

However, these geothermal waters contain low and variable DOC concentrations that do not always correspond with hydrogen peroxide concentrations. The most apparent inconsistency between hydrogen peroxide concentrations and DOC concentrations was observed at Chocolate Pots. In August, the pool and the channel had similar hydrogen peroxide concentrations but different DOC concentrations. In fact, DOC concentrations were < 1.0 mg/l in the pool and 4.95 mg/l in the channel. Similar observations were made at the other springs. This lack of a significant relationship between DOC and hydrogen peroxide concentrations suggests that additional pathways are responsible for hydrogen peroxide formation.

The primary candidate for an alternative pathway is the formation of hydrogen peroxide as a by-product in metal redox cycling. Zuo and Hoigne (1992) demonstrated hydrogen peroxide formation through the photoreduction of ferric-oxalates in atmospheric waters with as little as $1\mu M$ ferric iron. Additionally, Scully et al. (1996) observed higher than expected hydrogen peroxide concentrations in near neutral and slightly acidic wetland and bog waters with iron concentrations as low as 0.175mg/l ($\sim 3\mu M$). Zuo and Hoigne proposed that ferric iron complexes were photoreduced to ferrous iron (equation 17). The ferrous iron then reacted with the hydroperoxyl radical (HO_2/O_2^-) forming hydrogen peroxide (equation 18). They demonstrated that hydrogen peroxide formation rates increased with increasing ferric iron concentrations. If similar processes occur in geothermal waters, then photo-reactions with iron could be a major source for hydrogen peroxide formation. In fact, these geothermal waters contain iron concentrations that are as much as 10-times the concentrations observed by Scully et al. (1996). Additionally, ferrous iron concentrations at 3 sites exhibited diel cycling that coincided with hydrogen peroxide cycling; that is, higher hydrogen peroxide concentrations were observed with higher ferrous iron concentrations. Although total iron concentrations were higher at Chocolate Pots than at Nymph Lake-iron spring, the day-night change in ferrous iron concentrations was ~ 0.9 mg/l ($16\mu M$) at both locations. This suggests a causal-effect mechanism where the higher iron concentrations are responsible for hydrogen peroxide formation.

$$Fe(III) \rightarrow Fe(II) \quad\quad\quad\quad (17)$$
$$HO_2/O_2^- + Fe(II) \rightarrow H_2O_2 + Fe(III) \quad\quad\quad\quad (18)$$
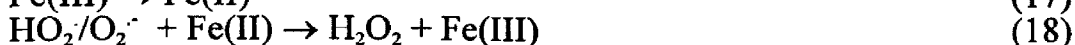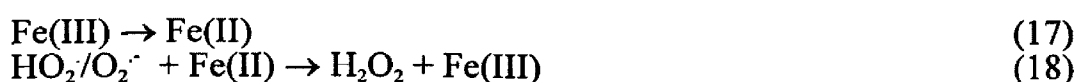
Besides iron concentrations, water pH also affects hydrogen peroxide formation. Zuo and Hoigne (1992) determined that hydrogen peroxide formation rates through metal redox reactions were controlled by pH. Below pH 4.8, the dominant species is the hydroperoxyl radical that has greater reactivity with ferrous iron to form hydrogen peroxide (2-3 orders of magnitude greater) than the reaction with ferric iron to form oxygen (equations 19-20). Above pH 4.8, the dominant species is the superoxide radical which reacts more quickly with ferric iron to form oxygen than with ferrous iron to form hydrogen peroxide (equations 21-22) (Zuo and Hoigne, 1992). Thus, at lower pH, the dominant product should be hydrogen peroxide. This was indeed the case where hydrogen peroxide yield was 3-4 times greater at Nymph Lake-iron spring (pH ~3.40) than at Chocolate Pots pool (pH ~5.75). Additionally, hydrogen peroxide yield was apparently higher in the Nymph Lake-iron channel than in the Nymph Lake-iron pool. If hydrogen peroxide yield from iron is the same within a given system, than the difference in hydrogen peroxide yield in the Nymph Lake-iron channel and the Nymph Lake-iron pool must be due to other factors.

$$HO_2 + Fe(II) \rightarrow H_2O_2 + Fe(III) \qquad k=1.2 \times 10^6 \qquad (19)$$
$$HO_2 + Fe(III) \rightarrow O_2 + Fe(II) \qquad k=<10^4 \qquad (20)$$
$$O_2^- + Fe(II) \rightarrow H_2O_2 + Fe(III) \qquad k=1.0 \times 10^7 \qquad (21)$$
$$O_2^- + Fe(III) \rightarrow O_2 + Fe(II) \qquad k=1.5 \times 10^8 \qquad (22)$$
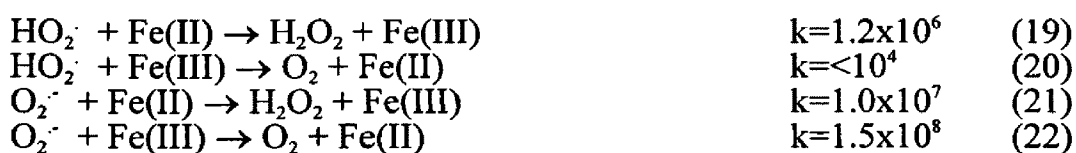
In addition to dissolved metals and pH, several other factors may influence hydrogen peroxide concentrations within a system. These factors are 1) mixing within the water column, 2) different formation rates and mechanisms, and 3) different degradation rates and mechanisms.

Mixing of hydrogen peroxide throughout the water column may greatly affect surface hydrogen peroxide concentrations. The channels are only a few inches deep with undoubtedly constant hydrogen peroxide concentrations throughout the water column. In contrast, the pools range from <0.5 meter deep to several meters deep. The super-heated waters entering the pool from the vent probably cool as they rise in the water column and contact the atmosphere. These 'cooler' waters may sink into the water column taking hydrogen peroxide and oxygen with them. The extent of this theoretical water cycling is unknown and warrants further investigation with hydrogen peroxide depth profiles.

Hydrogen peroxide formation rates in the pools may be less than in the channels as a result of lower DO concentrations in the pool. Although DO was not measured in the pools, the oxygen concentrations were undoubtedly low due to the high pool temperatures which limit oxygen solubility. The oxygen concentration in the pools may be controlled not only by temperature but also by surface area. A larger surface area allows for a greater air-water flux of oxygen. Also, water vapor over the pool may absorb oxygen as it cools. When the water vapor cools, it condenses and drops into the pool providing an additional source of oxygen to the pool. In other environments, this contribution is extremely small but in these geothermal waters it may be sufficient to allow for hydrogen peroxide formation.

While high oxygen concentrations in the channels may result in greater hydrogen peroxide formation, biological activity may also contribute to hydrogen peroxide formation. Stevens et al (1973) reported biological (photosynthetic) hydrogen peroxide formation in marine and freshwater cyanobacteria. If similar processes occur in the

cyanobacteria and other photosynthetic microbes in these geothermal waters, then biological activity may contribute to hydrogen peroxide formation in these waters. While this was not determined, biological formation of hydrogen peroxide may account for higher hydrogen peroxide concentrations in the Chocolate Pots channel in July despite lower DOC and iron concentrations than in the pool. Higher hydrogen peroxide concentrations were also observed at the Nymph Lake-iron channel than at the Nymph Lake-iron pool despite similar DOC and iron concentrations.

An additional cause for lower net hydrogen peroxide yield in the pools may be greater hydrogen peroxide degradation in the pools than in the channels. This may occur through hydrogen peroxide oxidation of sulfide (Millero et al, 1989) where sulfide cycled inversely to hydrogen peroxide cycling and where sulfide concentrations were higher in the pools than the channels. In particular, lower hydrogen peroxide concentrations in the pools coincided with higher sulfide concentrations. This suggests that hydrogen peroxide concentrations may be partially controlled through degradation by sulfide.

Besides sulfide oxidation by hydrogen peroxide, other factors may be responsible for hydrogen peroxide degradation. This is especially evident at night where decreasing hydrogen peroxide concentrations indicated hydrogen peroxide decay exceeded formation. Another possible pathway for hydrogen peroxide degradation is the chemical interaction of hydrogen peroxide with ferrous iron. Hydrogen peroxide concentrations at night decreased as relative ferrous iron concentrations decreased and ferric iron concentrations increased. This cycling of iron and hydrogen peroxide is consistent with hydrogen peroxide degradation through Fentons reactions (equations 23-24) (Zuo and

Hoigne, 1992). This reaction is extremely slow and is only noticeable at night when ferric iron accumulates due to a lack of photoreduction.

$$Fe(II) + H_2O_2 \rightarrow Fe(III) + HO^{\cdot} + HO^{-} \qquad k=76 \qquad (23)$$
$$Fe(II) + HO^{\cdot} \rightarrow Fe(III) + HO^{-} \qquad (24)$$

Another mechansim for hydrogen peroxide decay may be biological degradation. This process was not determined in the field study but it was examined in the laboratory study.

Laboratory experiments

The laboratory experiments successfully addressed questions concerning hydrogen peroxide formation by irradiating samples with specific regions of the solar spectrum. Hydrogen peroxide degradation was studied by differentiating between particulate and non-particulate matter and between biotic and abiotic processes.

Hydrogen peroxide decay

In these surface geothermal waters, hydrogen peroxide decay was mediated primarily by particulate matter (> 0.2 μm) that was not stable during autoclaving. This particulate matter was most likely microbes. Hydrogen peroxide degradation also occurred to a much smaller extent through the interactions of non-particulate and abiotic matter. Hydrogen peroxide degradation occurred through chemical reactions involving metals in Fentons type reactions (equations 23-24) and, to a lesser extent, Haber-Weiss type reactions (equation 25) (Zuo and Hoigne, 1992). In these waters, the metals possibly involved in these reactions may include iron, manganese, and arsenic. In fact in this study, net ferric iron concentrations increased at night with a corresponding decrease in ferrous iron and hydrogen peroxide concentrations.

$$Fe(II) + H_2O_2 \rightarrow Fe(III) + HO^{\cdot} + HO^{-} \qquad k=76 \qquad (23)$$
$$Fe(II) + HO^{\cdot} \rightarrow Fe(III) + HO^{-} \qquad (24)$$
$$Fe(III) + H_2O_2 \rightarrow Fe(II) + HO_2^{\cdot} + H^{+} \qquad k=\text{very slow} \quad (25)$$
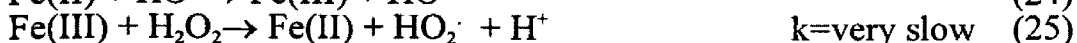
Hydrogen peroxide formation

If hydrogen peroxide formation proceeds by the same pathways (photochemical reactions with DOC and metals) in surface geothermal waters as observed by Scully et al., (1996) in iron-rich wetland and bog waters, then both UVB and UVA radiation should play significant roles in hydrogen peroxide formation. Additionally, while UVB should be the more efficient energy source as demonstrated by Cooper et al. (1994), UVA radiation should contribute the most to the overall formation of hydrogen peroxide as demonstrated by Scully et al. (1996). This was indeed the case in the controlled hydrogen peroxide formation studies where UVB radiation was 3-5 times more efficient than UVA radiation while UVA radiation formed approximately twice as much hydrogen peroxide as UVB radiation. Possible sources for hydrogen peroxide formation with these energy sources are the interaction of DOC with UV radiation and the interaction of metals with UV radiation. While DOC absorbs in the solar spectral region of 290-400nm, several iron complexes and species (iron hydroxide, iron oxalates) absorb in the solar spectral region of 290-570nm. In acidic waters, iron hydroxides $(Fe(OH)^{+2})$ are the dominant iron species. These iron complexes absorb in the solar spectral region 290-400nm (Zuo and Hoigne, 1992). The ferric ion, which is also present in acidic waters, absorbs in the 290-340nm solar spectral region (Zuo and Hoigne, 1992). Iron oxalate complexes absorb in the solar spectral region of 290-570nm (Zuo and Hoigne, 1992). Therefore, hydrogen peroxide formation with UVA radiation may occur through metal redox cycling.

When regions of the solar spectrum were combined through the use of filtered solar radiation, net hydrogen peroxide formation changed. In these laboratory experiments using natural solar radiation, UVA-PAR formed more hydrogen peroxide than did PAR. In contrast, hydrogen peroxide formation with UVB-UVA-PAR was less than with UVA-PAR alone. Hence, UVB may affect hydrogen peroxide concentrations in these surface geothermal waters by either degrading hydrogen peroxide or by disrupting a hydrogen peroxide formation pathway. To distinquish between these possibilities, experiments using UVB, UVA, and UVB-UVA light sources were conducted in a laboratory cabinet.

In the controlled light experiments, hydrogen peroxide formation when UVB-UVA was the energy source was equivalent to the sum of that produced by UVA and UVB as separate sources. This indicates that UVB radiation did not degrade hydrogen peroxide and that hydrogen peroxide formation is indeed additive for the two energy sources. Therefore, UVB radiation may instead interfere in hydrogen peroxide formation with PAR by blocking a production pathway as might occur with biological formation.

To determine if biological formation of hydrogen peroxide does occur, unfiltered water and unfiltered-autoclaved water samples were exposed to filtered solar radiation. Net hydrogen peroxide formation was greater in the water containing living organisms than in the water containing killed organisms suggesting that living organisms may indeed mediate hydrogen peroxide formation. While the net hydrogen peroxide formation in the autoclaved water was similar for all energy sources, the higher net hydrogen peroxide formation in unfiltered water exposed to UVA-PAR and the lower net hydrogen

peroxide formation in the unfiltered water exposed to UVB-UVA-PAR suggests that

UVB may indeed disrupt biological hydrogen peroxide formation.

CHAPTER 5: CONCLUSIONS

Hydrogen peroxide was found in surface geothermal waters at concentrations comparable to those observed in marine and freshwaters. These concentrations exhibited diel cycling suggesting photochemical formation. In other surface waters, the primary photochemical mechanism for hydrogen peroxide formation involves dissolved organic carbon (DOC) and UVB radiation (280-320nm). While UVB radiation (280-320nm) forms more hydrogen peroxide per watt of solar energy than UVA radiation (320-400nm), UVA is responsible for the majority of hydrogen peroxide formation in these waters. At the lower energy UVA radiation, hydrogen peroxide formation occurs primarily through metal redox cycling. Therefore, the primary pathway for hydrogen peroxide formation in geothermal waters is through metal redox cycling.

Hydrogen peroxide concentrations at depth depend on mixing (Zika et al., 1985) and the depth to which different regions of the solar spectra penetrate the water (Scully et al., 1996). Because UVA radiation can penetrate to greater depths than UVB radiation, it may be responsible for greater than expected hydrogen peroxide formation at depth in clear geothermal waters. The depth to which UV radiation penetrates the water column and the depth at which hydrogen peroxide forms could greatly influence microbial ecology and evolution.

Additionally, hydrogen peroxide formation and degradation through metal redox cycling affects the oxidation state and the bioavailabilty of the metals which may affect biological processes. This in-turn may also affect microbial ecology and evolution.

The first microorganisms probably lived at depths to escape the harmful effects of UV radiation (Sagan, 1973). These microbes probably utilized metals as an energy source (Brock et al, 1994) and as a shield against UV radiation. When the first photosynthetic organisms evolved, the oxygen formed was probably harmful to the organisms. To neutralize the oxygen, these organisms may have utilized natural chemical reactions with metals to convert oxygen to the superoxide radical, then to hydrogen peroxide, and finally

to water. Eventually, the microbes probably mediated hydrogen peroxide degradation by utilizing intracellular and/or extracellular metals in chemical reactions (Calvin, 1959). This method for hydrogen peroxide degradation may have been the first step in the development of hydrogen peroxide neutralizing enzymes with successive steps in enzyme development providing greater protection from hydrogen peroxide.

In this study, hydrogen peroxide degradation was mediated primarily by the microbes that inhabit the geothermal waters. It is not known whether these microbes mediate hydrogen peroxide degradation through enzymatic processes such as peroxidase and/or catalase or whether they mediate hydrogen peroxide degradation through chemical reactions such as Fentons type or Haber-Weiss reactions. The genetically close relationship of these microbes to the earliest microbes suggests that some of these microbes may use the latter less efficient methods to neutralize hydrogen peroxide.

While this study focused on iron-rich hot springs, similar hydrogen peroxide concentrations may be observed in other iron-rich environments (i.e. acid mine drainage). Besides iron, other redox sensitive metals such as arsenic and manganese may also be responsible for hydrogen peroxide formation in geothermal waters and other surface waters. Understanding how metal redox cycling and hydrogen peroxide affect microbial ecology and evolution will be beneficial in distinguishing fossils of early organisms from non-biotic crystalline forms preserved in Precambrian rocks.

APPENDIX A – Pilot Study

Experimental Design

Two hot springs in Yellowstone National Park (Sulphide Spring and Black Sand Pool) were selected to determine the existence of hydrogen peroxide in surface geothermal waters. Hot spring selection criteria were accessibility, proximity to electricity, and water pH.

Site selection criteria were water temperatures in the pool and in the runoff channels. The pools and one or two sites in the run-off channels were sampled to determine if temperature affected hydrogen peroxide concentrations. The pool sites were near the outflow channels and the channel sites were 3-30 meters downstream from the pool.

Sampling was conducted during the afternoons of May 10 and 11, 1996.

Results and Discussion

Analysis of two hot springs indicated hydrogen peroxide is present in geothermal waters (Table A1). Hydrogen peroxide concentrations at Black Sand Pool varied with time of day and sunlight exposure. Hydrogen peroxide concentrations were higher in late afternoon than in early afternoon and higher at sunlit sites than at shaded sites. Early afternoon hydrogen peroxide concentrations were higher in the channel (100 nM) than in the pool (60 nM). Late afternoon hydrogen peroxide concentrations were highest at the pool (275 nM) and lowest at a shaded site (110 nM). Late afternoon hydrogen peroxide concentrations decreased at a shaded site and increased slightly at a site exposed to sunlight. Hydrogen peroxide concentrations at Sulphide Pool also varied between the pool and the channel site. Hydrogen peroxide concentrations were higher in the pool (140 nM) than in the channel (80 nM).

Conclusions

Hydrogen peroxide is present in surface geothermal waters. Hydrogen peroxide concentration variations between shaded sites and sunlit sites suggest that hydrogen peroxide formation is through photochemical processes. Concentrations vary between

pool sites and channel sites which may be a consequence of shading rather than different rates of formation.

Table A1: Hydrogen peroxide pilot study						
	distance from pool	pH	temp (°C)	H2O2 concentration (nM)		sunlight
Black Sand Pool				1:30PM	4:00PM	
pool		8.10	85.0	60	275	sun
channel	15 meters	8.30	63.7	80	110	shade
channel	30 meters	8.93	21.4	100	160	sun
Sulphide Spring					3:00PM	
pool		5.38	70.8		140	sun
channel	1 meter	NA	NA		NA	shade
channel	3 meters	5.88	57.2		80	sun
NA - not analyzed			hydrogen peroxide method detection limit (MDL) 32.6 nM			

APPENDIX B - Light meter comparison

ceptometer	foot-candle
21	0.08
24	0.008
68	0.22
76	0.28
100	0.38
107	0.4
257	0.98
261	1
414	2.6
478	2.2
480	1.5
609	3.5
672	2.8
705	3.9
743	3.3
754	2.5
758	2.65
764	2.9
771	3.5
794	2.9
861	3.6
914	3.1
938	3.4
984	4
985	3.3
989	3.6
1031	4
1100	4
1173	3.5
1197	4.3
1216	3.4
1223	3.3
1391	4.55
1401	4.45
1405	4.1
1409	3.8
1449	4.2
1519	5
1533	5.1
1541	5.6
1545	5.1
1645	5.8
1668	5.9
1677	5.2
1690	5.9
1716	6
1719	5.3
1726	5.9
1743	6
1743	6
1759	5.59
1767	5.78
1747	6
1771	6
1806	>6

Comparison curve for ceptometer and foot-candle meter

$y = 0.0034x$
$R^2 = 0.9184$

light readings in foot-candles (y-axis)

light readings in PAR (μmole/m^2/sec) (x-axis)

—◆— foot-candle —— Linear (foot-candle)

	Black Sand Pool				Chocolate Pots				Nymph Lake					
	pool		channel		pool		channel		sulfur pool		iron pool		channel	
	July	August	July	August	July	August	July	August	July	August	July	August	July	August
DOC (mg/l)														
8:00AM	1.41	<0.5	1.65	1.46	4.75	1.97	0.93	0.62	2.24	0.59	0.95	5.57	0.88	4.36
Noon	0.69	<0.5	1.9	<0.5	2.35	<0.5	1.11	6.73	2.33	<0.5	0.72	2.7	0.91	4.49
4:00PM	<0.5	<0.5	2.36	<0.5	2.65	<0.5	0.75	4.72	2.5	<0.5	0.84	4.91	0.81	<0.5
8:00PM	<0.5	<0.5	2.38	<0.5	2.1	0.58	0.71	8.56	3.38	<0.5	1.05	0.63	0.97	5.67
Midnight	<0.5	<0.5	1.08	2.25	4.28	<0.5	0.71	0.55	2.42	4.5	0.85	4.54	0.97	<0.5
4:00AM	0.5	<0.5	<0.5	0.98	0.85	1.38	0.75	8.5	2.42	3.6	0.86	4.34	0.9	1.6
8:00AM	1.2	NA	<0.5	NA	3.1	NA	1.61	NA	1.85	NA	1.7	NA	0.97	NA
Noon	2.28	NA	<0.5	NA	0.74	NA	1.72	NA	2.17	NA	1.05	NA	0.91	NA
4:00PM	2.53	NA	0.53	NA	2.11	NA	0.62	NA	5.18	NA	0.79	NA	NA	NA
8:00PM	NA	NA	<0.5	NA	0.7	NA	1.67	NA	2.1	NA	1.08	NA	1.35	NA
Midnight	2.57	NA	4.18	NA	1.34	NA	2.06	NA	1.6	NA	1.61	NA	2.58	NA
average	1.60	<0.5	1.42	0.90	2.27	0.90	1.15	4.95	2.56	1.70	1.05	3.78	1.13	2.75
Dissolved sulfide (mg/l)														
8:00AM	0.11	0.12	0.01	<0.01	NA	0.04	NA	0.03	0.24	NA	0.09	NA	0.03	NA
Noon	0.09	0.06	0.03	<0.01	0.12	0.02	0.03	0.01	0.19	0.12	0.03	0.03	0.05	0.03
4:00PM	0.11	0.04	0.02	<0.01	<0.01	0.01	<0.01	<0.01	0.16	0.15	0.05	0.03	0.04	0.02
8:00PM	0.11	0.06	0.02	<0.01	0.1	<0.01	0.01	<0.01	0.12	0.10	0.12	0.11	0.03	0.02
Midnight	0.11	0.05	0.05	<0.01	0.03	<0.01	0.02	<0.01	0.07	0.12	0.06	0.08	0.03	0.01
4:00AM	0.12	0.05	0.01	<0.01	0.06	0.01	<0.01	0.03	0.15	0.05	0.10	0.04	0.02	<0.01
8:00AM	0.11	0.07	0.01	<0.01	0.01	0.04	0.01	0.04	0.16	0.20	0.06	0.06	0.03	<0.01
Noon	0.08	0.07	0.01	<0.01	<0.01	<0.01	<0.01	<0.01	0.11	0.15	0.03	<0.01	0.03	<0.01
4:00PM	0.13	0.06	0.01	<0.01	0.01		0.01		0.15	0.14	0.04	<0.01	0.03	<0.01
8:00PM	0.11	0.08	0.02	<0.01	<0.01		0.01		0.10	0.12	0.05	0.08	0.02	<0.01
Midnight	0.14	0.07	0.02	<0.01	0.01	NA	0.01	NA	0.12	0.12	0.10	0.08	0.04	0.01
average	0.11	0.07	0.02	<0.01	0.03		0.01		0.14	0.13	0.07	0.06	0.03	0.01
DO (mg/l)														
8:00AM	NA	NA	4.00	2.20	2.35	ND	5.50	4.50	NA	NA	NA	NA	NA	NA
Noon	NA	NA	4.80	9.80	0.30	ND	6.90	4.50	NA	NA	NA	NA	5.37	4.60
4:00PM	NA	NA	5.80	7.50	0.60	ND	4.90	4.70	NA	NA	NA	NA	5.43	4.60
8:00PM	NA	NA	5.20	4.40	0.20	NA	4.80	NA	NA	NA	NA	NA	5.38	4.40
Midnight	NA	NA	2.80	3.50	ND	NA	4.60	NA	NA	NA	NA	NA	5.40	4.60
4:00AM	NA	NA	4.60	3.20	ND	NA	4.50	NA	NA	NA	NA	NA	5.46	4.70
8:00AM	NA	NA	3.50	4.00	0.20	NA	5.10	NA	NA	NA	NA	NA	5.40	4.30
Noon	NA	NA	7.80	7.20	1.00	NA	5.25	NA	NA	NA	NA	NA	5.40	4.10
4:00PM	NA	NA	5.10	8.70	1.20	NA	5.05	NA	NA	NA	NA	NA	5.50	4.30
8:00PM	NA	NA	6.10	4.30	ND	NA	4.50	NA	NA	NA	NA	NA	5.37	4.30
Midnight	NA	NA	3.90	3.20	0.40	NA	5.10	NA	NA	NA	NA	NA	5.39	4.30
average	NA	NA	4.87	5.27	0.57	ND	5.11	4.56	NA	NA	NA	NA	5.41	4.42
H_2O_2 (nM) MDL=25 nM														
8:00AM	162	154	201	<DL	59	48	30	47	81	NA	50	NA	<DL	NA
Noon	205	125	74	270	290	155	136	94	104	NA	107	NA	274	NA
4:00PM	311	189	83	345	184	178	334	392	203	217	324	244	358	309
8:00PM	92	201	51	128	<DL	239	378	266	149	108	157	107	188	111
Midnight	51	40	<DL	50	43	86	40	139	127	38	160	27	115	29
4:00AM	103	89	67	41	29	139	40	66	115	40	130	35	31	29
8:00AM	168	190	25	58	<DL	88	51	244	108	32	103	90	<DL	90
Noon	200	402	85	244	158	361	203	290	443	130	381	150	394	121
4:00PM	128	495	417	87	100	445	483	633	101	298	356	175	242	500
8:00PM	190	330	158	90	75	287	394	178	203	130	173	155	133	134
Midnight	142	195	61	48	80	NA	NA	NA	79	75	101	34	47	44
average	159	219	122	136	113	203	209	235	156	119	186	113	198	152

NA= not analyzed
ND= not detected

| | Black Sand Pool | | | | Chocolate Pots | | | | Nymph Lake | | | | | |
| | pool | | channel | | pool | | channel | | sulfur pool | | iron pool | | channel | |
	July	August	July	August	July	August	July	August	July	August	July	August	July	August
soluble iron (mg/l)														
8:00AM	ND	ND	ND	ND	8.84	10.08	ND	ND	ND	NA	4.68	NA	3.35	NA
Noon	ND	ND	ND	ND	6.94	8.23	ND	ND	ND	ND	3.92	2.71	3.58	2.26
4:00PM	ND	ND	ND	ND	6.33	9.80	ND	ND	ND	ND	2.91	2.28	2.92	2.32
8:00PM	ND	ND	ND	ND	8.20	10.12	ND	ND	ND	ND	4.4	3.69	3.68	2.85
Midnight	ND	ND	ND	ND	8.50	10.03	ND	ND	ND	ND	4.62	4.04	3.38	2.99
4:00AM	ND	ND	ND	ND	9.20	10.24	ND	ND	ND	ND	4.75	3.77	3.41	2.6
8:00AM	ND	ND	ND	ND	8.30	10.35	ND	ND	ND	ND	3.44	3.21	2.33	2.18
Noon	ND	ND	ND	ND	5.90	8.82	ND	ND	ND	ND	3.83	1.98	2.87	1.33
4:00PM	ND	ND	ND	ND	7.81	8.95	ND	ND	ND	ND	3.39	1.76	2.68	1.31
8:00PM	ND	ND	ND	ND	6.84	9.24	ND	ND	ND	ND	3.98	3.54	3.46	2.71
Midnight	ND	ND	ND	ND	9.13	NA	ND	NA	ND	ND	4.50	3.61	3.53	2.57
average	ND	ND	ND	ND	7.82	9.59	ND	ND	ND	ND	4.04	3.06	3.20	2.31
ferrous iron (mg/l)														
8:00AM	ND	ND	ND	ND	4.31	5.13	ND	ND	ND	ND	2.49	NA	1.96	NA
Noon	ND	ND	ND	ND	3.76	4.25	ND	ND	ND	ND	2.45	1.66	2.10	1.33
4:00PM	ND	ND	ND	ND	3.40	4.85	ND	ND	ND	ND	2.25	1.57	1.83	1.43
8:00PM	ND	ND	ND	ND	4.16	5.06	ND	ND	ND	ND	2.10	1.87	1.98	1.57
Midnight	ND	ND	ND	ND	4.16	4.96	ND	ND	ND	ND	2.39	2.01	1.95	1.60
4:00AM	ND	ND	ND	ND	4.52	4.81	ND	ND	ND	ND	2.37	1.95	1.88	1.51
8:00AM	ND	ND	ND	ND	4.25	5.05	ND	ND	ND	ND	1.34	1.37	0.94	1.08
Noon	ND	ND	ND	ND	3.44	4.35	ND	ND	ND	ND	2.08	1.07	1.82	0.77
4:00PM	ND	ND	ND	ND	4.35	4.94	ND	ND	ND	ND	1.90	0.95	1.57	0.84
8:00PM	ND	ND	ND	ND	3.33	4.65	ND	ND	ND	ND	1.95	1.79	1.82	1.47
Midnight	ND	ND	ND	ND	4.43	NA	ND	NA	ND	ND	2.30	1.79	1.99	1.41
average	ND	ND	ND	ND	4.01	4.81	ND	ND	ND	ND	2.15	1.60	1.80	1.30
ferric iron (mg/l)														
8:00AM	ND	ND	ND	ND	4.53	4.95	ND	ND	ND	ND	2.19	NA	1.39	NA
Noon	ND	ND	ND	ND	3.18	3.98	ND	ND	ND	ND	1.47	1.05	1.48	0.93
4:00PM	ND	ND	ND	ND	2.93	4.95	ND	ND	ND	ND	0.66	0.71	1.09	0.89
8:00PM	ND	ND	ND	ND	4.04	5.06	ND	ND	ND	ND	2.30	1.82	1.70	1.28
Midnight	ND	ND	ND	ND	4.34	5.07	ND	ND	ND	ND	2.23	2.03	1.43	1.39
4:00AM	ND	ND	ND	ND	4.68	5.43	ND	ND	ND	ND	2.38	1.82	1.53	1.09
8:00AM	ND	ND	ND	ND	4.05	5.30	ND	ND	ND	ND	2.10	1.84	1.39	1.10
Noon	ND	ND	ND	ND	2.46	4.47	ND	ND	ND	ND	1.75	0.91	1.05	0.56
4:00PM	ND	ND	ND	ND	3.46	4.01	ND	ND	ND	ND	1.49	0.81	1.11	0.47
8:00PM	ND	ND	ND	ND	3.51	4.59	ND	ND	ND	ND	2.03	1.75	1.64	1.24
Midnight	ND	ND	ND	ND	4.70	NA	ND	NA	ND	ND	2.20	1.82	1.54	1.16
average	ND	ND	ND	ND	3.81	4.78	ND	ND	ND	ND	1.89	1.46	1.40	1.01

APPENDIX D - ICP Analysis

Method: BASICSED, Run date: 9/13/96										
Sample Name	Type	Mode	Al3082	As1890	B_2497	Ca3158	Cd2265	Co2286	Cr2677	Cu3247
Blank	Std	IR	-0.148	-0.00771	1.12024	5.62124	0.15232	0.30403	0.19611	0.4175
SED2	Std	IR				2127.71	485.442	276.568		979.177
SED3	Std	IR	1351.19							
SED4	Std	IR		18.2139	934.658				449.272	
BLANK	Unk	CONC	0.019	0.009	0.0007	-0.0035	0.001	0.0035	-0.0005	-0.0005
Blank	Std	IR	0.41	0.037	0.4543	10.76	0.3103	0.5208	0.3122	0.0376
BLANK1	Unk	CONC	-0.001	-0.006	-0.003	0.0354	0.0023	0.0017	0.0005	0.001
Blank	Std	IR	0.146	0.008	0.6646	5.88	0.1646	0.3673	0.1553	0.3445
BLANK2	Unk	CONC	0.002	-0.002	-0.002	-0.0087	0.0008	-0.001	0.0009	0.0002
COMPOSITE	Unk	CONC	10.3	1.05	1.028	10.63	1.066	1.069	1.019	1.032
USGS T121	Unk	CONC	0.091	0.008	0.0949	6.028	0.0097	0.0052	0.0189	0.005
Nymph Lake collection date 6/30/96										
sulfur pool 1200	Unk	CONC.	0.166	4.14	7.665	1.685	0	-0.0004	0.008	-0.0037
sulfur pool 2400	Unk	CONC	0.155	4.03	7.426	1.616	0.0001	-0.0003	0.0087	-0.0072
iron pool 1200	Unk	CONC	1.42	0.358	1.78	6.658	0.0003	-0.0006	0.0088	-0.0073
iron pool 2400	Unk	CONC	1.36	0.375	1.759	6.611	0.0009	-0.0001	0.0087	-0.0074
iron channel 1200	Unk	CONC	1.51	0.297	1.879	7.048	0.0005	-0.0007	0.0082	-0.0068
iron channel 2400	Unk	CONC	1.42	0.359	1.832	6.792	0.0007	-0.0005	0.0083	-0.0075
Chocolate Pots collection date 7/1/96										
pool 1200	Unk	CONC	0.112	0.053	0.4713	23.4	0.0003	-0.0003	0.0043	-0.0037
pool 2400	Unk	CONC	0.151	0.051	0.4627	23.8	0.0007	0.0007	0.0036	-0.0036
channel 1200	Unk	CONC	0.066	0.024	0.4689	23.5	0.0008	-0.0009	0.0039	-0.0036
channel 2400	Unk	CONC	0.071	0.035	0.4665	24.16	0.001	0.0011	0.0039	-0.0035
COMPOSITE	Unk	CONC	10.1	1.03	1.018	10.82	1.074	1.076	1.022	1.004
10ppm Li	Std	IR								
Li Blank	Std	IR								
10ppm Li	Std	IR								
10ppm Li	Unk	CONC	0.005	0.005	0.0003	-0.0247	0.0008	0.0009	-0.001	0.0001
Black Sand Pool collection date 7/13/96										
pool 1200	Unk	CONC	0.476	1.73	3.344	0.3991	0.0013	0.0017	0.0084	-0.0077
channel 1200	Unk	CONC	0.443	1.8	3.563	0.4264	0.0005	0.0008	0.012	-0.0093
channel 1200.3	Unk	CONC	0.454	1.7	3.451	0.41	-0.0007	-0.0008	0.0145	-0.0096
pool 2400	Unk	CONC	0.442	1.65	3.307	0.383	0.0001	-0.0007	0.0114	-0.0082
channel 2400	Unk	CONC	0.452	1.81	3.594	0.4271	0.0006	0.0017	0.0089	-0.0076
channel 2400.3	Unk	CONC	0.451	1.72	3.419	0.4072	-0.0002	0.0005	0.0121	-0.0085
channel 2400.3 REP	Unk	CONC	0.452	1.8	3.554	0.4181	0.0009	0.0014	0.0102	-0.0085
COMPOSITE	Unk	CONC	9.86	1.03	1.019	10.68	1.064	1.059	1.014	0.989
Nymph Lakecollection date 8/6/96										
sulfur pool 1200	Unk	CONC	0.25	3.87	7.296	1.764	0.0017	0.0015	0.0074	-0.0064
sulfur pool 1200 DU	Unk	CONC	0.244	3.85	7.181	1.764	0.0013	0.0015	0.0077	-0.0066
sulfur pool 2400	Unk	CONC	0.176	3.88	7.287	1.702	0.0012	0.0001	0.0089	-0.0063
sulfur pool 2400 SPI	Unk	CONC	1.34	5.79	7.251	57.56	0.0013	0.0018	0.0071	-0.0083
iron pool 1200	Unk	CONC	1.06	0.285	1.811	6.825	0.002	0.0002	0.0069	-0.0066
iron pool 2400	Unk	CONC	1.08	0.357	1.814	7.025	0.0011	-0.0006	0.0238	-0.007
iron channel 1200	Unk	CONC	1.12	0.215	1.88	7.098	0.0008	0.0001	0.0064	-0.0063
iron channel 2400	Unk	CONC	1.12	0.317	1.858	7.247	0.0013	0.0003	0.0079	-0.007
Chocolate Pots collection date 8/17/96										
pool 1200	Unk	CONC	0.146	0.046	0.4614	23.5	0.0017	0.0015	0.0032	-0.0037
pool 1200 DUPLICA	Unk	CONC	0.153	0.054	0.4579	23.9	0.0016	0.001	0.0042	-0.0041
pool 1200 SPIKE	Unk	CONC	1.3	2.77	1.861	73.8	0.0026	0.0033	0.0045	-0.006
pool 2400	Unk	CONC	0.148	0.046	0.4491	23.87	0.0022	0.0008	0.0031	-0.003
channel 1200	Unk	CONC	0.081	0.027	0.4559	23.69	0.0016	0.0017	0.0025	-0.0034
channel 2400	Unk	CONC	0.077	0.038	0.4516	24.17	0.0003	0.001	0.0043	-0.0029
COMPOSITE	Unk	CONC	10	1.03	1.031	10.81	1.072	1.073	1.019	0.9941
Black Sand Pool collection date 8/20/96										
pool 1200	Unk	CONC	0.453	1.67	3.274	0.3789	0.0017	0.0014	0.0089	-0.0057
pool 2400	Unk	CONC	0.444	1.67	3.31	0.4879	0.0011	0.0017	0.0114	-0.009
channel 1200	Unk	CONC	0.442	1.8	3.559	0.4216	0.0008	0.0014	0.011	-0.0091
channel 2400	Unk	CONC	0.429	1.79	3.507	0.4102	0.0006	0.001	0.0098	-0.009
COMPOSITE	Unk	CONC	9.99	1.05	1.032	11.12	1.098	1.092	1.039	0.9872
BLANK	Unk	CONC	0.002	0.002	0.0116	0.0049	0.0008	0.0008	0.0004	-0.0004
COMPOSITE	Unk	CONC	10	1.03	0.9989	11.05	1.09	1.09	1.035	0.9917

Method: BASICSED, Run date: 9/13/96

Sample Name	Fe2399	K_7664	Li6707	Mg2936	Mn2605	Mo2020	Na5895	Ni2316
Blank	0.5982	36.2015		-1.5781	0.15356	-0.08696	-29.255	0.25624
SED2				261.218	1171.04			
SED3	1293.04	1656.57				119.158	352.679	183.544
SED4								
BLANK	0.0065	-0.2769		-0.0237	0.0006	-0.0054	-0.0393	-0.0021
Blank	0.8434	46.88		-2.458	0.309	-0.1256	-34.6	0.2958
BLANK1	0.0066	0.1565		0.0369	0.0024	0.0006	0.065	0.0033
Blank	0.6206	32.06		-1.646	0.175	-0.1498	-30.48	0.2043
BLANK2	0.0016	-0.0004		-0.0014	0.0003	-0.0005	-0.0031	-0.0005
COMPOSITE	10.85	10.38		10.38	1.057	1.04	1.065	1.043
USGS T121	0.1676	0.4991		1.357	0.0326	0.0157	8.037	0.0091
Nymph Lake collection date 6/30/96								
sulfur pool 1200	0.1335	7.432		0.0309	0.0064	0.1295	452.6	-0.0184
sulfur pool 2400	0.1327	7.074		-0.0027	0.0054	0.1293	442.3	-0.0178
iron pool 1200	2.928	63.35		0.6841	0.1755	0.0013	115.5	-0.0205
iron pool 2400	2.929	61.73		0.6517	0.1726	-0.0003	112.4	-0.0191
iron channel 1200	2.582	68.47		0.7263	0.1879	0.0009	151.6	-0.0188
iron channel 2400	2.46	66.17		0.7078	0.1808	0.0008	121	-0.0197
Chocolate Pots collection date 7/1/96								
pool 1200	5.053	23.46		1.871	1.44	0.0096	114.9	-0.0118
pool 2400	5.912	23.81		1.903	1.457	0.0092	115.4	-0.0107
channel 1200	1.833	23.81		1.913	1.323	0.0111	116.7	-0.0099
channel 2400	1.897	24.03		1.908	1.358	0.0085	115.7	-0.0109
COMPOSITE	10.89	10.18		10.11	1.056	1.041	1.014	1.049
10ppm LI			3.26					
Li Blank			3.844					
10ppm Li			6608					
10ppm Li	0.0055	-0.1367	10.31	-0.0121	0.0002	0.0013	-0.0312	-0.0003
Black Sand Pool collection date 7/13/96								
pool 1200	0.1639	21.06	4.385	-0.0089	0.0003	0.0477	502.7	-0.0221
channel 1200	0.1741	22.15	4.47	-0.0281	0.0005	0.0534	527.9	-0.0271
channel 1200.3	0.1689	21.69	4.151	-0.0144	0.0006	0.0526	520.5	-0.0273
pool 2400	0.1541	20.81	4.129	-0.0158	0.0002	0.0481	504.5	-0.0218
channel 2400	0.1718	22.35	4.559	-0.0174	0.0002	0.0517	521.8	-0.0229
channel 2400.3	0.166	21.28	4.235	-0.0138	0.0002	0.0507	544.3	-0.0233
channel 2400.3 REPEAT	0.1725	21.61	4.345	-0.0217	0.0003	0.0499	514.8	-0.0223
COMPOSITE	10.69	9.873	-0.0011	10.01	1.033	1.025	0.9583	1.041
Nymph Lakecollection date 8/6/96								
sulfur pool 1200	0.1477	7.441	1.599	0.0067	0.0081	0.1258	433.1	-0.019
sulfur pool 1200 DUPLICATE	0.1491	7.43	1.608	-0.0051	0.0079	0.1247	425.6	-0.0196
sulfur pool 2400	0.1405	7.287	1.557	-0.0137	0.0062	0.1269	441.3	-0.02
sulfur pool 2400 SPIKE	22.88	25.7	1.267	9.994	1.007	0.6289	380	-0.0234
iron pool 1200	2.149	64.28	0.7566	0.6815	0.2004	-0.0002	137.8	-0.0195
iron pool 2400	2.515	64.84	0.7465	0.6911	0.2024	0.0012	138.1	-0.0205
iron channel 1200	1.729	67.39	0.7948	0.7195	0.204	-0.0004	145.8	-0.0197
iron channel 2400	1.921	68.06	0.7883	0.7063	0.209	0.0002	150.1	-0.0183
Chocolate Pots collection date 8/17/96								
pool 1200	5.853	23.4	0.7939	1.844	1.436	0.0085	113.2	-0.0112
pool 1200 DUPLICATE	5.918	23.56	0.7983	1.838	1.443	0.0072	113.6	-0.0105
pool 1200 SPIKE	27.22	38.9	0.6252	11.37	2.11	0.5314	159.9	-0.0139
pool 2400	5.919	23.42	0.8084	1.855	1.446	0.0066	113	-0.0109
channel 1200	1.45	23.6	0.8415	1.873	1.316	0.0071	113.3	-0.012
channel 2400	1.586	23.59	0.8117	1.882	1.361	0.0054	113.7	-0.0113
COMPOSITE	10.76	9.971	-0.0011	10.05	1.049	1.038	0.9904	1.05
Black Sand Pool collection date 8/20/96								
pool 1200	0.1674	20.1	4.031	-0.0272	0.0002	0.0476	486.9	-0.0241
pool 2400	0.1664	20.57	4.039	-0.0335	0.0005	0.0491	477	-0.0219
channel 1200	0.1769	21.35	4.32	-0.0236	0.0012	0.0529	518.3	-0.0262
channel 2400	0.1683	22.04	4.301	-0.0357	0.0005	0.0505	538.8	-0.0232
COMPOSITE	11.03	9.937	-0.002	10.08	1.066	1.058	0.9528	1.074
BLANK	0.0042	-0.0217	-0.0014	-0.0357	0.0003	0	-0.0322	-0.0015
COMPOSITE	10.99	10.25	-0.0009	· 10.07	1.057	1.053	1.012	1.066

Method: BASICSED, Run date: 9/13/96								
Sample Name	P_1782	Pb2203	S_1820	Se1960	Si2124	Sr3464	Ti3361	Zn2138
Blank	0.12272	0.21029	0.18439	-0.28615	0.14986	-0.3581	-0.11163	1.152
SED2		20.5504				264.213		687.618
SED3							1719.44	
SED4	10.6105		11.5594	15.504	561.393			
BLANK	0.0105	-0.0058	-0.0334	-0.0015	0.0189	-0.0015	0.0012	-0.0004
Blank	0.1133	0.2364	0.1253	-0.4106	0.5504	-0.8511	-0.2466	0.5328
BLANK1	0.0001	0.0068	-0.0045	-0.0018	-0.0302	0.0062	0.0006	0.0016
Blank	0.1072	0.1954	0.1196	-0.2903	0.2052	-0.3954	0.0127	0.7974
BLANK2	0.0024	-0.0055	0.003	-0.0024	-0.0038	0.0009	0.0005	0.0001
COMPOSITE	0.999	1.07	1.136	1.043	10.57	1.057	1.044	0.9999
USGS T121	0.0065	0.0108	1.929	0.0014	2.455	0.0493	-0.0003	0.0225
Nymph Lake collection date 6/30/96								
sulfur pool 1200	-0.4425	-0.0026	26.1	0.0042	138	-0.0266	0.0005	0.0205
sulfur pool 2400	-0.4271	0.0052	25.43	-0.0001	135.9	-0.0273	0.0006	0.0095
iron pool 1200	-0.409	-0.0009	93.16	-0.0169	131.3	-0.0091	-0.0002	0.0506
iron pool 2400	-0.4137	0.0007	90.37	-0.0032	128.9	-0.009	-0.0005	0.0422
iron channel 1200	-0.4553	0.0011	97.84	-0.0116	139.4	-0.0054	-0.0009	0.042
iron channel 2400	-0.4301	-0.0127	93.84	0.0087	135.3	-0.0055	-0.0007	0.0463
Chocolate Pots collection date 7/1/96								
pool 1200	-0.1455	0.0044	12.12	-0.0646	55.58	0.051	-0.0021	-0.002
pool 2400	-0.1666	-0.0075	12.31	-0.0293	56.88	0.0536	-0.0016	0.002
channel 1200	-0.142	-0.0068	12.37	-0.0429	56.36	0.05	-0.0014	-0.0015
channel 2400	-0.1508	-0.0001	12.36	-0.018	56.71	0.0496	-0.0018	0.0046
COMPOSITE	0.9853	1.092	1.13	1.006	10.4	1.075	1.031	0.9949
10ppm Li								
Li Blank								
10ppm Li								
10ppm Li	-0.0029	-0.0163	0.0499	-0.0035	0.0078	0.0015	0.0006	-0.0046
Black Sand Pool collection date 7/13/96								
pool 1200	-0.5493	-0.0048	6.873	-0.0111	178.4	-0.0345	0.0022	0.0035
channel 1200	-0.594	0.0019	7.174	-0.0162	186.6	-0.0426	0.0014	0.0003
channel 1200.3	-0.5528	0.0212	6.775	-0.018	176.8	-0.0433	0.001	0.0023
pool 2400	-0.5094	0.0052	6.521	-0.0243	167.5	-0.0368	0.0013	-0.0002
channel 2400	-0.564	0.0013	7.22	-0.0216	184	-0.0366	0.0016	0.006
channel 2400.3	-0.5669	-0.0021	6.83	-0.0321	175.7	-0.036	0.0014	0.0045
channel 2400.3 REPEAT	-0.5658	-0.006	7.153	-0.0201	180.8	-0.0365	0.0017	0.0057
COMPOSITE	0.9879	1.03	1.132	0.9923	10.44	1.064	1.012	0.9845
Nymph Lakecollection date 8/6/96								
sulfur pool 1200	-0.4226	-0.0169	53	-0.0333	137.1	-0.0267	0.0012	0.012
sulfur pool 1200 DUPLICATE	-0.4131	-0.0176	50.7	-0.0208	136	-0.0259	0.0012	0.0117
sulfur pool 2400	-0.4232	-0.0023	50.67	-0.0384	139	-0.0259	0.0009	0.0068
sulfur pool 2400 SPIKE	2.107	-0.0008	35.98	-0.0158	174.2	1.081	-0.0034	1.01
iron pool 1200	-0.4091	0.0035	88.61	-0.0065	130.7	-0.007	-0.0004	0.035
iron pool 2400	-0.4009	-0.0044	87.5	0.0031	131.1	-0.0101	-0.0003	0.0327
iron channel 1200	-0.429	-0.0038	93.28	-0.0122	138	-0.0095	-0.0001	0.0285
iron channel 2400	-0.4272	-0.0036	90.97	-0.0122	136	-0.0085	0.0002	0.0305
Chocolate Pots collection date 8/17/96								
pool 1200	-0.1355	-0.0014	12.37	-0.0516	55.92	0.0513	-0.0018	0.0085
pool 1200 DUPLICATE	-0.1426	0.0183	12.47	-0.0408	56.39	0.0521	-0.0015	0.0088
pool 1200 SPIKE	2.268	-0.0032	10.05	-0.0402	109.9	1.12	-0.0055	0.9975
pool 2400	-0.1426	-0.0095	12.56	-0.0474	56.7	0.0509	-0.0015	0.006
channel 1200	-0.1373	-0.0185	12.91	-0.0494	56.81	0.0531	-0.0013	0.0037
channel 2400	-0.1508	-0.0031	12.76	-0.0136	56.68	0.0522	-0.0014	0.0084
COMPOSITE	0.9812	1.093	1.089	0.9944	10.41	1.074	1.025	0.988
Black Sand Pool collection date 8/20/96								
pool 1200	-0.5381	0.0094	6.614	-0.011	174.9	-0.0362	0.0014	0.0017
pool 2400	-0.5405	0.0061	6.612	-0.0064	173.1	-0.0362	0.0015	0.0117
channel 1200	-0.5703	-0.0206	7.253	-0.0165	188.4	-0.0418	0.0018	-0.0007
channel 2400	-0.5658	-0.0066	7.027	-0.0509	180.9	-0.0347	0.0018	0.0033
COMPOSITE	0.9845	1.098	1.266	0.9836	10.66	1.104	1.03	0.9952
BLANK	-0.0025	-0.0039	0.0329	-0.0175	0.0181	0.0006	0.0006	-0.0004
COMPOSITE	0.9822	1.112	1.136	0.9833	10.43	1.101	1.03	0.9935

Sample name	dilution factor	fluoride	chloride	sulfate
Run date: 7/15/96				
autocal1		1.00	1.00	6.00
autocal2		5.00	5.00	30.00
autocal3		10.00	10.00	60.00
std1		0.89	0.87	6.46
std2		4.18	4.29	27.23
std3		8.75	8.92	53.85
Nymph lake collection date 6/30/96				
sulfur pool 0800	X1	16.71	>10	45.83
sulfur pool 1600	X1	17.07	>10	46.42
sulfur pool 2400	X1	16.94	>10	44.73
iron pool 0800	X1	2.35	>10	146.31
iron pool 1600	X1	2.69	>10	146.51
iron pool 2400	X1	2.50	>10	146.36
iron channel 0800	X1	2.51	>10	146.61
iron channel 1600	X1	2.67	>10	146.26
iron channel 2400	X1	2.69	>10	146.53
Chocolate Pots collection date 7/1/96				
pool 0800	X1	4.30	24.54	28.89
pool 1600	X1	4.06	24.67	29.07
pool 2400	X1	4.46	25.33	29.71
channel 0800	X1	4.13	24.73	28.99
channel 1600	X1	3.94	24.97	29.79
channel 2400	X1	4.16	25.47	30.68
Black Sand Pool collection date 7/13/96				
pool 0800	X1	26.91	>10	15.30
pool 1600	X1	27.95	>10	15.76
pool 2400	X1	28.47	>10	16.00
channel 0800	X1	29.35	>10	17.62
channel 1600	X1	30.00	>10	18.09
channel 2400	X1	30.21	>10	18.12
std1		0.97	1.25	5.95
std2		4.92	5.01	29.85
std3		10.05	10.12	59.98
Nymph lake collection date 6/30/96 repeat analysis				
sulfur pool 0800	X1	18.64	>10	51.81
sulfur pool 1600	X1	19.55	>10	51.89
sulfur pool 2400	X1	19.30	>10	49.76
std1		0.96	0.92	6.13
std3		9.95	9.95	61.15
std 3ppm F & Cl		2.71	2.73	
std 15ppm F & Cl		14.35	14.85	
std 30ppm F & Cl		27.77	27.67	
std1		0.98	1.41	6.07
std3		9.36	9.48	59.41
Nymph lake collection date 6/30/96				
sulfur pool 0800	X25	21.72	439.10	64.47
sulfur pool 1600	X25	18.88	421.60	63.57
sulfur pool 2400	X25	19.64	421.70	64.81
iron pool 0800	X10	4.26	98.48	247.20
iron pool 1600	X10	4.37	99.76	260.10
iron pool 2400	X10	3.94	98.32	268.60
iron channel 0800	X10	4.61	107.30	275.10
iron channel 1600	X10	4.00	102.60	279.30
iron channel 2400	X10	4.24	104.00	268.60
Black Sand Pool collection date 7/13/96				
pool 0800	X20	28.26	306.10	30.55
pool 1600	X20			
pool 2400	X20			
channel 0800	X20	29.46	326.10	30.55
channel 1600	X20	29.76	341.50	32.80
channel 2400	X20	30.01	328.80	31.40
std 15ppm F & Cl		14.98	15.51	
std 30ppm F & Cl		28.60	28.36	
std1		0.98	1.19	6.36
std3		10.23	10.40	61.33

BIBLIOGRAPHY

Brick, Christine M and Johnnie N Moore (1996). Diel variations of trace metals in the upper Clark Fork River, Montana. *Environ. Sci Technol.*, 30:1953-1960.

Brock, Thomas D (1978). *Thermophilic Microorganisms and Life at High Temperatures*, Springer Series in Microbiology; Springer-Verlag: New York.

Brock, Thomas D, Michael T Madigan, John M Martinko, and Jack Parker (1994). "Molecular Systematics and Microbial Evolution." In *Biology of Microorganisms*, 7th Edition, Prentice Hall: Englewood Cliffs, New Jersey; pp.692-717.

Brown, Chris F. (1997). Iron Cycling in Yellowstone National Park; unpublished Senior Thesis, University of Montana.

Calvin, Melvin (1959). Evolution of enzymes and the photosynthetic apparatus. *Science*, 130:1170-1174.

Christian, Gary (1977). *Analytical Chemistry*. 2nd Edition,Wiley and Sons: New York; pp. 325-328.

Collienne, R.H. (1983). Photoreduction of iron in the epilimnion of acidic lakes. *Limnol. Oceanogr.*, 28:83-100.

Cooper, William and David Lean (1989). Hydrogen peroxide concentration in a northern lake: Photochemical formation and diel variability. *Environ. Sci Technol.*, 23:1425-1428.

Cooper, William and David Lean (1992). "Hydrogen peroxide dynamics in marine and fresh water systems." In *Encyclopedia of Earth System Science*, Vol 2; W. A. Nierenber editor, Academic: San Diego, pp527-535.

Cooper, WJ, DRS Lean and JH Carey (1989). Spatial and temporal patterns of hydrogen peroxide in lake waters. *Can. J. Fish. Aquat. Sci.*, 46:1227-1231.

Cooper, William J, Chihwen Shao, David RS Lean, Andrew S Gordon, and Frank E Scully Jr (1994). "Factors affecting the distribution of H_2O_2 in surface waters." In *Environmental Chemistry of Lakes and Reservoirs*, Lawrence A Baker editor; ACS Advances in Chemistry Series No. 237; American Chemical Society: Washington, DC; pp391-422.

Cooper, William, Rod G Zika, Robert G Petasne and John MC Plane (1988). Photochemical formation of H_2O_2 in natural waters exposed to sunlight. *Environ. Sci Technol.*, 23:1425-1428.

Cooper, William J, Rod G Zika, Robert G Petasne and Anne M. Fischer(1989). "Sunlight-induced photochemistry of humic substances in natural waters: major reactive species." In *Aquatic Humic Substances:Influence on Fate and Treatment of Pollutants,* IH Suffet and Patrick MacCarthy editors; Advances in Chemistry 219; American Chemical Society: Washington, DC; pp 333-362.

Dean , R.B. and W.J. Dixon (1951). Simplified statistics for small numbers of observations. *Anal. Chem.*, 4:636-638.

Fournier, Robert O. (1989). Geochemistry and dynamics fo Yellowstone National Park hydrothermal system. *Ann. Rev. Earth Planet. Sci.*, 17:13-53.

Gaede, Wolfgang and Rudi van Eldik (1994). Kinetics of the oxidation of chromium (II) by hydrogen peroxide. Effect of different anions, temperaure, and pressure. *Inorg. Chem.*, 33:2204-2208.

Gottschalk, Gerhard (1986). *Bacterial Metabolism.* Springer-Verlag: New York.

Gunz, Dieter W and Michael R Hoffmann (1990). Atmospheric chemistry of peroxides: A review. *Atmospheric Environment*, 24A(7):1601-1633.

Halliwell, Barry and John M.C. Gutteridge (1984). Oxygen toxicity, oxygen radicals, transition metals and disease. *Biochem. J.* 219:1-14.

Holm, Thomas R, Gregory K George and Michael J Barcelona (1987). Fluorometric determination of hydrogen peroxide in groundwater. *Anal. Chem.*, 59:582-586.

Larsen, Ingvar L., Norbert A. Hartmann, and Jerome J. Wagner (1973). Estimating precision for the method of standard additions. *Anal. Chem.*, 45:1511-1513.

Margulis, Lynn (1981). *Symbiosis in Cell Evolution.* WH Freeman and Company: San Francisco.

McKnight, DM, BA Kimball, and KE Bencala (1988). Iron photoreduction and oxidation in an acidic mountain stream. *Science* 240:637-640.

Millero, Frank J, Arthur LeFerriere, Marino Fernandez, Scott Hubinger, and J Peter Hershey (1989). Oxidation of H_2S with H_2O_2 in natural waters. *Environ. Sci Technol*, 23:209-213.

Millero, Frank J, and Sara Sotolongo (1989). The oxidation of Fe(II) with H_2O_2 in seawater. *Geochim Cosmochim Acta*, 53:1867-1873.

Moffett, James W and Oliver C. (1990). An investigation of hydrogen peroxide chemistry in surface waters of Vineyard Sound with $H_2{}^{18}O_2$ and $^{18}O_2$. *Limnol. Oceanogr.*, 35:1221-1229.

Moffett, James W and Rod G Zika (1987). Reaction kinetics of hydrogen peroxide with copper and iron in seawater. *Environ. Sci Technol.*, 21:804-810.

Nealson, Kenneth H (1983). "The Microbial Iron Cycle." In *Microbial Geochemistry*, WE Krumbein editor, Blackwell Scientific Publications: Oxford, pp 159-190.

Nealson, Kenneth H (1983). "The Microbial Manganese Cycle." In *Microbial Geochemistry*, WE Krumbein editor, Blackwell Scientific Publications: Oxford, pp 191-221.

Ott, R. Lyman (1993). *An introduction to statistical methods and data analysis.* Duxbury Press: Belmont, CA.

Palenik, B, OC Zafiriou, and FMM Morel (1987). Hydrogen peroxide production by marine phytoplankter. *Limnol. Oceanogr.* 32(6):1365-1369.

Palenik, B and FMM Morel (1987). Dark Production of H_2O_2 in the Sargasso Sea. *Limnol. Oceanogr.* 33(6):1606-1611.

Palenik, B and FMM Morel (1990). Amino acid utilization by marine phytoplankton: A novel mechanism. *Limnol. Oceanogr.* 35(2):260-269.

Pettine, M, Frank J Millero (1990). Chromium speciation in seawater; the probable role of hydrogen peroxide. *Limnol. Oceanogr.* 35(3):730-736.

Sagan, Carl (1973). Ultraviolet selection pressure on the earliest organisms. *J. of Theoret. Biol.,* 39:195-200.

Scully, NM, DRS Lean, DJ McQueen and WJ Cooper (1996a). Photochemical formation of hydrogen peroxide in lakes: Effects of dissolved organic carbon and ultraviolet radiation. *Can. J. Fish. Aquat. Sci.*, 52:2675-2681.

Scully, NM, DRS Lean, DJ McQueen and WJ Cooper (1996B). Hydrogen peroxide formation: The interaction of ultraviolet radiation and dissolved organic carbon in lakewaters along a latitude (43-75°N) gradient. *Limnol. Oceanogr.,*41:540-548.

Sharma, Virender K and Frank J Millero (1989). The oxidation of cu(I) with H_2O_2 in natural waters. *Geochim Cosmochim Acta*, 53:2269-2276.

Standard Methods For the Examination of Water and Wastewater (1985) 16th edition; Mary Ann H. Franson, managing editor. Published jointly by American Pubic Health Association, American Water Works Association, and Water Pollution Control Federation; American Public Health Association, Washington D.C.

Stevens SE, C.O.P Patterson and Jack Meyers (1973). The production of hydrogen peroxide by bluegreen algae: A survey. *J. Phycol.* 9:427-430.

Stookey, Lawrence L. (1970). Ferrozine-A new spectrophotometric reagent for iron. *Anal. Chem.*, 42:779-781.

Sunda, W.G., S.A. Huntsman, and G.R. Harvey (1983). Photoreduction of manganese oxides in seawater and its geochemical and biological implications. *Nature*, 301:234-236.

Zika, Rod G, Eric S Saltzman WL Chameides and DD Davis (1982). H_2O_2 Levels in Rainwater Collected in South Florida and the Bahama Islands. *J. Geophys. Res.*, 87: 5115-5017.

Zika, Rod G, James W Moffett, Robert G Petasne, William J Cooper and Eric S Saltzman (1985). Spatial and temporal variations of hydrogen peroxide in Gulf of Mexico waters. *Geochim Cosmochim Acta*, 49:1173-1184.

Zuo, Yuegang and Jurg Hoigne (1992). Formation of hydrogen peroxide and deposition of oxalic acid in atmospheric water by photolysis of iron(III)-oxalato complexes. *Environ. Sci. Technol.*, 26:1014-1022.